

ELECTROMAGNETIC EFFECTS OF ATMOSPHERIC GRAVITY WAVES

by

Jon F. Claerbout

S.B., M.I.T.

(1960)

S.M., M.I.T.

(1963)

SUBMITTED IN PARTIAL FULFILLMENT

OF THE REQUIREMENTS FOR THE

DEGREE OF DOCTOR OF

PHILOSOPHY

at the

MASSACHUSETTS INSTITUTE OF TECHNOLOGY

June 1967

Signature of Author Jon F. Claerbout
Department of Geology and Geophysics

Certified by RSC
Thesis Supervisor

Accepted by RSC Lindgren
Chairman, Departmental Committee
on Graduate Students

WITHDRAWN
FROM
MIT LIBRARIES
AUG 1 1969
MASS. INST. TECH.

ELECTROMAGNETIC EFFECTS OF ATMOSPHERIC GRAVITY WAVES

by Jon F. Claerbout

Submitted to the Department of Geology and Geophysics on

May 12, 1967

in partial fulfillment of the requirements for the degree of

Doctor of Philosophy

Continuous observations of pressure fluctuations at gravity wave periods (5-30 minutes) in eastern Massachusetts show that the only important pressure fluctuations not associated with moving weather sources are pressure fluctuations associated with the jet stream. These fluctuations appear to be non-dispersive and move a little slower than the maximum overhead jet stream velocity. The coupling between gravity wave modes and fluctuations in the jet stream is examined to investigate the pumping of energy from the jet stream into the upper atmosphere. There are two major problems in understanding the nature of the disturbance at the critical altitude where the velocity of the disturbance matches the velocity of the mean wind. The first problem involves the origin of the disturbance in the vicinity of such a critical altitude. Theoretically, the energy flux emitted is amplified by the wind shear as the wave moves away from the critical altitude. The second problem involves a wave originating elsewhere moving into a critical zone. A wave packet moving into a critical zone becomes so compressed before it reaches the critical altitude that the wind shear within the wave itself causes the atmosphere to become locally unstable. The exact mechanism for the transport of energy across a critical altitude is not known. If by symmetry it is presumed that the amplitude of the wave will be comparable on either side of the critical altitude, the wave amplitudes in the upper atmosphere can be predicted.

Energy propagation to the ionospheric D-region (80 km.) takes 10 hours under average conditions where typical amplitudes will be 10 meters/second. Shorter propagation times occur when mesospheric temperature gradients are low and winds above the jet stream are directed opposite to the jet. The waves are strongly reflected by temperature gradients in the

lower thermosphere, consequently, it takes a long time to accumulate any energy at height. Energy typically propagates upward to about 115 km where it is dissipated by electromagnetic forces in 20 to 1000 hours. The induced magnetic field when integrated back to the ground is an order or two magnitude less than the quiet-time ambient field. Therefore we have not observed a correlation between atmospheric pressure and the magnetic field on the ground but expect that pressure may be correlated to some measure of activity in the ionospheric D-region.

Thesis supervisor: Theodore R. Madden

Title: Professor of Geophysics

TABLE OF CONTENTS

	<u>Page</u>
Abstract	2
Table of Contents	4
List of Figures	6
List of Tables	7
Introduction	8
I) Acoustic Gravity Wave Formula Derivations	13
A) Stratified Wind and Temperature	13
1) From Basic Equations to Stratified Media	15
2) Energy and Momentum Principles	24
3) Instabilities of Waves Interacting with High Altitude Winds	37
B) With Ionization and Maxwell's Equations	47
1) Continuity Equations	49
2) Conductivity of a Moving Partially Ionized Gas	51
3) Canonical Form of Tensor Conductivity, Choice of Coordinates	57
4) Electrical Phenomena with Prescribed Neutral Velocity	67
5) Wave-Guide Integration Formulas	74
II) Results of Calculations	78
A) Pure Acoustic Gravity	78
1) Dispersion Curves	80
1.1) Free Space Curves	80
1.2) Thermal Effects	83
1.3) Jet Stream Effects	87
1.4) Vertical Energy Transport	91
2) Particle Motions for Lamb Wave and Jet Wave	95
B) Acousto-Electromagnetic	103
1) Ionospheric Winds, Two Dimensional Conductivities	103
2) Gravity Wave Dissipation and Heating	110
3) Lamb Wave V, J, D, E, H , and $V \cdot \text{Grad } P$	114
4) Westerly Jet Wave	122
5) Finite Transverse Wavelength	125
III) Data Acquisition and Interpretation	129
A) Instrumentation	130
B) Selected Data Samples	138
C) Spectrum and Plane Wave Interpretation	144
D) Correlation with Jet Stream Behavior	151

Appendices

A) Transformations of First Order Matrix Differential Equations	161 161
B) Sturm-Liouville Formulation of Acoustic Gravity Wave Problem	163
C) Atmospheric Constants and Basic Physical Formulas	167
References	169
Acknowledgement	173
Biographical Note	174

FIGURES AND PLATES

<u>Number</u>	<u>Title</u>	<u>Page</u>
Section I-A-2		
1	Wave emitted by wind over undulating surface	27
Section I-A-3		
1	Wave packet approaching critical height	38
Section I-B-3		
1	Graph of crossconductivities	65
Section II-A		
1.1	Free space dispersion curves	81
1.2	Group velocity of acoustic-gravity waves	82
1.3	Altitude scaling of properties of gravity waves	84
1.4	Effect of thermosphere on dispersion curves	85
1.5	Dispersion curves for a jet stream model	89
1.6	Expanded scale of figure II-A-1.5	90
1.7	Expanded scale of figure II-A-1.6	91
2.1	Particle motions of Lamb wave in T-J model	96
2.2	Particle motions of jet wave in T-J model	98
2.3	Particle motions in a linear wind profile	99
2.4	A wave with source at jet stream altitude	101
2.5	A wave traveling slower than the jet stream	102
Section II-B		
2.1	Vertical energy transport and e.m. decay time	112
3.1	Motions of Lamb wave in a realistic atmosphere	115
3.2	Charge drift caused by Lamb wave	116
3.3	Electric field caused by Lamb wave	117
3.4	Electric currents caused by Lamb wave	119
3.5	Magnetic field caused by Lamb wave	120
3.6	Electrical effects of eastward going Lamb wave	121
4.1	Electrical effects of jet wave in T-J model	123
4.2	Jet wave in a realistic temperature model	124
5.1	Jet wave with finite transverse wavelength	128
Section III-A		
1	Map showing pressure recording sites	131
2	Microbarograph array data collection system	132
3	Microbarograph design	134
4	Functional diagram of pressure transducer	135
5	Gain and phase of barograph system	136
6	Pressure comparison between two instruments	137

Number	<u>Title</u>	<u>Page</u>
Section III-B		
1	Pressure transient of a moving weather front	139
2	Pressure transient associated with the jet stream	139
3	Pressure data of Jan. 2-8, 1967	141
4	Pressure data of Jan. 9-15, 1967	142
Section III-C		
1	Insignificant dispersion of jet waves	145
2	Coherency among pressure observations	147
3	Crosspower of Cambridge-Weston pressure	149
Section III-D		
1	Profiles of temperature, wind, and instability	152
2	500 millibar map April 3-5, 1966	153
3	Association of pressure with stability criteria	155

TABLES

Section I-B-3		
1	Ionospheric properties and derived conductivities	64
Section I-B-5		
1	Equations for waveguide integration	76
Section II-B		
1.1	Ionospheric properties for wind calculations	107
1.2	Ionospheric effects of a horizontal wind	108
1.3	Ionospheric effects effects of a horizontal E-field	109

INTRODUCTION

This thesis is concerned with the propagation, generation, and dissipation of gravity waves in the atmosphere. In Eastern Massachusetts the observed gravity waves are generated principally in the jet stream and are thought to propagate up to the ionosphere where they are dissipated by electromagnetic processes. Gravity wave phenomena are in-between high frequency meteorology and low frequency sound. The wave periods (3-60 minutes) are much shorter than the earth's rotation period which is important in meteorology, but the wave periods are so long that when multiplied by the speed of sound they imply a quarter wavelength comparable to the atmospheric scale height. Sound propagation at such periods is profoundly influenced by gravity hence the term "acoustic-gravity wave."

These gravity waves, like gravity waves on water, have elliptical particle motions. Water waves, however, are constrained to the surface of the water, but these waves are internal to the atmosphere. Indeed, one of their most interesting features is vertical propagation. Under simplifying assumptions these waves preserve the quantity ρv^2 (ρ is the air density and v is the wave particle velocity) while propagating vertically. Since the atmospheric density decreases an order of magnitude in 15 to 20 kilometers altitude the wave particle velocity may get quite large at high altitudes. Because of this, gravity waves have been thought to explain small scale high altitude winds and ionospheric

disturbances. Small scale (one kilometer vertical wavelength) high altitude (40-200 kilometers) winds have been observed by meteor trails, rocket exhaust trails, and falling spheres.

(For many references see Hines, Murphy et.al., Dickenson). These winds have been attributed to gravity waves, but the observations are so transient that a quantitative comparison of theory and data is difficult. Movement of ionospheric inhomogenities observed by scattering of radio waves is also attributed (Martyn 1950, Hines 1960) to gravity waves but again quantitative study is difficult.

Much attention has been given to waves propagating long distances from exploding volcanoes and nuclear explosions (Cox, Donn and Ewing, Pierce, Press and Harkrider, Pfeffer and Zarichney). These wave sources are rare; more frequent sources have been suggested (Hines, Pierce, Dickenson) to be storms and strong cumulus convection. While this may be true, our pressure observations over the course of 14 months have shown no waves emitted by storms which travel any faster than the storms themselves. On the other hand, of frequent occurrence were disturbances of jet stream speed. Theoretically these faster disturbances can be expected to propagate to the ionosphere much more readily than disturbances of weather front speed.

The strength of these "jet waves" may be explained by the strong wind shear at jet stream altitudes. When the wind shear (which has physical dimensions of frequency) becomes comparable to the atmospheric vertical resonance fre-

quency the atmosphere becomes dynamically unstable. At any height where this frequency ratio predicts instability one may expect a disturbance to form and be swept over ground observers at the speed of the wind at that height. A height where a gravity wave velocity matches a wind velocity is called a critical height; here coupling may occur and the wave can be amplified. Theory predicts the vertical energy flux of a gravity wave to be amplified by the wind shear as the wave emerges from the critical height. As the waves propagate vertically they may encounter more critical heights. These may act as barriers or they may transmit the energy; this is an important topic for future research. In any case the waves emerging from the last critical height propagate upward having their energy amplified by the wind shear and their amplitude further magnified by the decreasing atmospheric density.

Propagation upward to the ionospheric D-region (80 km) will take about 10 hours. This travel time is quite variable depending on the wind and thermal state of the intervening air. The particle velocities at this altitude, if they can pass through the critical heights without energy loss, will be about 10 meters per second in both horizontal and vertical directions. This should be measurable by some independent means.

Further propagation into the ionosphere is greatly retarded by strong thermal gradients. Typically, disturbance energy is going so nearly horizontal that it reaches 115 kilometers only after 20 to 1000 hours. In this amount of

time the disturbance will be well spread out in space and will be dissipated by electromagnetic processes. Greatly diminished amounts of energy may get further up and still be important because the amplitudes continue to increase for awhile due to the decreasing ρ .

When the gravity wave neutral air molecules drag ions and electrons across the earth's magnetic field electric currents are set up which in turn induce magnetic fields. The currents (.3 microamps / meter²) that we extrapolate from the pressure data are quite comparable to other currents thought to be present in the ionosphere. Due to the fairly short (20 km) vertical wavelengths of the wave, the effects of the currents tend to cancel in the production of magnetic fields. When the magnetic fields are integrated back to earth they are smaller than the observed quiet-time variations by one or two orders of magnitude.

In the first chapter of this thesis we derive the basic properties of atmospheric gravity waves as previously deduced by Lamb, Eckart, Martyn, Hines and Pierce. Our deduction and conclusions on energy and momentum flow of these waves differ somewhat from other studies by Eliasson and Palm and by Bretherton. We also discuss difficulties in the linear theory at the critical height. There is a fairly extensive discussion of electrical conductivity in a windy ionosphere. Finally we derive the necessary formulas to calculate the electromagnetic effects of atmospheric gravity waves. The reader may prefer to skim the first chapter for its essential definitions and ideas and go on to the second.

In the second chapter we present numerous results of applying the formulas of the first chapter to various simplified and realistic temperature, wind, and ionization models of the atmosphere. The simplified models have been included in order to make clearer the underlying causes of various phenomena.

In the third and final chapter we present pressure array data, its collection, and its interpretation with emphasis on the relation between the observed pressure fluctuations and the state of the jet stream.

I Acoustic Gravity Waves in a Stratified Atmosphere

Section 1 begins with the established acousto-hydrodynamic equations. They are linearized and specialized to a temperature and wind stratified atmosphere. The trial solutions consist of altitude dependent (z -dependent) ambient values plus perturbations which are sinusoidal in x , y , and t but have arbitrary z -dependence. With the substitution of these trial solutions, the hydrodynamic equations become linear differential equations with z as the independent variable and the perturbations as dependent variables. We explore different choices of integrating factors with the dependent variables and come up with a choice of variables which will be continuous even though the temperature and wind may be stratified into layers with abrupt changes at the layer interfaces.

In section 2 we derive formulas for wave energy density and flow. It turns out that energy flux is divergent for a wave propagating across zones of wind shear because energy is exchanged between the wave and the ambient stratified wind. It is another quadratic function of the wave variables, the momentum flux, which is non-divergent when the wave flows across wind shear.

There are two circumstances under which the energy density of the waves may become negative: (1) The temperature lapse is so strong that the heavy cold air on top of

the lighter warm air is such as to make the atmosphere unstable. (2) The wind shear (which has dimensions of frequency) is greater than twice the atmospheric vertical free resonance frequency. The first condition corresponds to static instability of the atmosphere and the second to dynamic instability.

In section 3 we consider waves whose horizontal phase velocity equals at some altitude (called the critical height) the velocity of the mean wind. As a wave of fixed horizontal wavelength propagates to a critical height its frequency with respect to the ambient medium is doppler shifted to zero. In the low frequency limit the wave loses all acoustic character and becomes a gravity wave with a horizontal group velocity and zero vertical wavelength. In the vicinity of the critical height an exact solution is possible. The solution shows a divergence everywhere of the normally conserved wave momentum flux if the atmosphere is dynamically unstable according to condition (2) above. The role of critical heights and dynamic instabilities is crucial in an explanation of pressure fluctuations observed at the ground.

I-A-I From Basic Equations to Stratified Media

We use the conventional definitions: pressure p , density ρ , sound speed c , particle velocity $v=(u,v,w)$, angular frequency ω , wave numbers k and l , gravity g , and ratio or specific heats γ . As subscripts, x , z , and t are partial derivatives. A bar over a quantity indicates its time average. A tilde over a quantity represents the perturbation part due to the presence of a wave. By a stratified media we mean one in which the media properties are functions of only the vertical z coordinate. We take plus z upward. The trial solutions are:

$$(1) \quad \begin{bmatrix} P \\ \rho \\ u \\ v \\ w \end{bmatrix} = \begin{bmatrix} \bar{p}(z) \\ \bar{\rho}(z) \\ \bar{u}(z) \end{bmatrix} + \begin{bmatrix} \tilde{p}(z) \\ \tilde{\rho}(z) \\ \tilde{u}(z) \\ \tilde{v}(z) \\ \tilde{w}(z) \end{bmatrix} e^{-i\omega t + ikx + ilz}$$

Linearization means that products of elements in the right-hand vector will be ignored as being small. The equations of adiabatic state (energy), momentum conservation, and mass conservation are:

$$(2a) \quad \frac{Dp}{Dt} = c^2 \frac{D\rho}{Dt}$$

$$(2b,c,d) \quad \rho \frac{D\vec{v}}{Dt} = \rho \vec{g} - \nabla p$$

$$(2e) \quad \frac{\partial}{\partial t} \rho + \nabla \cdot (\rho \vec{V}) = 0$$

We expand out the substantial derivatives in this set

$$(3a) \quad \rho_t + \vec{V} \cdot \nabla \rho = c^2 [\rho_t + \vec{V} \cdot \nabla \rho]$$

$$(3b,c,d) \quad \rho (\vec{V}_t + \vec{V} \cdot \nabla \vec{V}) = \rho \vec{g} - \nabla p$$

$$(3e) \quad \rho_t + \nabla \cdot (\rho \vec{V}) = 0$$

The substantial derivative of an arbitrary scalar variable

Ψ is

$$\begin{aligned} (4) \quad \frac{D\Psi}{Dt} &= \Psi_t + \vec{V} \cdot \nabla \Psi \\ &= \Psi_t + [\bar{u} + \tilde{u}, \tilde{v}, \tilde{w}] \begin{bmatrix} ik\tilde{\Psi} \\ i\ell\tilde{\Psi} \\ \bar{\Psi}_z \end{bmatrix} \\ &= \Psi_t + ik\bar{u}\tilde{\Psi} + \tilde{w}\bar{\Psi}_z \\ &= -i\Omega\tilde{\Psi} + \tilde{w}\bar{\Psi}_z \end{aligned}$$

Applying this to the components of the vector variable \vec{V} we get
(5)

$$\frac{D\vec{V}}{Dt} = -i\Omega \begin{bmatrix} \tilde{u} \\ \tilde{v} \\ \tilde{w} \end{bmatrix} + \tilde{w} \begin{bmatrix} \bar{u}_z \end{bmatrix}$$

In (4) and (5) we introduced the definition of a Doppler

frequency

$$(6) \quad \Omega = \omega - \vec{k} \cdot \vec{v} = \omega - k \bar{u}$$

Utilizing (4) and (5) we linearize the principal set (3)

$$(7a) \quad -i\Omega \tilde{\rho} + \bar{\rho}_z \tilde{W} = c^2 [-i\Omega \bar{\rho} + \bar{\rho}_z \tilde{W}]$$

$$(7b) \quad \bar{\rho} (-i\Omega \tilde{u} + \bar{u}_z \tilde{W}) = -i k \tilde{\rho}$$

$$(7c) \quad \bar{\rho} (-i\Omega \tilde{v} + 0) = -i l \tilde{\rho}$$

$$(7d) \quad \bar{\rho} (-i\Omega \tilde{W} + 0) = -\tilde{\rho} g - \tilde{P}_z$$

$$(7e) \quad \rho_t + \bar{\rho} (\nabla \cdot \vec{v}) + \vec{v} \cdot (\nabla \rho) = 0$$

$$\rho_t + (\bar{\rho} + \tilde{\rho}) (ik\tilde{u} + il\tilde{v} + \tilde{W}_z) + ik\tilde{\rho}\bar{u} + \bar{\rho}_z \tilde{W} = 0$$

$$-i\Omega \tilde{\rho} + (\bar{\rho} \tilde{W})_z + ik\tilde{\rho}\bar{u} + il\tilde{\rho}\bar{v} = 0$$

Next we solve for $\tilde{\rho}$, \tilde{u} , \tilde{v} , \tilde{P}_z , and $(\bar{\rho} \tilde{W})_z$ respectively

$$(8a) \quad \tilde{\rho} = \frac{1}{c^2} \tilde{P} + \frac{i}{\Omega} \left(\frac{1}{c^2} \bar{P}_z - \bar{\rho}_z \right) \tilde{W}$$

$$(8b) \quad \tilde{u} = \frac{1}{\bar{\rho}} \frac{k}{\Omega} \tilde{\rho} - \frac{i \bar{u}_z}{\Omega} \tilde{W}$$

$$(8c) \quad \tilde{v} = \frac{l}{\Omega \bar{\rho}} \tilde{\rho}$$

$$(8d) \quad \tilde{p}_z = -g\tilde{\rho} + i\Omega\bar{\rho}\tilde{w}$$

$$(8e) \quad (\bar{\rho}\tilde{w})_z = i\Omega\tilde{\rho} - i\bar{\rho}(k\tilde{u} + l\tilde{v})$$

Substituting (8a), and (8b) and (8c) into (8d) and (8e) we get the basic linearized equations for acoustic gravity disturbances in a wind and temperature stratified atmosphere.

$$(9d) \quad \frac{d}{dz} \begin{bmatrix} \tilde{\rho} \\ \bar{\rho}\tilde{w} \end{bmatrix} = \begin{bmatrix} -g/c^2 & i(\Omega - \frac{g}{\Omega\bar{\rho}}(\frac{l}{c^2}\bar{p}_z - \bar{p}_z)) \\ i(\frac{\Omega}{c^2} - \frac{k^2+l^2}{\Omega}) & -\frac{k}{\Omega}\bar{u}_z - \frac{l}{\bar{\rho}}(\frac{l}{c^2}\bar{p}_z - \bar{p}_z) \end{bmatrix} \begin{bmatrix} \tilde{\rho} \\ \bar{\rho}\tilde{w} \end{bmatrix}$$

(9e)

It is useful to put equations (9d) and (9e) into a form where the matrix of coefficients has the following properties:

- 1) it contains no z derivatives
- 2) it is constant in a constant temperature constant wind velocity region;
- 3) it contains no complex numbers, and its trace is zero.

Then the solutions will have the following properties:

- 1) continuous functions of z ; even if wind and temperature are discontinuous at layer boundaries
- 2) sinusoidal or exponential in a constant temperature constant wind region.

To facilitate manipulating these equations, we freely use two transforms described in Appendix A.

First we apply the weighting transform with g^{-1} on the first variable and $-i$ on the second variable. Here we assume g is independent of altitude and define $V_p = \frac{\Omega}{k}$

$$(10) \quad \frac{d}{dz} \begin{bmatrix} \tilde{P}/g \\ \bar{\rho} \tilde{W} / i \end{bmatrix} = \begin{bmatrix} -g/c^2 & -\frac{\Omega}{g} + \frac{1}{\Omega} \left(-\frac{g}{c^2} - \frac{\bar{\rho}_z}{\bar{\rho}} \right) \\ g \left(\frac{\Omega}{c^2} - \frac{\Omega}{V_p^2} \right) & \frac{\Omega_z}{\Omega} + \frac{g}{c^2} + \frac{\bar{\rho}_z}{\bar{\rho}} \end{bmatrix} \begin{bmatrix} \tilde{P}/g \\ \bar{\rho} \tilde{W} / i \end{bmatrix}$$

Apply Ω^{-1} on second variable

$$(11) \quad \left[\frac{d}{dz} - \begin{bmatrix} -g/c^2 & -\frac{\Omega^2}{g} - \frac{g}{c^2} - \frac{\bar{\rho}_z}{\bar{\rho}} \\ g \left(\frac{1}{c^2} - \frac{1}{V_p^2} \right) & \frac{g}{c^2} + \frac{\bar{\rho}_z}{\bar{\rho}} \end{bmatrix} \right] \begin{bmatrix} \tilde{P}/g \\ \bar{\rho} \tilde{W} / i \Omega \end{bmatrix}$$

Do the addition transformation on the first variable

$$(12) \quad \left[\frac{d}{dz} - \begin{bmatrix} -g/V_p^2 & -\frac{\Omega^2}{g} + \frac{g}{V_p^2} \\ g\left(\frac{1}{c^2} - \frac{1}{V_p^2}\right) & \frac{\bar{\rho}_z}{\bar{\rho}} + \frac{g}{V_p^2} \end{bmatrix} \right] \begin{bmatrix} \frac{\tilde{P}}{g} + \frac{\bar{\rho}\tilde{W}}{i\Omega} \\ \frac{\bar{\rho}\tilde{W}}{i\Omega} \end{bmatrix}$$

Now on the second variable use the weight W

$$W = \bar{P}/\bar{\rho} = \frac{c^2}{\gamma} ; \quad \frac{W_z}{W} = \frac{\bar{P}_z}{\bar{P}} - \frac{\bar{\rho}_z}{\bar{\rho}} = \frac{\gamma g}{c^2} - \frac{\bar{\rho}_z}{\bar{\rho}}$$

$$(13) \quad \left[\frac{d}{dz} - \begin{bmatrix} -g/V_p^2 & \frac{\gamma}{c^2}\left(-\frac{\Omega^2}{g} + \frac{g}{V_p^2}\right) \\ \frac{c^2 g}{\gamma}\left(\frac{1}{c^2} - \frac{1}{V_p^2}\right) & g\left(-\frac{\gamma}{c^2} + \frac{1}{V_p^2}\right) \end{bmatrix} \right] \begin{bmatrix} \frac{\tilde{P}}{g} + \frac{\bar{\rho}\tilde{W}}{i\Omega} \\ \frac{\bar{\rho}\tilde{W}}{i\Omega} \end{bmatrix}$$

Finally apply the weight $w = \bar{P}^{-1/2}$; $\frac{w_z}{w} = \frac{\gamma g}{2c^2}$ to both variables and g/γ to the first variable

$$(14) \quad \left[\frac{d}{dz} - \begin{bmatrix} g\left(\frac{\gamma}{2c^2} - \frac{k^2}{\Omega^2}\right) & -\frac{\Omega^2}{c^2} + \frac{g^2 k^2}{c^2 \Omega^2} \\ \left(1 - c^2 \frac{k^2}{\Omega^2}\right) & -g\left(\frac{\gamma}{2c^2} - \frac{k^2}{\Omega^2}\right) \end{bmatrix} \right] \begin{bmatrix} \bar{P}^{-1/2} \left(\frac{\tilde{P}}{g} + \frac{\bar{\rho}\tilde{W}}{i\Omega} \right) \\ \bar{P}^{-1/2} \frac{\tilde{W}}{i\Omega} \end{bmatrix}$$

which is the "polished" form of the equations. These

equations were derived in a different way by Pierce (1966).

The following algebraic deduction shows how the first field variable is related to the divergence of velocity:

$$\nabla \cdot \vec{V} = ik \tilde{u} + il \tilde{v} + \frac{d\tilde{w}}{dz}$$

Use (8e)

$$= i(k\tilde{u} + l\tilde{v}) + \frac{1}{\bar{\rho}} [i\Omega \tilde{\rho} - i\bar{\rho}(k\tilde{u} + l\tilde{v})] - \tilde{w} \frac{d\bar{\rho}}{dz}$$

Use (8a)

$$= \frac{1}{\bar{\rho}} \left\{ i\Omega \left[\frac{\tilde{p}}{c^2} + \frac{i}{\Omega} \left(\frac{\bar{p}_z}{c^2} - \bar{\rho}_z \right) \tilde{w} \right] - \tilde{w} \bar{\rho}_z \right\}$$

$$= \frac{i\Omega}{\bar{\rho} c^2} \tilde{p} + \frac{g}{c^2} \tilde{w}$$

$$= \frac{i\Omega}{\bar{\rho}^{1/2}} \left[\frac{1}{\delta \bar{\rho}^{1/2}} \left(\tilde{p} + \frac{g\bar{\rho}\tilde{w}}{i\Omega} \right) \right]$$

$$= \frac{i\Omega}{\bar{\rho}^{1/2}} \quad \gamma_1$$

$$(15) \quad \gamma_1 = \frac{\bar{\rho}^{1/2}}{i\Omega} \nabla \cdot \vec{V}$$

The procedure of deriving (14) from (9) was orig-

inally a difficult one, and the presentation of a sequence of unmotivated algebraic steps seemed impossible to avoid. It would be valuable to know just how broad a class of problems can be reduced to a polished form by the weighting and addition transformations and to know if the reduction can proceed in a systematic way. This might be in the literature on Lyapunov transformations but a cursory investigation has failed to find it. For example, it would be nice to know if a polished form is possible for a layer of constant Brunt frequency. If so, extremely realistic atmospheric models would be constructed with very few layers.

In summary, in this section we have deduced equation (14) from fundamentals. This equation can be integrated to produce the state of the media at one position given the state at another. It shows that the variables $\Omega^{-1} \nabla \cdot \tilde{\mathbf{v}}$ and $\frac{\tilde{w}}{\Omega}$ are continuous functions of height even though the temperature and wind may be discontinuous.

Since one expects the vertical velocity to be continuous at layer boundaries why is it that \tilde{w}/Ω is continuous rather than \tilde{w} ? Consider a point where the boundary is deformed to a sine wave with wind on one side and not the other. At the zero crossing of the sine wave the particles on the windless side may have no vertical velocity, but by virtue of the wind, particles

on the other side are sliding up or down the sine wave on its steepest slope. An observer moving along with the particles interprets $\frac{\tilde{W}}{-i\Omega}$ as the amplitude of the deformed boundary and that is why it must be the same to observers on either side of the boundary.

One also expects the total pressure to be continuous at the deformed boundary. The wave pressure is augmented by a pressure due to the deformation of the boundary. Thus the total pressure

$$\tilde{p} + \frac{d\bar{P}}{dz} \delta z = \tilde{p} + (-\rho g) \frac{\tilde{W}}{-i\Omega} = \tilde{p} + \frac{\rho g \tilde{W}}{i\Omega}$$

is continuous as equation (14) shows.

In the next sections we use equation (14) to study the transport of energy and momentum by acoustic gravity waves.

I-A-2 Energy and Momentum Principles

In this section we will derive formulas for energy density, momentum density, and transport of these densities in a stratified medium. In the simplest type of wave propagation the phase velocity and the group or energy velocity have the same direction and speed. Bringing in gravity causes these velocities to differ in both direction and speed. Bringing in a stratified wind causes further complication because the energy in a wave packet is not conserved as the packet propagates from one altitude to another. In a media at rest $\frac{1}{4} \text{Re} \tilde{P} \tilde{W}^*$ is identified as the vertical energy flux. If $\frac{1}{4} \text{Re} \tilde{P} \tilde{W}^*$ does not vanish at a boundary of the system, it represents the power flowing into the system at the boundary. We will subsequently show that $\text{Re} \frac{\tilde{P} \tilde{W}^*}{\Omega}$ is altitude invariant in a region of no sources. Hence, the quantity $\text{Re} \tilde{P} \tilde{W}^*$ is not constant in a windy medium where Ω is z-dependent. Since $\frac{1}{4} \text{Re} \tilde{P} \tilde{W}^*$ represents the amount of power which may be absorbed by a viscous absorber, it is clear that an observer at some altitude seeing a wave can have no idea how much power it took to generate the wave unless he knows the ratio of his translation speed to the source's translation speed.

The situation is not so strange as it may seem. Consider an observer riding on a flat car in a railroad

switching yard full of flatcars. If he sees a snowball flying over his flatcar he cannot tell how much energy went into launching the snowball unless he knows the relative velocity of the flatcar from which it was launched. If a steady state were set up by continuous snowball-throwing, there is one thing all flatcar observers would agree on and that is the momentum flux or mass current perpendicular to the tracks.

In our acoustic-gravity wave problem the constancy in z of $\text{Re} \frac{\tilde{p}\tilde{w}^*}{\Omega}$ can also be interpreted as a current, not a current of energy or mass but as related to a vertical current of horizontal momentum. This will be interpreted more fully after we verify that $\text{Re} \frac{\tilde{p}\tilde{w}^*}{\Omega}$ is indeed altitude invariant.

Take equation (I-A-9)

(1)

$$\frac{d}{dz} \begin{bmatrix} \tilde{p} \\ \tilde{p}\tilde{w} \end{bmatrix} = \begin{bmatrix} -g/c^2 & i\left(\Omega - \frac{g}{\Omega\bar{\rho}}\left(\frac{\bar{p}_z}{c^2} - \bar{\rho}_z\right)\right) \\ i\left(\frac{\Omega}{c^2} - \frac{k \cdot k}{\Omega}\right) & -\frac{\Omega_z}{\Omega} - \frac{1}{\bar{\rho}}\left(\frac{\bar{p}_z}{c^2} - \bar{\rho}_z\right) \end{bmatrix} \begin{bmatrix} \tilde{p} \\ \tilde{p}\tilde{w} \end{bmatrix}$$

Introducing the definition of Brunt frequency ω_b

(2)

$$\omega_b^2 = \frac{g}{\bar{\rho}} \left(\frac{1}{c^2} \bar{p}_z - \bar{\rho}_z \right)$$

and recalling the equilibrium equation $\bar{p}_z = -\bar{\rho}g$
and utilizing transformations in Appendix A we get

$$(3) \quad \frac{d}{dz} \begin{bmatrix} \tilde{p} \\ \frac{\tilde{w}}{-i\Omega} \end{bmatrix} = \begin{bmatrix} -g/c^2 & \bar{\rho}(\Omega^2 - \omega_b^2) \\ \frac{1}{\bar{\rho}} \left(-\frac{1}{c^2} + \frac{k^2}{\Omega^2} \right) & +g/c^2 \end{bmatrix} \begin{bmatrix} \tilde{p} \\ \frac{\tilde{w}}{-i\Omega} \end{bmatrix}$$

We abbreviate this

$$(4) \quad \frac{d}{dz} \begin{bmatrix} X_1 \\ X_2 \end{bmatrix} = \begin{bmatrix} A_{11} & A_{12} \\ A_{21} & -A_{11} \end{bmatrix} \begin{bmatrix} X_1 \\ X_2 \end{bmatrix}$$

Now we can get an equation for $X_1 X_2^*$ as follows

$$\begin{aligned} \frac{d}{dz} (X_1 X_2^*) &= \frac{dX_1}{dz} X_2^* + X_1 \frac{dX_2^*}{dz} \\ &= (A_{11} X_1 + A_{12} X_2) X_2^* + X_1 (A_{21} X_1 - A_{11} X_2)^* \end{aligned}$$

$$(5) \quad = A_{21}^* X_1 X_1^* + A_{12} X_2 X_2^*$$

$$(6) \quad \frac{d}{dz} \frac{\tilde{p} \tilde{w}^*}{i\Omega^*} = \frac{1}{\bar{\rho}} \left(-\frac{1}{c^2} + \left(\frac{k^2}{\Omega^2} \right)^* \right) \tilde{p} \tilde{p}^* + \bar{\rho} (\Omega^2 - \omega_b^2) \frac{\tilde{w} \tilde{w}^*}{\Omega \Omega^*}$$

This we may split into real and imaginary parts

$$(7) \quad \frac{d}{dz} \Im_m \frac{\tilde{p} \tilde{w}^*}{\Omega} = \frac{1}{\bar{\rho}} \left(-\frac{1}{c^2} + \Re \frac{k^2}{\Omega^2} \right) \tilde{p} \tilde{p}^* + \bar{\rho} (\Re \Omega^2 - \omega_b^2) \frac{\tilde{w} \tilde{w}^*}{\Omega \Omega^*}$$

$$(8) \quad \frac{d}{dz} \left(-\text{Re} \frac{\tilde{P}\tilde{W}^*}{\Omega^*} \right) = -\frac{1}{\bar{\rho}} \left(\text{Im} \left(\frac{k^2}{\Omega^2} \right)^* \right) \tilde{P}\tilde{P}^* + \bar{\rho} \left(\text{Im} \Omega^2 \right) \frac{\tilde{W}\tilde{W}^*}{\Omega\Omega^*}$$

Equation (8) shows that in a source free region in the steady state (ω, k real) that $\text{Re} \frac{\tilde{P}\tilde{W}^*}{\Omega}$ is constant, independent of z we can define a current F by the formula

$$(9) \quad F = \frac{k}{\pi} \text{Re} \frac{\tilde{P}\tilde{W}^*}{\Omega}$$

where F has the dimensions of momentum density per unit volume times velocity. Having also physical dimensions of force per unit area it is a stress. Without the π it is called the Reynolds stress.

We will now show that F is the time rate of momentum lost by a uniform wind blowing over a unit area of a perfectly rigid sinusoidally undulating ground. The situation is depicted in figure 1.

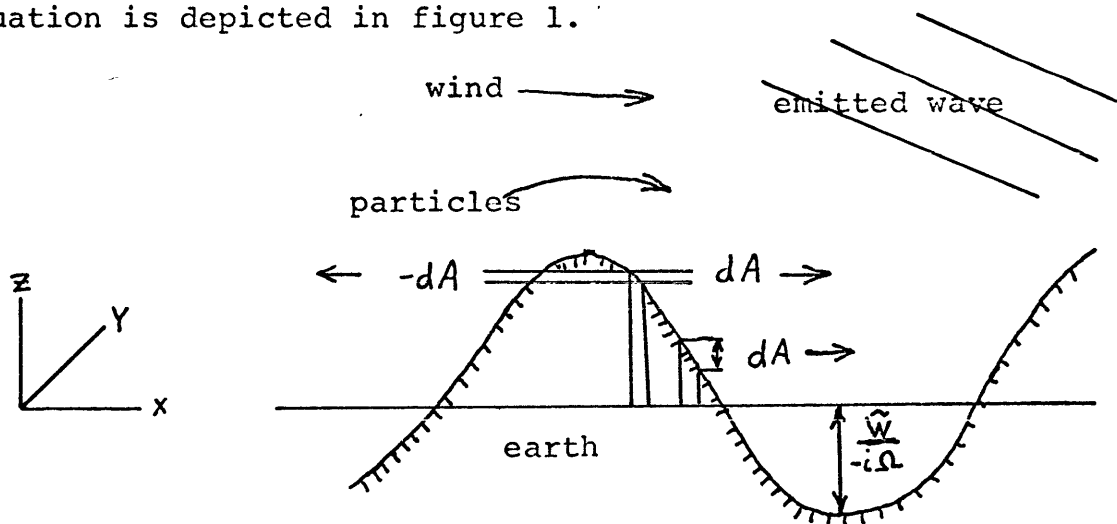


Figure 1

The lost momentum is accounted for by the radiation to infinity of an acoustic-gravity wave. If the atmosphere is topped by a rigid boundary of if frequencies and velocities are such that the disturbance is evanescent then investigation whows that F vanishes by virtue of \tilde{p} and \tilde{w} being out of phase. The force acting on the ground in the horizontal direction is proportional to the pressure times the effective area. The amount of area for the force to act on in the horizontal direction is proportional to the amplitude of the ground displacement. Both pressure and area are sinusoidal functions of x . A negative pressure acting on a negative area gives a force in the same horizontal direction as a positive force on a positive area. In $1/4$ wavelength along x the area is $\frac{\tilde{w}}{\Omega} dy$. Thus the area per unit length on the x -axis is $\text{Re}(dA)$ where

$$dA = \frac{4}{\lambda_x} \frac{\tilde{w}}{\Omega} e^{ikx} dy$$

The integral of the pressure times the effective area over one wavelength along the x -axis is the force.

$$\text{Force} = \int_0^{\lambda_x} (\text{Re } \tilde{p})(\text{Re } dA) dx = \frac{4}{2} \text{Re} \frac{\tilde{p}\tilde{w}^*}{\Omega} dy$$

Hence the shearing force per unit area acting on the ground is

$$F = \text{Force/area} = \frac{2}{\lambda_x} \text{Re} \frac{\tilde{p}\tilde{w}^*}{\Omega} = \frac{k}{\pi} \text{Re} \frac{\tilde{p}\tilde{w}^*}{\Omega}$$

The momentum density M of the waves may be defined by its continuity equation.

$$(10) \quad 0 = \frac{\partial M}{\partial t} + \text{div } F = 0$$

Taking k real, this becomes

$$(11) \quad 0 = \frac{\partial M}{\partial t} + \frac{d}{dz} \left(\frac{k}{\pi} \text{Re} \frac{\tilde{P}\tilde{W}^*}{\Omega^*} \right)$$

In the case where ω is real we have already shown the right hand term to be zero. Generalizing to complex ω $\omega = \omega_r + i\omega_i$; we will be able to define $\frac{\partial M}{\partial t}$. Since M is a quadratic function of field variables and either of the field variables is

$$(12) \quad \varphi = \varphi(z) e^{ikx - i\omega_r t} e^{\omega_i t}$$

then

$$\varphi\varphi^* = \varphi(z)\varphi^*(z) e^{2\omega_i t}$$

and

$$\frac{\partial}{\partial t} \varphi\varphi^* = 2\omega_i \varphi\varphi^*$$

So we may substitute $\frac{\partial}{\partial t} M = 2\omega_i M$ into (11) and also bring (8) into (11) getting

$$(13) \quad 2\omega_i M = \frac{k}{\pi} \left\{ \frac{1}{\bar{\rho}} \left(\partial_m \frac{k^2}{\Omega^2} \right) \tilde{P}\tilde{P}^* + \bar{\rho} \left(\partial_m \Omega^2 \right) \frac{\tilde{W}\tilde{W}^*}{\Omega\Omega^*} \right\}$$

Take $\Omega = \Omega_r + i\omega_i$ to be complex, but keep k real. Thus we are considering a time transient problem with sources and sinks to be of infinite extent in x and y . For algebraic simplicity take $|\omega_i| \ll |\Omega_r|$. Then

(13) gives the momentum density as

$$(14) \quad M = \frac{k}{\pi\Omega_r} \left\{ \frac{1}{\bar{\rho}} \frac{k^2}{\Omega_r^2} \tilde{P}\tilde{P}^* + \bar{\rho} \tilde{W}\tilde{W}^* \right\}$$

Now using the momentum continuity equation (10) and the knowledge that the energy current is $1/4 \operatorname{Re} \tilde{P}\tilde{W}$ we will derive a continuity equation for energy density and it shows how gradients of the mean flow can amplify waves going through them. Expand out equation (11)

$$\begin{aligned} 0 &= \frac{\partial M}{\partial t} + \frac{d}{dz} \operatorname{Re} \frac{k}{\pi} \frac{\tilde{P}\tilde{W}^*}{\Omega^*} \\ &= \frac{\partial}{\partial t} \left(\frac{\pi}{k} M \right) + \frac{d}{dz} \left[\frac{(\operatorname{Re} \tilde{P}\tilde{W}^*)(\operatorname{Re} \Omega)}{\Omega\Omega^*} - \omega_i \operatorname{Im} \frac{\tilde{P}\tilde{W}^*}{\Omega\Omega^*} \right] \end{aligned}$$

Again use $\omega_i \ll \Omega_r$ so $\Omega\Omega^* = \Omega_r^2$.

$$(15) \quad 0 = \frac{\partial}{\partial t} \left(\frac{\pi}{k} M \right) - \frac{d\Omega_r}{dz} \operatorname{Re} \tilde{P}\tilde{W}^* + \frac{1}{\Omega_r} \frac{d}{dz} \operatorname{Re} \tilde{P}\tilde{W}^* - \omega_i \frac{d}{dz} \left[\operatorname{Im} \frac{\tilde{P}\tilde{W}^*}{\Omega_r^2} \right]$$

Multiply by $\frac{\Omega_r}{2}$ and identify $2\omega_i$ with $\frac{\partial}{\partial t}$

$$(16) \quad 0 = \frac{\partial}{\partial t} \frac{1}{2} \left[\frac{\pi\Omega_r M}{k} - \frac{\Omega_r}{2} \frac{d}{dz} \left(\operatorname{Im} \tilde{P}\tilde{W}^* \right) \right] + \frac{k}{2} \frac{d\bar{u}}{dz} \operatorname{Re} \frac{\tilde{P}\tilde{W}^*}{\Omega_r} + \frac{d}{dz} \frac{1}{2} \operatorname{Re} \tilde{P}\tilde{W}^*$$

We identify the rightmost term with the divergence of energy flux. The center term is wave amplification due to the flux of wave momentum across the mean wind shear. The leftmost term is the time derivative of the energy density E and we next examine it further.

$$(17) \quad 2E = \frac{\pi \Omega_r}{k} M - \frac{\Omega_r}{2} \frac{d}{dz} \int_m \frac{\tilde{p} \tilde{w}^*}{\Omega_r^2}$$

$$= \frac{\pi \Omega_r}{k} M - \frac{1}{2} \frac{d}{dz} \int_m \frac{\tilde{p} \tilde{w}^*}{\Omega_r} + \frac{d \Omega_r}{2 dz} \int_m \frac{\tilde{p} \tilde{w}^*}{\Omega_r}$$

Now let ω be real and substitute (14) into the first term and (7) into the second

$$2E = \left[\frac{1}{\bar{\rho}} \left(\frac{k}{\Omega} \right)^2 \tilde{p} \tilde{p}^* + \bar{\rho} \tilde{w} \tilde{w}^* \right] - \frac{1}{2} \left[\frac{1}{\bar{\rho}} \left(-\frac{1}{c^2} + \frac{k^2}{\Omega^2} \right) \tilde{p} \tilde{p}^* + \bar{\rho} (\Omega^2 - \omega_b^2) \frac{\tilde{w} \tilde{w}^*}{\Omega^2} \right] + \frac{\Omega_r}{2 \Omega} \int_m \frac{\tilde{p} \tilde{w}^*}{\Omega}$$

$$(18) \quad E = \frac{1}{4} \left\{ \frac{1}{\bar{\rho}} \left(\frac{k}{\Omega} \right)^2 \tilde{p} \tilde{p}^* + \bar{\rho} \left(1 + \frac{\omega_b^2}{\Omega^2} \right) \tilde{w} \tilde{w}^* - \frac{d \bar{u}}{dz} \frac{k}{2 \Omega} \int_m \frac{\tilde{p} \tilde{w}^*}{\Omega} \right\}$$

A 1/4 scale appears instead of a 1/2 because \tilde{p} and \tilde{w} are the peak, not the R.M.S. amplitudes of the sinusoidal time dependence. Now we have derived expressions for momentum density (formula 14) and energy density (formula 18) in terms of the two complex variables \tilde{p} and \tilde{w} . The media could also be described at a point by giving two independent complex variables representing upgoing and downgoing wave solutions. It could be described by giving four real quantities, say pressure, density and two components of velocity. By means of the equations of motion any of these descrip-

tions can be derived from the others so they are mathematically equivalent. Some choices give a more intuitive feel for the situation than others. For example take the horizontal component of Newton's equation

$$(I-A-7b) \quad \bar{\rho} (-i\Omega \tilde{u} + \bar{u}_z \tilde{W}) = -ik \tilde{P}$$

$$\bar{\rho} \left(\tilde{u} + \bar{u}_z \frac{\tilde{W}}{-i\Omega} \right) = \frac{k}{\Omega} \tilde{P}$$

$$\bar{\rho} \left(\tilde{u} + \frac{d\bar{u}}{dz} \delta z \right) = \frac{k}{\Omega} \tilde{P}$$

$$(19) \quad \bar{\rho} \tilde{u}_p = \frac{k}{\Omega} \tilde{P}$$

and use it as a substitution to eliminate \tilde{P} from (14)

$$(20) \quad M = \frac{k}{\pi\Omega} \bar{\rho} \left(\tilde{u}_p \tilde{u}_p^* + \tilde{W} \tilde{W}^* \right)$$

Equation (20) may be interpreted as

$$(20a) \quad \text{horiz momentum density} \sim \frac{\text{(kinetic energy density)}}{\text{(horiz ambient phase vel)}}$$

Likewise introducing the horizontal component of Newton's equation (19) into the momentum flux definition (9) we get

$$(21) \quad F = \frac{k}{\pi} \text{Re} \frac{\tilde{P} \tilde{W}^*}{\Omega} = \frac{\bar{\rho}}{\pi} \text{Re} \tilde{u}_p \tilde{W}^*$$

In this form it is easier to understand that it represents the vertical flow of horizontal momentum. With formulas (20) and (21) conservation of momentum density (11) becomes

(22)

$$0 = \frac{\partial}{\partial t} \left[\frac{k}{\Omega} \bar{\rho} (\tilde{u}_p \tilde{u}_p^* + \tilde{w} \tilde{w}^*) \right] + \frac{d}{dz} (\bar{\rho} \operatorname{Re} \tilde{u}_p \tilde{w}^*)$$

Likewise introducing the horizontal component of Newton's equation (19) into the energy density (18) we get

$$(23) \quad 4E = \bar{\rho} (\tilde{u}_p \tilde{u}_p^* + \tilde{w} \tilde{w}^*) + \frac{\tilde{p} \tilde{p}^*}{\bar{\rho} c^2} + \bar{\rho} \omega_b^2 \left(\frac{w}{i\Omega} \right) \left(\frac{w}{-i\Omega} \right)^* - \frac{d\bar{u}}{dz} \frac{k}{\Omega} \int_{-\infty}^{\infty} \frac{\tilde{p} \tilde{w}^*}{\Omega}$$

The first term is clearly the kinetic energy of a parcel. The second term is the potential energy of adiabatic compression. In the third term the factor $\rho \omega_b^2$ is like a spring constant and the factor $\left(\frac{w}{-i\Omega} \right) = \delta z$ is the vertical displacement. Gravity appears explicitly when the definition of ω_b^2 is substituted giving

$$g \left(\frac{1}{c^2} \frac{d\bar{p}}{dz} - \frac{d\bar{\rho}}{dz} \right) (\delta z)^2 = \text{gravitational adiabatic compression energy} + \text{density stratification perturbation energy}$$

The fourth term in (23) is an interaction energy between the wave and the wind shear. Consider a wind layer; when its boundaries are distorted into sinusoids the centri-

fugal force inside the layer does work against the boundaries as the sinusoidal amplitude increases. Thus the bigger the wave the more energy has been put into it by the mean flow. This is quite the reverse of the usual effect of the density stratification where the wave acts to increase the potential energy in the mean stratification. We will next see that the fourth term acts to give the wave a negative energy density.

The possibility of a negative wave energy density arises not just from the wind shear term. It could also come from the gravitational term if the density were stratified with the (potentially) heaviest air on top. A precise condition for the positiveness of the energy quadratic comes by writing (18) in matrix form

$$(24) \quad E = \frac{1}{4} \begin{bmatrix} \tilde{p} & \tilde{w} \end{bmatrix}^* \begin{bmatrix} \frac{1}{\bar{\rho}} \left(\frac{1}{c^2} + \frac{k^2}{\Omega^2} \right) & -\frac{i}{2} \frac{d\bar{u}}{dz} \frac{k}{\Omega^2} \\ +\frac{i}{2} \frac{d\bar{u}}{dz} \frac{k}{\Omega^2} & \bar{\rho} \left(1 + \frac{\omega_b^2}{\Omega^2} \right) \end{bmatrix} \begin{bmatrix} \tilde{p} \\ \tilde{w} \end{bmatrix}$$

The Hermitian matrix is positive definite if its trace and determinant are positive. Thus for positive energy we must have

$$0 < \frac{1}{\bar{\rho}} \left(\frac{1}{c^2} + \frac{k^2}{\Omega^2} \right) + \bar{\rho} \left(1 + \frac{\omega_b^2}{\Omega^2} \right)$$

$$0 < \frac{\Omega^4}{k^2} \left\{ \left(\frac{\Omega^2}{c^2 k^2} + 1 \right) \left(\Omega^2 + \omega_b^2 \right) - \frac{1}{4} \left(\frac{d\bar{u}}{dz} \right)^2 \right\}$$

The first inequality is satisfied if the atmosphere has a stable temperature stratification. The second inequality may be violated in strong wind shears. This gives rise to dynamic instability described in the next section.

Somewhat different developments by Bretherton (1966) and Elaissen and Palm (1960) have not included the term which is negative in the presence of wind shear.

In summary, we have begun with the equation of motion and found a quadratic scalar function of the state variables which for the steady state is altitude invariant in a source free region. This quadratic function represents the momentum lost per unit area per second of a wind blowing over a sinusoidally undulating ground. Therefore we identified this quadratic as a vertical current of momentum. With frequency complex this current has a divergence which we equate to the time rate of change of a density which we call the momentum density. With this continuity equation plus the definition of energy flux we derived another continuity equation we called the continuity of energy equation. On solving for the energy it was found to contain the familiar terms of acoustics plus new terms due to density and wind stratification. If the new terms had not been so unfamiliar it might have been preferable to begin the discussion with the energy density definition and to have worked back to the energy and momentum continuity equations. Finally we noted that

negative energy densities may arise and that this is associated with instability of ambient state of the atmosphere.

I-A-3 The Instability of Waves Interacting
with High Altitude Winds

Coupling is frequently observed between two phenomena which move at the same speed. Here we will study what happens to acoustic gravity waves propagating at a velocity which equals that of the wind. Since the wind velocity is generally a continuously changing function of height one is concerned with a discrete set of points called critical heights where the wind speed equals the horizontal component of the wave speed. Of particular interest in the real atmosphere are the jet stream winds. Their speed frequently exceeds 20% of the speed of sound. The first thing to notice about a critical height z_c is that an observer moving with the wind at the critical height sees the frequency of the disturbance doppler shifted to zero. In the precise treatment the doppler frequency $\Omega = \omega - ku$ occurs as a divisor which leads to some mathematical complexity. An idea of what happens to the wave may be gotten by seeing what happens in a wind-free, isothermal medium when the frequency is lowered keeping the horizontal wavelength fixed. The phase velocity becomes vertical, the group velocity and particle motions become horizontal, and the vertical wavelength becomes very small. The progress of a wave packet emitted from the ground heading toward the critical height is depicted below in figure 1.

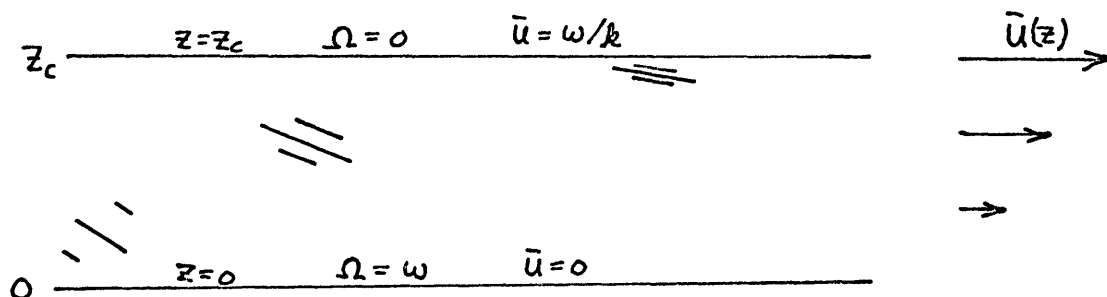


Figure 1

If there is a continuing source on the ground the momentum density of the wave builds up to infinity at the critical height. Also very large shears develop in the wave itself.

In the solutions we will develop for the vicinity of the critical height we can see the effect of increasing the wind shear. Above a certain critical shear the solutions blows up catastrophically. Looking back to the solution in a stable wind shear we recall that the shear in the wave itself blows up at z_c . Thus, any real wave of finite amplitude at the ground creates the conditions for instability at some point below z_c .

An attempt to give an intuitive idea of this so-called Richardson instability goes as follows:

Gravity will tend to stabilize the atmosphere with the densest layer on the bottom. However, if the bottom layer has a lot of kinetic energy in the form of wind, there is no energetic reason why it could not move up to replace a less dense layer losing some of its wind energy

to do it. Perturbation on the stratified wind flow may tend to grow with time just like kinks in a water hose tend to grow because of the centrifugal force on the water. Stability will be assured only if the gravitational energy of some perturbed state is greater than the wind kinetic energy available for the perturbation. Specifically let two altitudes in a wind stratified incompressible fluid be separated by a distance dz have a horizontal velocity difference du and a density difference $d\rho$. Then the stability condition is

Kinetic energy < potential energy

$$\begin{aligned} \frac{1}{2} \rho (du)^2 &< g (d\rho) (dz) \\ \frac{1}{2} \rho \left(\frac{du}{dz} dz \right)^2 &< g \left(\frac{d\rho}{dz} dz \right) dz \\ \frac{1}{2} \left(\frac{du}{dz} \right)^2 &< \frac{g}{\rho} \frac{d\rho}{dz} \end{aligned}$$

The right hand side is the square of the Brunt frequency of an incompressible fluid (formula I-A-2.2) and the inequality is within a factor of 2 of the Richardson stability criterion.

We begin the analytical deduction with formula

(I-A-1.9)

$$\frac{d}{dz} \begin{bmatrix} \tilde{p} \\ \bar{\rho} \tilde{w} \end{bmatrix} = \begin{bmatrix} -g/c^2 & i \left(\Omega - \frac{g}{\bar{\rho}} \left(\frac{\bar{p}_z}{c^2} - \bar{\rho}_z \right) \right) \\ i \left(\frac{\Omega}{c^2} - \frac{h^2}{\Omega} \right) & -\frac{h}{\Omega} \bar{u}_z - \frac{1}{\bar{\rho}} \left(\frac{\bar{p}_z}{c^2} - \bar{\rho}_z \right) \end{bmatrix} \begin{bmatrix} \tilde{p} \\ \bar{\rho} \tilde{w} \end{bmatrix}$$

In the vicinity of $\Omega = 0$ we may drop all terms without Ω in the denominator.

$$(1) \quad \frac{d}{dz} \begin{bmatrix} \tilde{p} \\ \frac{\tilde{\rho} \tilde{w}}{i} \end{bmatrix} = \frac{1}{\Omega} \begin{bmatrix} 0 & \frac{g}{\bar{\rho}} \left(\frac{\bar{p}_z}{c^2} - \bar{\rho} \right) \\ -k^2 & -k \bar{u}_z \end{bmatrix} \begin{bmatrix} \tilde{p} \\ \frac{\tilde{\rho} \tilde{w}}{i} \end{bmatrix}$$

Now it is convenient to introduce the definition of the Brunt frequency ω_b .

$$(2) \quad \omega_b^2 = \frac{g}{\bar{\rho}} \left(\frac{\bar{p}_z}{c^2} - \bar{\rho}_z \right) \cong \frac{g}{T} \left(\frac{\partial T}{\partial z} + 9.5 \text{ } ^\circ\text{C/km} \right)$$

If we take the wind profile to be a linear function

$$u(z) = u_0 + u_1 z \quad \text{of altitude near the singularity,}$$

then we have

$$(3) \quad \frac{1}{\Omega} = \frac{1}{\omega - k(u_0 + u_1 z)} = \frac{(-k u_1)^{-1}}{z - u_1^{-1}(\frac{\omega}{k} - u_0)} = \frac{(-k u_1)^{-1}}{z - z_c}$$

Substituting (2) and (3) into (1) gives

$$(4) \quad \frac{d}{dz} \begin{bmatrix} \tilde{p} \\ \frac{\tilde{\rho} \tilde{w}}{i} \end{bmatrix} = \frac{1}{z - z_c} \begin{bmatrix} 0 & -\omega_b^2 / k u_1 \\ k / u_1 & 1 \end{bmatrix} \begin{bmatrix} \tilde{p} \\ \frac{\tilde{\rho} \tilde{w}}{i} \end{bmatrix}$$

Taking ω_b constant near the singularity we can integrate (4) in the vicinity of z_c . Let the matrix of coefficients be temporarily denoted by A and the solution vector by x . Then (4) is written

$$(5) \quad (z - z_c) \frac{d}{dz} x = A x$$

Define a new independent variable y by $e^y = (1 - z/z_c)$

Then

$$\frac{dz}{dy} = -z_c e^y = -z_c (1 - z/z_c) = (z - z_c)$$

and

$$(z - z_c) \frac{d}{dz} = (z - z_c) \frac{dy}{dz} \frac{d}{dy} = \frac{d}{dy}$$

So (5) becomes

$$(6) \quad \frac{d}{dy} x = A x$$

This equation may be integrated to give the solution x_+ at a point y_+ from the solution x_- at y_- . Integration of (6) gives

$$(7) \quad x_+ = e^{A(y_+ - y_-)} x_- = \left[e^{A \ln \frac{z_c - z_+}{z_c - z_-}} \right] x_- = \mathbb{P} x_-$$

Let the matrix \mathbb{P} be expanded by Sylvester's theorem.

$$(8) \quad \mathbb{P} = \left[\text{adj}(A - \lambda_1 I) \right] e^{\lambda_1 \ln \frac{z_c - z_+}{z_c - z_-}} + \left[\text{adj}(A - \lambda_2 I) \right] e^{\lambda_2 \ln \frac{z_c - z_+}{z_c - z_-}}$$

Here "adj" represents matrix adjoint and λ_1 and λ_2 are the eigenvalues of A . The eigenvalues are the solution of

$$(9) \quad 0 = \det(A - \lambda I) = \det \begin{vmatrix} -\lambda & -\omega_b^2 / k u_1 \\ -k u_1 & 1 - \lambda \end{vmatrix}$$

$$(10) \quad 0 = \lambda^2 - \lambda - \omega_b^2 / u_1^2$$

$$(11) \quad \begin{aligned} \lambda &= 1/2 \pm \sqrt{1/4 - \omega_b^2 / u_1^2} \\ &= 1/2 \pm i\sqrt{R - 1/4} \\ &= 1/2 \pm i\mu \end{aligned}$$

The quantity R as we have seen earlier is called the Richardson number by meteorologists and is a measure of the dynamic stability of the atmosphere. It is usually greater than $1/4$ so we will take μ as real until later when we consider instability. The adjoint matrices in (8) are

$$(12) \quad \begin{bmatrix} -1/2 - i\mu & -\omega_b^2 / k u_1 \\ k / u_1 & 1/2 - i\mu \end{bmatrix}, \quad \begin{bmatrix} -1/2 + i\mu & -\omega_b^2 / k u_1 \\ k u_1 & 1/2 + i\mu \end{bmatrix}$$

The adjoints in (12) correspond to solutions of oppositely directed flux. This follows since the columns in the adjoints are proportional to $[\tilde{P}, \frac{\tilde{P}\tilde{W}}{i}]^T$ so $\text{Re} \frac{\tilde{P}\tilde{W}^*}{\Omega}$ is negative (downward) for the plus eigenvalue and positive (upward) for the minus eigenvalue. The momentum flux associated with each of these solutions was shown in the last section to be a constant. The analysis actually breaks down at any point where $\Omega = 0$ as may be seen by re-examining formula I-A-2.8 By means of (7) and (8) we

will attempt to carry the integration across the critical height. Take the upward going wave and look at the z_- dependent part of the momentum flux.

$$\operatorname{Re} \frac{1}{\Omega} \tilde{p} \tilde{w}^* \sim \frac{z_c - z_-}{z_c - z_+} \left| e^{(1/2 - i\mu) \ln \frac{z_c - z_+}{z_c - z_-}} \right|^2$$

As long as z_+ and z_- are on the same side of z_c the logarithm is real and the above quantity is a constant equal to unity. If z_- stays fixed but z_+ migrates to the other side of z_c the flux undergoes a jump at z_c . Evaluating it where $|z_+ - z_c| = |z_- - z_c|$ we get the amount of the jump.

$$\begin{aligned} \operatorname{Re} \frac{\tilde{p} \tilde{w}^*}{\Omega} &\sim (-1) \left| e^{(1/2 - i\mu) \ln(-1)} \right|^2 \\ &\sim - \left| (-1)^{1/2 - i\mu} \right|^2 \\ &\sim - \left| (e^{\pm i\pi})^{(1/2 - i\mu)} \right|^2 \\ &\sim - e^{\pm 2\pi\mu} \end{aligned}$$

The sign ambiguity has been resolved by Booker and Bretherton by consideration of an initial value problem. In it one takes ω hence z_c to be complex. Complex integration shows that the wave is attenuated by an amount $e^{-2\pi\mu}$ on traversal of the critical height.

Hines and Reddy did the problem from a slightly different point of view and got a different answer. In-

stead of integrating first ($dz \rightarrow 0$) and then letting the imaginary part of ω go to zero, they did it in reverse order. They took ω real and integrated in steps of width Δz . If the singular point is kept at a layer boundary it has no effect even as ($\Delta z \rightarrow 0$) and $\text{Re} \frac{\tilde{p}\tilde{w}^*}{\Omega}$ stays constant.

In any case, one may calculate that the time it takes to propagate a disturbance through z_c is infinity.

$$\begin{aligned} \text{time} &= \int_{z_-}^{z_+} \text{momentum density } dz / \text{momentum flux} \\ &\sim \int_{z_-}^{z_+} \frac{dz}{(z_c - z)^2} \quad / \text{const.} \\ &\sim \frac{1}{(z_+ - z_c)} \xrightarrow{z_+ \rightarrow z_c} \infty \end{aligned}$$

If one observes a continuing random disturbance on one side of a critical height and is to decide the amplitude of the disturbance on the other side of the critical height none of the above analyses are appropriate because of further complications. These complications have to do with non-linearity and instability which for real finite amplitudes arise before the disturbance gets to z_c .

Formulas (4) to (8) show that at $z = z_+$

$$(13) \quad \tilde{p} \sim \tilde{w} \sim e^{(1/2 \pm i\mu) \ln \left(\frac{z_c - z}{z_c - z_-} \right)} \sim (z_c - z)^{1/2}$$

Reference to the equations of motion shows that

$$(14) \quad \tilde{p} \sim \tilde{u} \sim (z_c - z)^{-1} e^{(1/2 + i\mu) \ln \frac{z_c - z}{z_c - z_0}} \sim (z_c - z)^{-1/2}$$

Differentiating gives

$$(15) \quad \tilde{u}_z = \frac{d\tilde{u}}{dz} \sim (z_c - z)^{-3/2}$$

The further complication is that (14) and (15) diverge at the critical height. For any realistic non-zero amplitude (14) implies we get into problems of non-linearity even before the critical height is reached. Formula (15) implies that the wind shear of the wave itself will become very large and violate the Richardson stability criterion before the critical height is reached. A numerical calculation in section III-D shows that for realistic parameters under the jet stream the stability criterion is violated before the non-linearity criterion.

This leads us to consider the Richardson number R in the dynamically unstable region $0 < R < 1/4$ or μ imaginary. From (13) we see that there is a solution of the form

$$\tilde{p} \sim \tilde{w} \sim (z_c - z)^{1/2 + \epsilon} \quad \epsilon > 0$$

This implies an altitude dependent vertical flux of horizontal momentum

$$\text{Re} \frac{\tilde{p}\tilde{w}}{\Omega} \sim (z_c - z)^{2\epsilon}$$

However formula (I-B-8) implies that this flux is altitude independent if ω is real. Thus ω must be complex.

I-B Gravity Wave Formulation with Ionization

In sections 1 and 2 we develop formulas for the motion of ions and electrons in a region of space where neutral molecules have a prescribed velocity and there is a prescribed electric field. This is done essentially by writing a vector force equation for both ions and electrons and inverting the 6×6 matrix. The use of a vector operator method enables one to treat the 6×6 matrix as a 2×2 matrix and solve for the exact inverse. This method contrasts with the usual derivations in that it remains algebraically simple even when numerical approximations among frequencies and mass ratios are not made.

In section 3 we consider various coordinate axes along which the trans-conductivity matrices can be expressed. The canonical set of coordinates have one vector along the magnetic field and the other two rotating around it in opposite directions. The algebra of a many ion problem is greatly simplified in the canonical coordinates where "cross-terms" never arise. When the ambient vector fields are at some oblique angle it is advantageous to select coordinates which are oblique and along the angles of the vector fields. We have chosen a set of oblique axes and made altitude profiles of the d.c. conductivity.

In section 4 we take as known the conductivities just derived and the acoustic-gravity wave solutions of chapter

I-A and develop formulas for the electromagnetic effects. The technique is similar to the technique used in section I-A. Solutions are assumed sinusoidal in time and lateral extent and an ordinary differential equation is derived from the physical laws. The equation is numerically integrated upward through the ionosphere and the application of boundary conditions determines the constants multiplying the homogeneous solutions. The particular solution is found by convoluting the homogeneous solutions with the sources. Sources for the calculation of currents and electric fields are the neutral acoustic-gravity motions and sources for the magnetic fields are the currents.

In section 5 we bring together all the equations mentioned into a large system and review some of the approximations inherent in the formulation. We discuss the full problem of simultaneous interaction between neutral and charged particles.

I-B-1 Continuity Equations

The conservation equations for ions and electrons of number densities n_i and n_e are

$$(1) \quad \frac{\partial}{\partial t} n_i + \nabla \cdot (n_i v_i) = Q_i$$

$$(2) \quad \frac{\partial}{\partial t} n_e + \nabla \cdot (n_e v_e) = Q_e$$

where Q_i and Q_e are ion and electron rates of production minus rates of recombination.

The equation of charge neutrality is

$$(3) \quad 0 = n_i e_i + n_e e_e$$

The equation of charge conservation is

$$(4) \quad Q_i e_i + Q_e e_e = 0$$

The definition of electrical current J is

$$(5) \quad J = n_i e_i v_i + n_e e_e v_e = n_i e_i (v_i - v_e)$$

The definition of negative or positive charge density q is

$$(6) \quad q = (n_i e_i - n_e e_e) / 2 = n_i e_i = -n_e e_e$$

Multiply (1) by e_i and (2) by e_e . Add to get (7), and subtract to get (8).

$$(7) \quad \frac{\partial}{\partial t} \rho + \nabla \cdot \mathbf{J} = 0$$

$$(8) \quad \frac{\partial}{\partial t} (2q) + \nabla \cdot (qV_i + qV_e) = 2Q_i e_i$$

Equation (7) is an approximation which neglects displacement currents. This approximation is dropped in section I-B-3 because it becomes inconsistent with Maxwell's equation which implicitly and exactly contain the law of conservation of charge.

Equation (8) suggests defining ionization drift rate D by

$$(9) \quad D = (V_i + V_e) / 2$$

The final equation for ionization production and transport is

$$(10) \quad \frac{\partial}{\partial t} q + \nabla \cdot (qD) = Q_i e_i$$

I-B-2 Momentum Equations, Conductivity of a
Moving Partially Ionized Gas

Let interger subscripts refer to species, that is, to ions, electrons, or neutrals. Scalars should be considered to be multiplied by a 3 x 3 identity matrix. The scalar definitions are: number density n , particle mass m , density ρ , charge e , excitation $e^{-i\omega t}$, collision frequency ν , and scattering efficiency α . Vector definitions are: velocity V , magnetic field B , electric field E , electric current J , pressure gradient ∇p . Individual components of a vector are referenced by the coordinate subscripts x , y , or z . We write the linearized momentum equations for a 3 specie interacting gas without external forces.

$$\begin{aligned}
 (1) \quad m_1 n_1 \dot{V}_1 &= n_1 n_2 \alpha_{12} (V_2 - V_1) + n_1 n_3 \alpha_{13} (V_3 - V_1) \\
 m_2 n_2 \dot{V}_2 &= n_2 n_1 \alpha_{21} (V_1 - V_2) + n_2 n_3 \alpha_{23} (V_3 - V_2) \\
 m_3 n_3 \dot{V}_3 &= n_3 n_1 \alpha_{31} (V_1 - V_3) + n_3 n_2 \alpha_{32} (V_2 - V_3)
 \end{aligned}$$

Conservation of momentum says the sum of the above equations is zero. The sum on the left side is evidently the time derivative of the total momentum of the gas, and the sum on the right side is

$$0 = n_1 n_2 (V_1 - V_2) (\alpha_{21} - \alpha_{12}) + n_1 n_3 (V_1 - V_3) (\alpha_{31} - \alpha_{13}) + n_2 n_3 (V_2 - V_3) (\alpha_{32} - \alpha_{23})$$

Since the velocities V_1 , V_2 , and V_3 may take on any orientation and magnitude, the velocity differences are independent, and we must have $\alpha_{ij} = \alpha_{ji}$. The result is the same as if we had considered only 2 species.

Now we add some hypothetical body forces to, for example, the first of (1)

$$m_1 n_1 \dot{V}_1 = n_1 n_2 \alpha_{12} (V_2 - V_1) + n_1 n_3 \alpha_{13} (V_3 - V_1) + e_1 n_1 (E - B \times V_1) - \nabla P$$

Divide by $m_1 n_1 = \rho_1$

$$(2) \quad 0 = \left(i\omega - \frac{n_2}{m_1} \alpha_{12} - \frac{n_3}{m_1} \alpha_{13} \right) V_1 + \frac{n_2}{m_1} \alpha_{12} V_2 + \frac{n_3}{m_1} \alpha_{13} V_3 + \frac{e_1}{m_1} (E - B \times V_1) - \frac{\nabla P}{\rho}$$

The form of equation (2) motivates some definitions.

Define collision frequencies by

$$(3) \quad \nu_{ij} = \alpha_{ij} n_j / m_i$$

and the gyro frequency by

$$(4) \quad \omega_i = e_i |B| / m_i$$

and let

$$(5) \quad U = \frac{1}{\sqrt{B \cdot B}} \begin{bmatrix} 0 & -B_z & B_y \\ B_z & 0 & -B_x \\ -B_y & B_x & 0 \end{bmatrix}$$

Notice that $U^3 = -U$; $U^2 \neq -I$

Define "diagonal collision frequencies" ν_{ij} by

$$(6) \quad i\omega = \sum_j \nu_{ij}$$

Utilizing these definitions formula (2) becomes

$$(7) \quad \nu_{11} V_1 + \nu_{12} V_2 + \nu_{13} V_3 + \omega_1 \left(\frac{E}{|B|} - U V_1 \right) - \frac{\nabla P}{\rho_1}$$

Now we particularize the discussion to ions, electrons, and neutrals having subscripts consecutively 1, 2, and 3. The set (1) with Maxwell forces on the ions and a pressure gradient on the neutrals becomes

$$(8) \quad \begin{bmatrix} -\frac{\omega_1 E}{|B|} \\ -\frac{\omega_2 E}{|B|} \\ \frac{\nabla P}{\rho_3} \end{bmatrix} = \begin{bmatrix} (\nu_{11} - \omega_1 U) & \nu_{12} & \nu_{13} \\ \nu_{21} & (\nu_{22} - \omega_2 U) & \nu_{23} \\ \nu_{31} & \nu_{32} & \nu_{33} \end{bmatrix} \begin{bmatrix} V_1 \\ V_2 \\ V_3 \end{bmatrix}$$

We have omitted ion pressure and electron pressure because they are insignificant in the ionosphere where we intend to apply this equation.

Equation (8) is a 9 x 9 set of scalar equations. It is our principal goal to derive a single vector equation

relating electric current, voltage, and neutral particle velocity. The electric current is proportional to the difference of ion and electron velocities, and the ionization drift is proportional to the sum. So we rearrange the first two variables

$$(9) \quad \begin{bmatrix} -\frac{\omega_1 E}{|B|} \\ -\frac{\omega_2 E}{|B|} \\ \frac{\nabla p}{\rho} \end{bmatrix} = \begin{bmatrix} (\nu_{11} - \omega_1 U - \nu_{12}) & (\nu_{11} - \omega_1 U + \nu_{12}) & \nu_{13} \\ (\nu_{21} - \nu_{22} - \omega_2 U) & (\nu_{21} + \nu_{22} - \omega_2 U) & \nu_{23} \\ (\nu_{31} - \nu_{32}) & (\nu_{31} + \nu_{32}) & \nu_{33} \end{bmatrix} \begin{bmatrix} \frac{1}{2}(V_1 - V_2) \\ \frac{1}{2}(V_1 + V_2) \\ V_3 \end{bmatrix}$$

The first two equations may be written as

$$(10) \quad - \begin{bmatrix} \nu_{13} \\ \nu_{23} \end{bmatrix} V_3 - \begin{bmatrix} \omega_1 \\ \omega_2 \end{bmatrix} \frac{E}{|B|} = \begin{bmatrix} (\nu_{11} - \nu_{12} - \omega_1 U) & (\nu_{11} + \nu_{12} - \omega_1 U) \\ (\nu_{21} - \nu_{22} + \omega_2 U) & (\nu_{21} + \nu_{22} - \omega_2 U) \end{bmatrix} \begin{bmatrix} \frac{1}{2}(V_1 - V_2) \\ \frac{1}{2}(V_1 + V_2) \end{bmatrix}$$

To solve for the current in terms of the electric field and the neutral velocity, it is necessary to invert the 6 x 6 scalar or 2 x 2 partitioned matrix in (10). This inverse is simply the adjoint over the determinant of the 2 x 2 partitioned matrix because all of the partitions commute with one another, each being a polynomial in the matrix U . In treating the problem of three or more charged particles, polynomials of higher degree than

quadratic will be formed in computing the adjoint and the determinant but can be reduced to a quadratic by repeated application of the formula $U^3 = -U$. Finally, we are able to invert the determinant at most quadratic in U by the following formula (a, b , and c are arbitrary scalars):

$$(11) \quad (a + bU + cU^2) \left(\frac{1}{a} + \frac{-bU + \frac{1}{a}(b^2 - ac + c^2)U^2}{(a-c)^2 + b^2} \right) = 1$$

which is verified readily with the substitution $U^3 = -U$.

We now invert (10) simultaneously absorbing a minus sign in the adjoint.

(12a, b,)

$$\begin{bmatrix} \frac{1}{2}(V_1 - V_2) \\ \frac{1}{2}(V_1 + V_2) \end{bmatrix} = \frac{1}{\det} \begin{bmatrix} (-\mathcal{V}_{21} - \mathcal{V}_{22} + \omega_2 U) (\mathcal{V}_{11} + \mathcal{V}_{12} - \omega_1 U) \\ (\mathcal{V}_{21} - \mathcal{V}_{22} + \omega_2 U) (-\mathcal{V}_{11} + \mathcal{V}_{12} + \omega_1 U) \end{bmatrix} \left\{ \begin{bmatrix} \omega_1 \\ \omega_2 \end{bmatrix} \frac{E}{|B|} + \begin{bmatrix} \mathcal{V}_{13} \\ \mathcal{V}_{23} \end{bmatrix} V_3 \right\}$$

where

$$(13) \quad \det = 2 \left[(\mathcal{V}_{11}\mathcal{V}_{22} - \mathcal{V}_{12}\mathcal{V}_{21}) - (\mathcal{V}_{22}\omega_1 + \mathcal{V}_{11}\omega_2)U + \omega_1\omega_2 U^2 \right]$$

The principle objective of this section is now complete for we have the exact statement for the electrical conductivity (12a) and the ionization drift coefficient (12b) of a partially ionized gas moving in a magnetic field. In section (3) we consider expressing the conductivities

along different axes and show a simpler way to treat the many ion problem.

I-B-3 Canonical Form of the Conductivity
Matrix, Choice of Coordinates

The unit cross product matrix U satisfies the characteristic equation $U^3 = -U$. Its eigenvalues satisfy the same equation and hence must be 0 , $-i$, and $+i$. The eigenvectors A_0 , A_1 , and A_2 of U must satisfy the equation $UA = \mu A$. The three eigenvectors may each be represented as a product of an operator Q with an arbitrary vector E as follows:

$$(1) \quad \begin{aligned} A_0 &= Q_0 E = (I + U^2) E \\ A_1 &= Q_1 E = 1/2 (iU - U^2) E \\ A_2 &= Q_2 E = 1/2 (-iU - U^2) E \end{aligned}$$

The proof that these A 's are indeed the eigenvectors of U follows by direct substitution into $UA = \mu A$. Actually, we have the condition $UQ = \mu Q$ satisfied.

$$(2) \quad \begin{aligned} UQ_0 &= U(I + U^2) = 0 \cdot (I + U^2) = \mu_0 Q_0 \\ UQ_1 &= U(iU - U^2)/2 = -i \cdot (iU - U^2)/2 = \mu_1 Q_1 \\ UQ_2 &= U(-iU - U^2)/2 = +i \cdot (-iU - U^2)/2 = \mu_2 Q_2 \end{aligned}$$

The Q operators commute with one another and are each Hermitian matrices since U is skew symmetric, iU is Hermitian, U^2 and I are symmetric. Thus $Q^* = Q$

and $Q^*Q = Q^2$.

The eigenvectors A are mutually orthogonal because we have the even stronger condition that the operators Q are mutually orthogonal. Proof is by computing products of each possible pair

$$\begin{aligned}
 (3) \quad Q_1 Q_0 &= Q_0 Q_1 = (I + U^2)(iU - U^2)/2 = 0 \\
 Q_2 Q_0 &= Q_0 Q_2 = (I + U^2)(-iU - U^2)/2 = 0 \\
 Q_2 Q_1 &= Q_1 Q_2 = (iU - U^2)(-iU - U^2)/4 = 0
 \end{aligned}$$

The Q matrices are idempotent which means that $Q^2 = Q$. Proof is by substitution

$$\begin{aligned}
 (4) \quad Q_0^2 &= (I + U^2)(I + U^2) = (I + U^2) = Q_0 \\
 Q_1^2 &= 1/2(iU - U^2)1/2(iU - U^2) = +1/2(iU - U^2) = Q_1 \\
 Q_2^2 &= 1/2(-iU - U^2)1/2(-iU - U^2) = +1/2(-iU - U^2) = Q_2
 \end{aligned}$$

In summary, the Q 's satisfy the relation

$$(5) \quad Q_i Q_j = \delta_{ij} Q_i = \delta_{ij} Q_j$$

and we have the fortunate property that products of linear combinations of the Q 's do not give rise to cross terms.

In the preceding section we showed how to calculate the conductivity matrix $\underline{\underline{\sigma}}$ as a linear combination of I , U , U^2 . The point of this section is to show how to find scalars λ_0 , λ_1 , and λ_2 so that the con-

ductivity matrix $\underline{\underline{\sigma}}$ is expressed as a linear combination of the Q 's

$$(6) \quad \underline{\underline{\sigma}} = \lambda_0 Q_0 + \lambda_1 Q_1 + \lambda_2 Q_2$$

Then the eigenvalues of the conductivity matrix $\underline{\underline{\sigma}}$ are simply λ_0 , λ_1 and λ_2 and the eigenvectors are A_0 , A_1 , and A_2 as may be seen by multiplying (6) through by each of the A 's getting

$$(7) \quad \underline{\underline{\sigma}} A_i = \underline{\underline{\sigma}} Q_i E = \lambda_i Q_i E = \lambda_i A_i$$

The central job in getting the conductivity matrix was inverting a matrix (equation I-B-2.10) by the adjoint over the determinant. Both adjoint and determinant were polynomials in U . Polynomials in U are easily represented in terms of the Q 's by the relations

$$(8) \quad \begin{aligned} I &= Q_0 + Q_1 + Q_2 \\ U &= i(Q_2 - Q_1) \\ U^2 &= -(Q_1 + Q_2) \end{aligned}$$

Then a polynomial in U expressed in terms of Q 's is

$$(9) \quad \begin{aligned} aI + bU + cU^2 &= a(Q_0 + Q_1 + Q_2) + ib(Q_2 - Q_1) - c(Q_1 + Q_2) \\ &= aQ_0 + [a - c - ib]Q_1 + [a - c + ib]Q_2 \end{aligned}$$

The first step in inverting the determinant is to

express it as a sum of Q 's. Say this is formula (9).

Then it is simple to invert.

Let \det^{-1} be denoted as

$$(10) \quad \det^{-1} = \alpha Q_0 + \beta Q_1 + \gamma Q_2$$

where α , β , and γ are unknown coefficients.

The meaning of inverse is that

$$(11) \quad \det \det^{-1} = I$$

Which in terms of the Q 's is

$$(12) \quad \left(a Q_0 + [(a-c)-ib] Q_1 + [(a-c)+ib] Q_2 \right) \left(\alpha Q_0 + \beta Q_1 + \gamma Q_2 \right) = Q_0 + Q_1 + Q_2$$

By the orthogonality of the Q 's there are no cross terms so α , β , and γ are readily identified and

$$(13) \quad \det^{-1} = \frac{Q_0}{a} + \frac{Q_1}{(a-c)-ib} + \frac{Q_2}{(a-c)+ib}$$

Recapitulating, the conductivity matrix is the inverse of a matrix (of formula I-B-2.10) whose elements are polynomials in U , or equivalently a sum of the Q 's. We invert this matrix just like ordinary matrices by the adjoint over the determinant. The determinant which is itself a sum of Q matrices is inverted with (13). The result is

$$\underline{\underline{\sigma}} = \frac{\text{num}}{\text{det}} = \frac{\text{num}}{a + bU + cU^2}$$

$$(14) \quad \underline{\underline{\sigma}} = \text{num} \frac{Q_0}{a} + \frac{Q_1}{(a+c) - ib} + \frac{Q_2}{(a-c) + ib}$$

$$(15) \quad \underline{\underline{\sigma}} = \lambda_0 Q_0 + \lambda_1 Q_1 + \lambda_2 Q_2$$

which gives the relation of a , b , and c to the λ_i .

For direct currents at low altitudes where collision frequencies dominate gyro frequencies we see by formula I=B-2.13 that a dominates b and c .

$$(I-B-2.13) \quad \text{det} \sim (\nu_{11}\nu_{22} - \nu_{12}\nu_{21}) - (\nu_{22}\omega_1 + \nu_{11}\omega_2)U + \omega_1\omega_2 U^2 \\ \sim a - bU + cU^2$$

Then by (14) and (15) all of the eigenvalues of the conductivity matrix become the same because physically the conductivity is becoming isotropic.

At high altitudes where the situation is reversed c dominates. Then λ_1 and λ_2 may be neglected. Then the current is the projection of E onto B taken in the direction of B since (15) becomes

$$(16) \quad \underline{\underline{\sigma}} \approx \lambda_0(I + U^2) = \frac{\lambda_0}{B \cdot B} \begin{bmatrix} B_x \\ B_y \\ B_z \end{bmatrix} \begin{bmatrix} B_x & B_y & B_z \end{bmatrix}$$

Choice of a basis is somewhat arbitrary and to counter-balance the good features of the canonical basis are the following considerations:

If one were interested in the slight deviation from isotropy at low altitudes, one would be taking the difference between two nearly equal eigenvalues. From a computing point of view it would be advantageous to work with the difference directly. This can be accomplished with another basis, say $I, U, I + U^2$. We find σ_i such that

$$(17) \quad \underline{\underline{\sigma}} = \sigma_0 \bar{I} + \sigma_1 U + \sigma_2 (I + U^2)$$

By Sylvester's theorem the eigenvalues $\lambda_0, \lambda_1, \lambda_2$ of $\underline{\underline{\sigma}}$ are found by substituting into (17) the eigenvalues $0, -i, i$ of U .

$$(18) \quad \begin{aligned} \lambda_0 &= \sigma_0 + \sigma_2 \\ \lambda_1 &= \sigma_0 - i\sigma_1 \\ \lambda_2 &= \sigma_0 + i\sigma_1 \end{aligned}$$

When the situation is physically isotropic σ_1 , and σ_2 are zero, but if it becomes very slightly anisotropic, we have a better numerical description with σ_0 , σ_1 , and σ_2 than with the eigenvalues λ_0 , λ_1 , and λ_2 .

Another reason to prefer the basis of formula (17) to the canonical basis is that no imaginary numbers are introduced. The imaginary components in the canonical representation arise because the axes are circularly polarized. Physically the vector IE points in the direction of E , UE is in the direction of $B \times E$, and $(I + U^2)E$ is along B (since its cross product with B , $U(I + U^2)E$ vanishes).

The conductivities for mean daytime conditions have been computed in the $I, U, I + U^2$ basis, tabulated in table I-B-3.1 and graphed on Figure I-B-3.1. They refer to the formulas

$$(19) \quad J = (\sigma_0^{JE} + \sigma_1^{JE}U + \sigma_2^{JE}(I+U^2))E + (\sigma_0^{JV} + \sigma_1^{JV}U + \sigma_2^{JV}(I+U^2))V_3$$

$$D = (\sigma_0^{DE} + \sigma_1^{DE}U + \sigma_2^{DE}(I+U^2))E + (\sigma_0^{DV} + \sigma_1^{DV}U + \sigma_2^{DV}(I+U^2))V_3$$

In this notation σ_0^{JE} is the Pederson conductivity, σ_1^{JE} , is the Hall conductivity and σ_2^{JE} is the conductivity along magnetic field lines. These are oblique coordinates unless E is perpendicular to B .

Finally we consider manipulating a large matrix M whose elements are linear combinations of Q 's. In the many ion problems, one wants to invert such a matrix.

Suppose M be written as

$$M = M_0 \otimes Q_0 + M_1 \otimes Q_1 + M_2 \otimes Q_2$$

Table I-B-3.1 Mean solar mid-latitude daytime ionospheric properties and derived conductivities.

H	T3	T2	C	GAMMA	DENSITY	N2	NU23	NU21	NU13
200	1235	1700	763	1.455	.28E-09	.32E 12	.13E 03	.34E 03	.30E 01
180	1123	1500	726	1.443	.57E-09	.25E 12	.24E 03	.32E 03	.59E 01
160	1020	1300	534	1.440	.11E-08	.20E 12	.45E 03	.31E 03	.12E 02
140	712	979	566	1.433	.35E-08	.16E 12	.12E 04	.38E 03	.36E 02
120	350	510	393	1.426	.26E-07	.14E 12	.67E 04	.77E 03	.27E 03
100	210	220	301	1.418	.50E-06	1.00E 11	.83E 05	.16E 04	.51E 04
80	160	150	262	1.415	.25E-04	.32E 10	.35E 07	1.00E 02	.25E 06
60	247	247	323	1.411	.35E-03	1.00E 03	.61E 08	.22E 01	.35E 07
40	264	283	333	1.407	.54E-02	1.00E 07	.10E 10	.20E 00	.54E 03

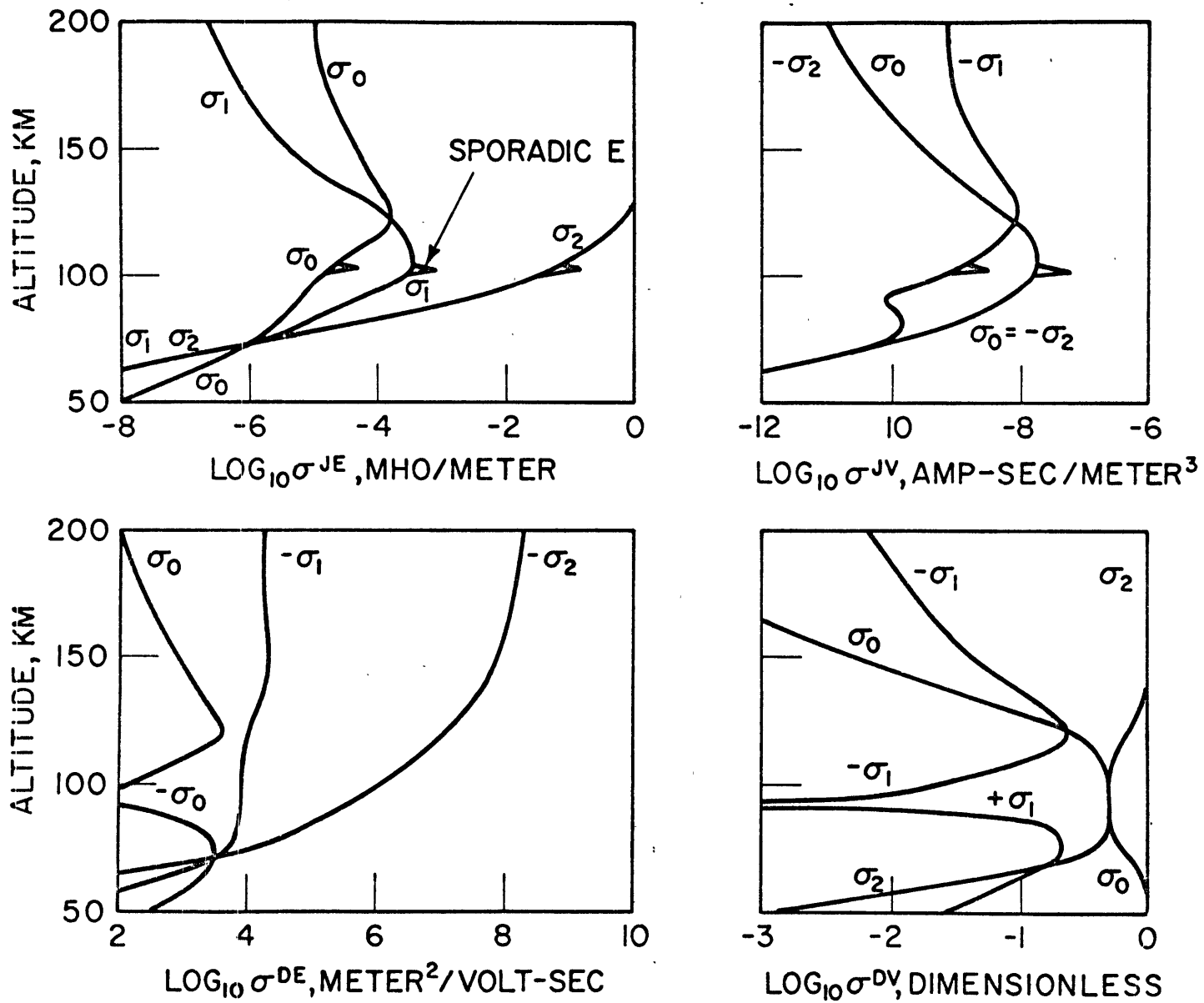
BASIS IS I,U,I+U*U

H	JE0	JE1	JE2	JV0	JV1	JV2
200	.13E-04	.19E-06	.19E 02	.12E-10	-.77E-09	-.12E-10
180	.20E-04	.69E-06	.13E 02	.36E-10	-.12E-08	-.36E-10
160	.31E-04	.13E-05	.74E 01	.11E-09	-.19E-08	-.11E-09
140	.78E-04	.14E-04	.29E 01	.35E-09	-.47E-08	-.85E-09
120	.18E-03	.25E-03	.54E 00	.15E-07	-.11E-07	-.15E-07
100	.13E-04	.27E-03	.33E-01	.16E-07	-.75E-09	-.16E-07
80	.25E-05	.76E-05	.23E-04	.46E-09	-.15E-09	-.46E-09
60	.45E-07	.77E-08	.13E-03	.46E-12	-.27E-11	-.46E-12
40	.28E-09	.29E-11	.30E-13	.17E-15	-.17E-13	-.17E-15

H	DE0	DE1	DE2	DV0	DV1	DV2
200	.13E 03	-.17E 05	-.19E 09	.11E-03	-.75E-02	.10E 01
180	.25E 03	-.17E 05	-.16E 09	.45E-03	-.15E-01	.10E 01
160	.49E 03	-.17E 05	-.12E 09	.17E-02	-.29E-01	1.00E 00
140	.15E 04	-.16E 05	-.55E 08	.16E-01	-.83E-01	.98E 00
120	.40E 04	-.11E 05	-.12E 08	.33E 00	-.24E 00	.68E 00
100	.26E 03	-.83E 04	-.10E 07	.50E 00	-.15E-01	.50E 00
80	-.25E 04	-.75E 04	-.23E 05	.55E 00	.15E 00	.45E 00
60	-.14E 04	-.24E 03	-.41E 02	.99E 00	.34E-01	.14E-01
40	-.87E 02	-.90E 00	-.94E-02	1.00E 00	.52E-02	.54E-04

Symbols not defined by formula 19 are: H, altitude in kilometers; T3, neutral temperature; T2, electron temperature; C, sound speed; GAMMA, ratio of specific heats; N2, electron density; NU23 electron-neutral collision frequency; NU21, electron-ion collision frequency; NU13, electron-neutral collision frequency.

Figure I-B-3.1 Graph of crossconductivities in formula (19)



where the \otimes is the Kronecker product. This means that each scalar element in M_i is considered to be multiplied by Q_i . By considering a few examples, it is easy to see that due to the non-interacting nature of the Q 's we have

$$\det M = \sum_{i=0}^2 (\det M_i) \otimes Q_i$$

$$\text{adjoint } M = \sum_{i=0}^2 (\text{adjoint } M_i) \otimes Q_i$$

$$M^{-1} = \sum_{i=0}^2 M_i^{-1} \otimes Q_i$$

The eigenvalues of M are the eigenvalues of M_0 , M_1 , and M_2 multiplied by the eigenvalues of the Q 's. The eigenvectors may be likewise attained.

I-B-4 Electrical Phenomena with Prescribed Neutral Velocity

Now we derive equations which enable us to calculate the electrical effects of acoustic gravity waves. In this section we take the behavior of the neutral atmosphere to be completely determined by the acoustic equations and we use the neutral particle velocities as sources to drive Maxwell's equations. Since we are concerned with millicycle per second frequencies we can drop time derivatives in Maxwell's equations and take the electric field E to be derivable from a potential ψ .

$$(1) \quad \nabla \psi = -\vec{E}$$

The divergence of electrical current \vec{J} vanishes

$$(2) \quad \nabla \cdot \vec{J} = 0$$

From section II-B-2 and 3 we have the electrical conductivity expression

$$(3) \quad \vec{J} = \underline{\underline{\sigma}} \vec{E} + \underline{\underline{\tau}} \vec{V}$$

where \vec{V} is the velocity of the neutral wind. Inserting (3) into (1) we get

$$\begin{aligned}
 \nabla \varphi &= -\underline{\underline{\sigma}}^{-1} \vec{J} + \underline{\underline{\sigma}}^{-1} \underline{\underline{T}} \vec{V} \\
 (4) \quad &= -\underline{\underline{r}} \vec{J} + \underline{\underline{s}} \vec{V}
 \end{aligned}$$

where $\underline{\underline{r}}$ is the resistivity matrix and $\underline{\underline{s}}$ will be called the source vector. We take solutions to be of the form

(5)

$$\begin{bmatrix} J_x \\ J_y \\ J_z \\ \varphi \end{bmatrix} = \begin{bmatrix} J_x(z) \\ J_y(z) \\ J_z(z) \\ \varphi(z) \end{bmatrix} e^{ikx + ily}$$

Inserting (5) into (4) and into (2) we get

(6)

$$\begin{bmatrix} \underline{\underline{r}} & ik \\ ik & il \\ \underline{\underline{\sigma}}^{-1} \underline{\underline{T}} & 0 \end{bmatrix} \begin{bmatrix} J_x \\ J_y \\ J_z \\ \varphi \end{bmatrix} = \begin{bmatrix} S_x \\ S_y \\ S_z \\ 0 \end{bmatrix}$$

Bringing terms without z derivatives to the right

$$(7) \quad \frac{d}{dz} \begin{bmatrix} 0 \\ 0 \\ \psi \\ J_z \end{bmatrix} = - \begin{bmatrix} & & & ik \\ & \underline{r} & & il \\ & & & 0 \\ ik & il & 0 & 0 \end{bmatrix} \begin{bmatrix} J_x \\ J_y \\ J_z \\ \psi \end{bmatrix} + \begin{bmatrix} S_x \\ S_y \\ S_z \\ 0 \end{bmatrix}$$

Interchanging the last two equations in set (7)

$$(8) \quad \frac{d}{dz} \begin{bmatrix} 0 \\ 0 \\ J_z \\ \psi \end{bmatrix} = - \begin{bmatrix} r_{xy} & r_{yx} & r_{xz} & ik \\ r_{yx} & r_{yy} & r_{yz} & il \\ ik & il & 0 & 0 \\ r_{zx} & r_{zy} & r_{zz} & 0 \end{bmatrix} \begin{bmatrix} J_x \\ J_y \\ J_z \\ \psi \end{bmatrix} + \begin{bmatrix} S_x \\ S_y \\ 0 \\ S_z \end{bmatrix}$$

Next we partition this 4 x 4 into a 2 x 2 of 2 x 2's

$$(9) \quad \frac{d}{dz} \begin{bmatrix} 0 \\ x_2 \end{bmatrix} = - \begin{bmatrix} A_{11} & A_{12} \\ A_{21} & A_{22} \end{bmatrix} \begin{bmatrix} x_1 \\ x_2 \end{bmatrix} + \begin{bmatrix} S_1 \\ S_2 \end{bmatrix}$$

solving the top equation for x_1 ,

$$(10) \quad x_1 = A_{11}^{-1} (-A_{12} x_2 + S_1)$$

and inserting back into the bottom of (9)

$$(11) \quad \frac{d}{dz} X_2 = (A_{21} A_{11}^{-1} A_{12} - A_{22}) X_2 + (-A_{21} A_{11}^{-1} S_1 + S_2)$$

This is the desired 2 x 2 set of equations which we may write symbolically as

$$(12) \quad \frac{d}{dz} \begin{bmatrix} J_z \\ \psi \end{bmatrix} = \begin{bmatrix} A(z) \end{bmatrix} \begin{bmatrix} J_z \\ \psi \end{bmatrix} + \begin{bmatrix} c(z) \end{bmatrix}$$

These equations are solved in principle by matrizants (Gantmacher Vol. 2 p. 131) and in practice by various numerical integration schemes. (Further details are in Appendix F.) There seems to be no point in writing out the elements of A explicitly since no simplifications arise with a general conductivity matrix.

Having calculated J_z and ψ by numerical integration of (12) one gets all the other variables by either of two routes. The first way is to use (10) to get J_x and J_y and then (4) to get E: The other way is to use (1) to get E using (12b) to get E_z and then (3) to get J. Both methods have been used as a check.

Finally we come to calculate the perturbation in the magnetic field H. For this we use $\text{curl } H = J$ and $\text{div } H = 0$. Arranging as a matrix

(13)

$$\begin{bmatrix} 0 & -\partial_z & il \\ \partial_z & 0 & -ik \\ -il & ik & 0 \\ ik & il & \partial_z \end{bmatrix} \begin{bmatrix} H_x \\ H_y \\ H_z \end{bmatrix} = \begin{bmatrix} J_x \\ J_y \\ J_z \\ 0 \end{bmatrix}$$

and interchanging the first and second rows

$$(14) \begin{bmatrix} \partial_z & 0 & -ik \\ 0 & \partial_z & -il \\ -il & ik & 0 \\ ik & il & \partial_z \end{bmatrix} \begin{bmatrix} H_x \\ H_y \\ H_z \end{bmatrix} = \begin{bmatrix} J_y \\ -J_x \\ J_z \\ 0 \end{bmatrix}$$

and replacing the third by ik times the third plus il times the fourth we get:

$$(15) \begin{bmatrix} \partial_z & 0 & -ik \\ 0 & \partial_z & -il \\ 0 & -(k^2+l^2) & il\partial_z \\ ik & il & \partial_z \end{bmatrix} \begin{bmatrix} H_x \\ H_y \\ H_z \end{bmatrix} = \begin{bmatrix} J_y \\ -J_x \\ ikJ_z \\ 0 \end{bmatrix}$$

Now it will be observed that the second and third of (15) constitute a 2 x 2 set for H_y and H_z .

$$(16) \quad \begin{bmatrix} \partial_z & -il \\ -(k^2+l^2) & il\partial_z \end{bmatrix} \begin{bmatrix} H_y \\ H_z \end{bmatrix} = \begin{bmatrix} -J_x \\ ikJ_z \end{bmatrix}$$

Rearranging

$$(17) \quad \frac{d}{dz} \begin{bmatrix} H_y \\ ilH_z \end{bmatrix} = \begin{bmatrix} 0 & 1 \\ (k^2+l^2) & 0 \end{bmatrix} \begin{bmatrix} H_y \\ ilH_z \end{bmatrix} + \begin{bmatrix} -J_x \\ ikJ_z \end{bmatrix}$$

In the event that $l = 0$ the above system is degenerate and one can use another set of variables

$$(18) \quad \frac{d}{dz} \begin{bmatrix} H_x \\ ikH_z \end{bmatrix} = \begin{bmatrix} 0 & 1 \\ (k^2+l^2) & 0 \end{bmatrix} \begin{bmatrix} H_x \\ ikH_z \end{bmatrix} + \begin{bmatrix} J_y \\ -ilJ_z \end{bmatrix}$$

In a departure from the usual situation the matrix is independent of the media and (17) and (18) have the homogeneous solution

$$(19) \quad \begin{bmatrix} H_x \\ H_y \\ H_z \end{bmatrix} \sim \begin{bmatrix} ik \\ il \\ \pm\sqrt{k^2+l^2} \end{bmatrix} e^{\pm\sqrt{k^2+l^2} z}$$

Usually one uses the damped homogeneous solution in a terminating halfspace. Here the situation differs because the halfspace (above the ionosphere) we envision is

not devoid of sources as the currents are prescribed from the solutions of equation (12). A halfspace inhomogeneous solution of $\text{curl } H = J$ is then

$$(20) \quad H = \frac{-\nabla \times J}{(k^2 + \ell^2 + m^2)}$$

as may be verified by substitution.

Consider a situation with a current free halfspace below $z = 0$, arbitrary currents between 0 and z_1 and halfspace currents above z_1 . Then matching solutions at z_1 we have

$$(21) \quad \alpha e^{Az_1} \begin{bmatrix} 1 \\ \sqrt{k^2 + \ell^2} \end{bmatrix} + e^{Az_1} \int_0^{z_1} e^{-Az} \begin{bmatrix} J_y \\ -i\ell J_z \end{bmatrix} dz = \beta \begin{bmatrix} 1 \\ -\sqrt{k^2 + \ell^2} \end{bmatrix} - \frac{\nabla \times J}{k^2 + \ell^2 + m^2}$$

where α is an unknown scale factor of the damped solution below $z = 0$ integrated to z_1 , and β is a scale factor for the damped solution in the upper halfspace. The second term is the source convolution below z_1 , and the fourth term likewise above z_1 . The matrix A is the matrix of formula (18). Equation (21) is two simultaneous equations for the two unknowns α and β . When they are solved for, the solution is known everywhere.

I-B-5 Wave Guide Mode Integration

Consider the analogy between neutrals characterized by ρ and \vec{V} and ionization characterized by q and \vec{D} . There is a formally identical continuity equation and formally similar momentum equation. The neutrals, however, have an equation of state which relates their density to a pressure whose gradient appears in the momentum equation. We have written no such equation of state for the ionization. The notion of an ion "pressure" for the first order wave motion seems inappropriate since the ionized atmospheric components do not even satisfy the zero order hydrostatic equation. It might seem that by dropping one variable (ion pressure) and one equation (ion state equation) we could still do the problem, but we cannot. Without an equation of state for ionized media, we have the dilemma that we have no equation with a $\frac{d\tilde{q}}{dz}$ term to integrate \tilde{q} , nor do we have an equation with which we can eliminate \tilde{q} from the set. A satisfactory procedure for the lower ionosphere is to ignore the ionized particle drift so far as the momentum equation for neutrals is concerned. In formula I-B-9c we set the drift \vec{D} equal to the neutral motion V_3 and include a gravity term, getting

(10) to (12)

$$\begin{aligned} \frac{1}{\rho} (\nabla \tilde{p} + \tilde{g} \tilde{\rho}) &= (\nu_{31} - \nu_{32}) \frac{\vec{J}}{2n_e e_1} + (\nu_{31} + \nu_{32}) \vec{D} + \nu_{33} \vec{V}_3 \\ &= (\nu_{31} - \nu_{32}) \frac{\vec{J}}{2n_e e_1} + i\omega \vec{V}_3 \end{aligned}$$

A posteriori we can calculate \vec{D} with formula I-C-2-12b from \vec{J} and \vec{V}_3 to see how long a time must elapse for \vec{D} to significantly change the initial ion distribution.

Other equations we will need are Maxwell's equations,

$$(1) \text{ to } (3) \quad \nabla \times \vec{E} + \mu \dot{\vec{H}} = 0$$

$$(4) \text{ to } (6) \quad \nabla \times \vec{H} - \epsilon \dot{\vec{E}} - \vec{J} = 0$$

the conductivity equation I-B-2.14 which we write as

$$(7) \text{ to } (9) \quad \vec{J} = \underline{\underline{\sigma}} \vec{E} + \underline{\underline{s}} \rho_3 \vec{V}_3$$

the equation of continuity for neutrals,

$$(13) \quad \frac{\partial \rho}{\partial t} + \nabla \cdot (\rho \vec{v}) = 0$$

and the equation of state for neutrals

$$(14) \quad \frac{Dp}{Dt} - c^2 \frac{D\rho}{Dt} = 0$$

Organizing all these together, and introducing a few simplifying definitions, we get Table I- B-5-1.

Table I-B-5.1 can be reduced by the method of section I-b-4 to a 6 x 6 first order linear differential equation. The coupling is severe enough that there seems to be no

	E_x	E_y	E_z	H_x	H_y	H_z	J_x	J_y	J_z	$\bar{p}u$	$\bar{p}v$	$\bar{p}w$	\bar{p}	\bar{p}	
$\text{curl } E + \mu \dot{H} = 0$		$-\frac{d}{dz}$	il	$-i\mu w$											①
		$\frac{d}{dz}$	$-ik$	$-i\mu w$											②
		$-il$	ik		$-i\mu w$										③
$\text{curl } H - J - e\dot{E} = 0$	$i\omega\epsilon$			$-\frac{d}{dz}$	il	-1									④
		$i\omega\epsilon$		$\frac{d}{dz}$	$-ik$	-1									⑤
			$i\omega\epsilon$	$-il$	ik		-1								⑥
$J - \sigma(E + v \times B) = 0$ $J - \sigma E + s\bar{p}V = 0$	$-\sigma_{xx}$	$-\sigma_{xy}$	$-\sigma_{xz}$				1			S_{xx}	S_{xy}	S_{xz}			⑦
	$-\sigma_{yx}$	$-\sigma_{yy}$	$-\sigma_{yz}$					1		S_{yx}	S_{yy}	S_{yz}			⑧
	$-\sigma_{zx}$	$-\sigma_{zy}$	$-\sigma_{zz}$						1	S_{zx}	S_{zy}	S_{zz}			⑨
$\bar{p} \frac{Dv}{Dt} - \bar{p}g + \nabla p + aJ = 0$							a			$-i\omega$				ik	⑩
								a		$-i\omega$				il	⑪
									a	$-i\omega$	g	$\frac{d}{dz}$			⑫
$\frac{\partial p}{\partial t} + \nabla(\bar{p}v) = 0$										ik	il	$\frac{\bar{p}}{\rho} + \frac{d}{dz}$	$-i\omega$		⑬
$\frac{Dp}{Dt} - c^2 \frac{Dp}{Dt} = 0$										$g - c^2 \frac{\bar{p}}{\rho}$	$i\omega c^2$	$-i\omega$			⑭

Table I-B-5.1 Complete set of equations for waveguide integration of electromagnetic-acoustic-gravity wave disturbance.

point in doing this in symbolic form. It may as well be done by computer as the integration proceeds. An advantage of doing it by computer is that the optimum pivot can be taken at each altitude; this may be very important since the dynamics are controlled by different equations at different altitudes.

An alternative method which may be faster and numerically more stable goes as follows: Take the electrical variables to be zero during the first integration. Then take the acoustic variables from the first integration to be sources to solve for the electromagnetic variables. Next take the electrical variables as sources on a second acoustic integration. Continuing in this manner one hopefully converges to a solution which also satisfies the 14 x 14 set on the table.

The first iteration is not necessarily satisfactory even if \vec{J} and \vec{D} influence the neutrals quite weakly. In chapter II we see that many gravity waves are deflected to propagate almost horizontally so that electromagnetic forces have a long time to act before the disturbance gets very high.

II Results of Calculations

The purpose of this chapter is to present machine integrations of some of the differential equations in the last chapter to see what kind of behavior is possible. First we describe well known (Hines) isothermal space properties. Since thermal gradients strongly influence the waves we then consider a succession of model atmospheres between isothermal and realistic.

Consideration of a simple jet stream model shows how it profoundly influences wave propagation with velocities comparable to the jet velocity. This is illustrated with particle velocity diagrams and dispersion curves. We are interested in the upward propagation of these disturbances and the fact that their vertical wavelengths are comparable to scale changes in temperature leads us to do a special calculation which shows the extreme importance of thermal gradients.

To get an idea of the importance of electromagnetic damping of gravity waves we first take up the electromagnetic damping of uniform ionospheric winds as a function of altitude. The damping of gravity waves is much more complex, but the overall energy loss rate turns out to be roughly the same function of altitude. Then we calculate the electromagnetic fields induced by some acoustic-gravity waves in some typical situations. Finally we consider

cellular rather than plane waves to see the effect of the changing current geometry on the magnetic fields.

In the end we have a quantitative picture of gravity waves emitted from the jet stream propagating upward to where they induce dissipative electromagnetic fields and die out.

II-A-1.1 Free Space Dispersion Curves

Figure (1) is the free space dispersion curve given by Hines (1960). It may be derived by specializing our layer integration formula (I-A-1-14) by replacing $\frac{d}{dz}$ by ik_z . The layer integration formula is then an eigenvector equation for the eigenvalue ik_z . Hines' dispersion relation may be thought of as the eigenvalue k_z as a function of k_x and ω . Selecting a certain frequency selects a curve. The direction of the propagation vector \vec{k} is given by a vector from the origin to the curve. This is the direction of the phase velocity. The group velocity is given by $\nabla_{\vec{k}} \omega$. It is perpendicular to the curve at the tip of the \vec{k} vector in the direction of increasing frequency (decreasing period). Notice that at the long (gravity wave) periods a \vec{k} vector with an upward vertical component implies a downward component of the group velocity. Also notice that in the long period limit all group velocities become horizontal and phase velocities become vertical. That limit must be approached in the jet stream when one observes a steady disturbance at the ground traveling at jet stream speed because an observer moving with the jet sees the disturbance frequency doppler shifted to zero.

Figure (2) gives a picture of group velocity magnitudes as a function of frequency and direction. It is notable that a low frequency cannot propagate vertically.

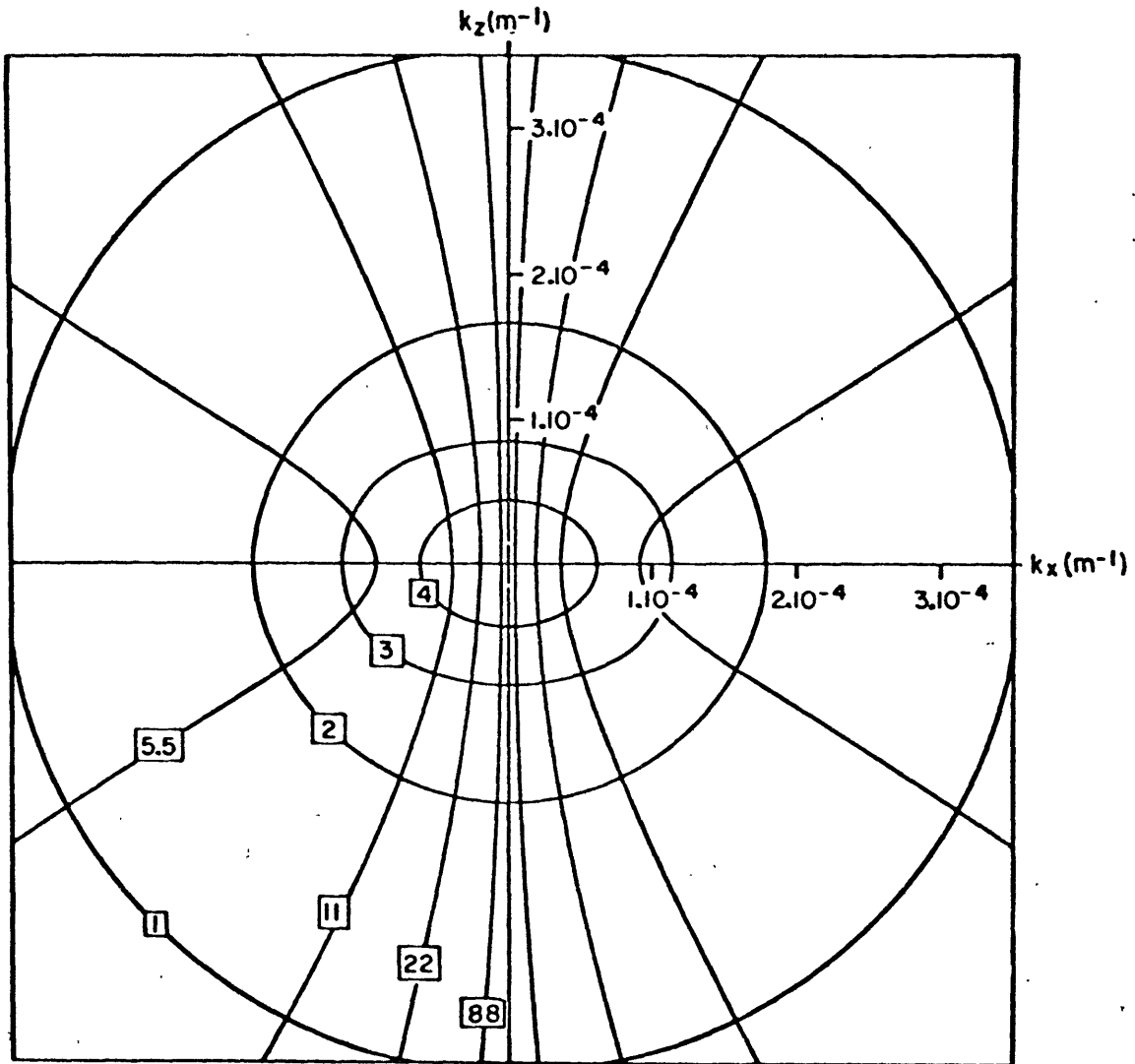


Figure II-A-1.1 After Hines (1960). Free space dispersion curves of acoustic gravity waves. The numbers in the boxes are periods in minutes.

Figure II-A-1.2 Group velocity of acoustic gravity waves as a function of period.

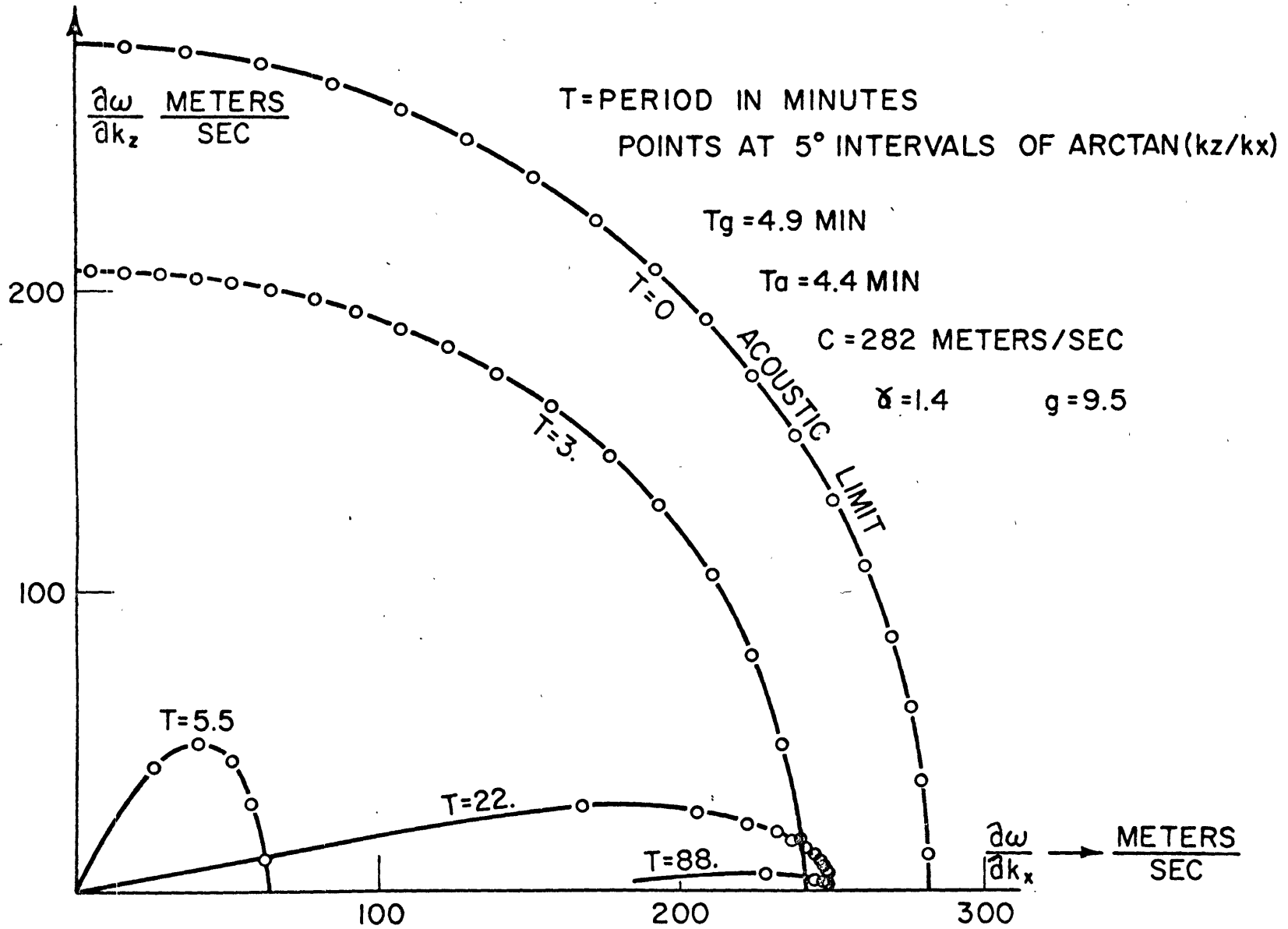


Figure (3) shows the altitude dependence of various parameters. One sees immediately that non-linearities will arise when weak but observable disturbances on the ground propagate to ionospheric altitudes.

II-A-1.2 Thermal Effects

With the mathematical formulation used in this thesis and the computer programs developed, there is no need to consider layer models for the atmosphere's temperature and wind structure. We still like layer models because of the insight they afford compared to realistic models for which cause and effect are harder to unscramble. Therefore we introduce the thermo-jet or T-J layer model. It shows all the principle modal behavior of a realistic model. The T-J model has a constant sound speed of 300 meters/sec between 0 and 100 km altitude, and 550 meters/sec above 100 km (thermosphere), and a 75 meter/sec jet stream between 8 and 10 km in an otherwise quiescent stmosphere. Figure 4 shows how dispersion curves undergo the transition from an isothermal atmosphere to the T-J model. Figure 4a applies to a thermosphere with a 301 meters/sec sound speed; 4b to 350 meters/sec; 4c to 450 meters/sec and figure 4d to a 550 meters/sec sound speed. Pluses and minuses refer to the sign of the dispersion relation. Where the sign changes a mode is possible. At some periods and phase velocities the half-space solution is not evanescent but is an outgoing wave

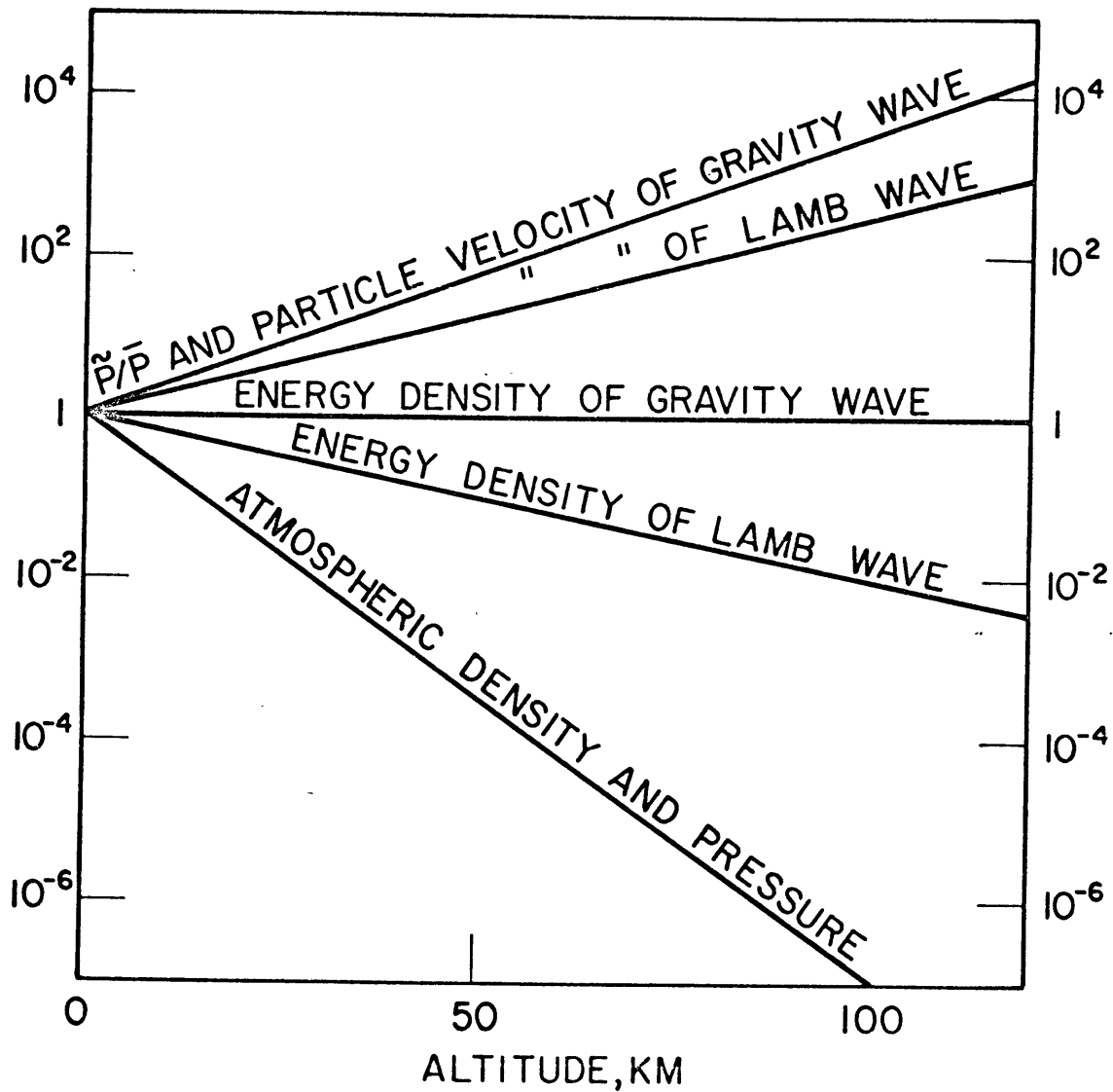
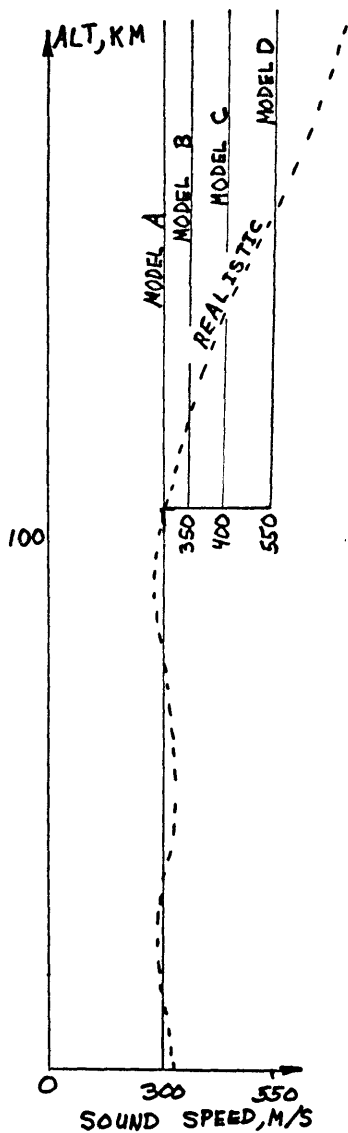
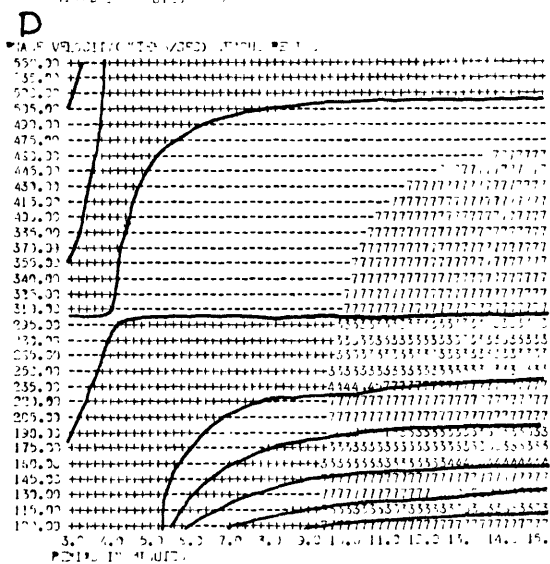
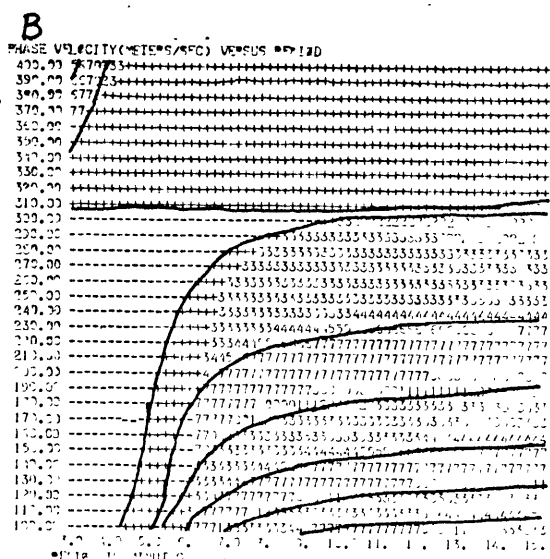
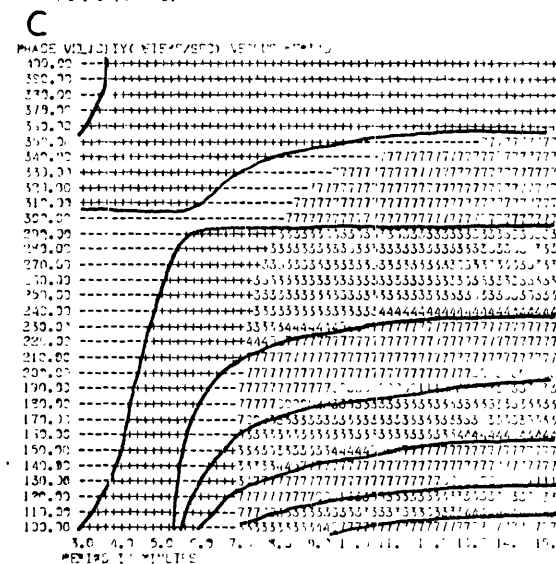
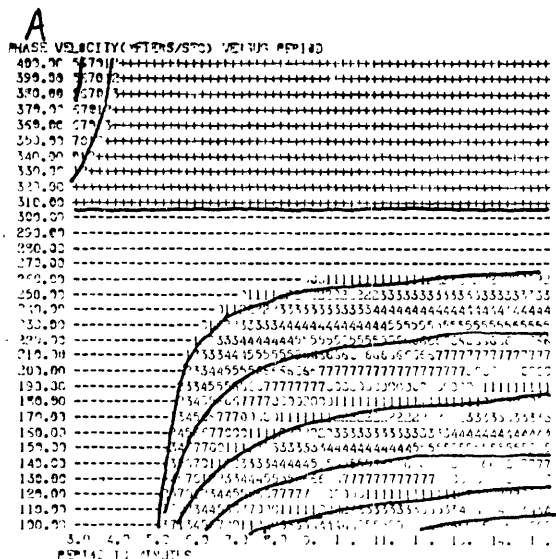


Figure II-A-1.3 Altitude scaling of various properties of acoustic gravity waves in a free space of constant temperature.

Figure II-A-1.4 Effect of thermosphere on dispersion



solution. In the nomenclature of I-A-2 "outgoing" means that the sign of the vertical wave number in the half-space is chosen to make the energy flux $\text{Re} \tilde{P} \tilde{W}^*$ positive. The numbers in the upper left hand corner of the dispersion diagram are vertically leaking acoustic waves. The numbers in the lower right are vertically leaking gravity waves. Modal solutions for these leaky waves require complex frequencies or complex horizontal wave numbers. We have instead kept the frequency real and put in a pressure source at jet stream level. In these regions of the $T-V_p$ plane numbers are printed which represent the octant of the phase angle of the source. The real part changes sign at practically the same frequency as the real part of the dispersion relation for a leaky mode so the leaky and non-leaky regions merge smoothly.

At 300 meters per second all models show a practically undispersed wave. In an isothermal atmosphere it is called the Lamb wave. The Lamb wave's particle motions are horizontal (or nearly so when the thermosphere is added) and so it is practically unaffected by gravity. The energy density is trapped near the ground, damping exponentially with a scale height of about 30 kilometers. In the isothermal atmosphere there are no nodes. When a thermosphere is added there are still no nodes for periods less than the atmospheric vertical resonance 4 minute periods. At larger periods there is a node around 100 km altitude. This is of mathematical

significance but not practical significance because the node is at high altitude on the tail of the energy distribution. At these longer periods another wave has become the fundamental mode. Its speed at the long period limit is about 500 meters/second. Its energy density is maximum at the 100 km thermosphere boundary and it damps off in both directions. In the limit of a very hot (light) thermosphere and very cold (heavy) air layer and long period (incompressible medium). This wave resembles a surface wave on water.

One expects high altitude (100 km) nuclear explosions to excite the 500 meter/second mode and near surface explosions to excite the 300 meter/second mode. Although there were a number of nuclear explosions during our year of observations, we failed to see any waves. This was due to their great distance (90°) and comparatively weak strength.

II-A-1.3 Jet Stream Effects

In figure 5 one sees the effect of the 75 meter/sec jet stream from 8 to 10 kilometers altitude is to cause a cluster point of modes around 75 meters per second. From figure 1 one sees that long period waves have a short vertical wavelength. This explains the cluster point. If an observer outside the jet sees a 76 meter/second wave, an observer inside sees a 1 meter/second wave with a very short vertical wavelength whose period is doppler shifted to be very long. Since the vertical wavelength gets arbitrarily

short, the mode number gets arbitrarily large, hence the cluster point in the mode diagram.

A modal diagram of this type showing velocities less than the jet stream speed is somewhat questionable due to the integration through two singular points. This was discussed extensively in section I-A-3. A computer program working with layers experiences no difficulty because the singular point is missed being at the point of discontinuity between layers. Below 75 meters/second one simply has a backward going wave in the jet coupled to a forward going wave outside the jet. An important reason for showing the modes below 75 meters/second is that if the T-J model were the real atmosphere, observational experience shows that the jet sources are probably located below the peak of the wind velocity profile.

The scales of figure 5 are expanded somewhat to make figure 6. The non-dispersed modes at short periods are gravity waves inside the jet and acoustic waves outside. Since acoustic waves do not propagate outside the jet the modal profile is strongly damped outside the jet. This is quite in agreement with our observations in the real atmosphere which show very little energy above the Brunt frequency. The Brunt frequency in the troposphere is actually lower (about 10 minutes) than the Brunt frequency in the T-J model due to the temperature lapse in the troposphere. Thus

PHASE VELOCITY (METERS/SEC) VERSUS PERIOD

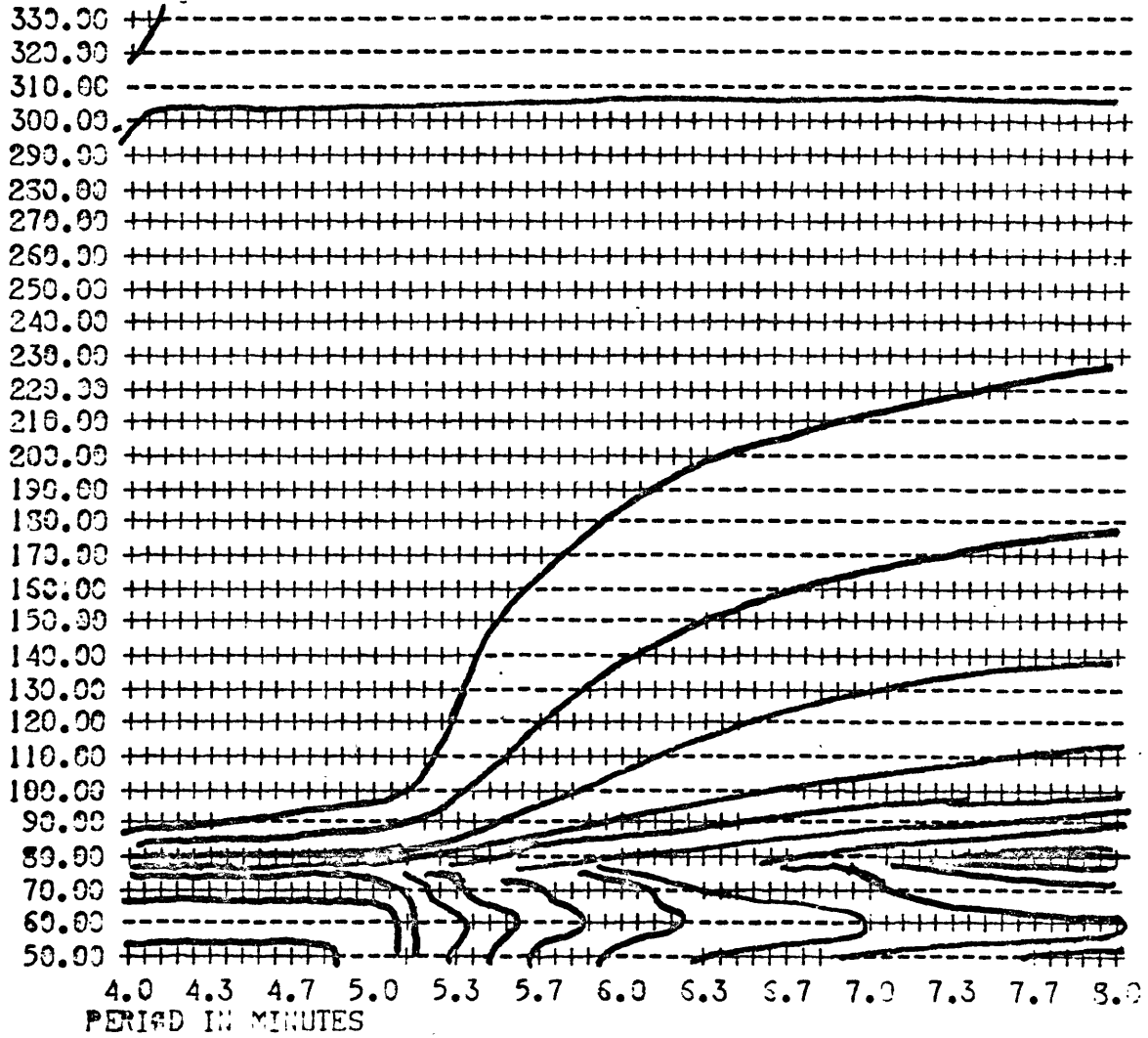


Figure II-A-1.5 Dispersion curves for a model with a jet-stream layer with a speed of 75 meters/second.

PHASE VELOCITY (METERS/SEC) VERSUS PERIOD

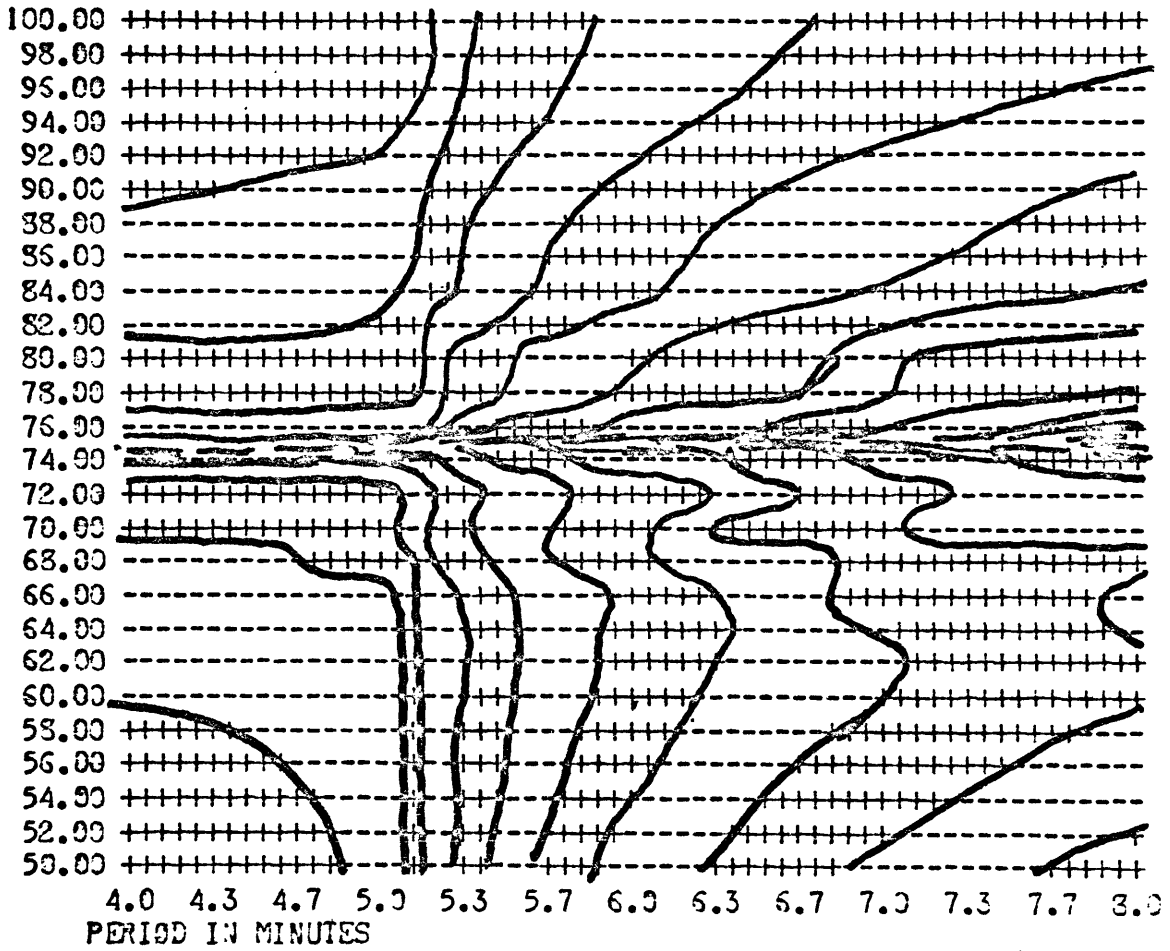


Figure II-A-1.6 This is figure 5 with an expanded phase velocity scale.

in a more realistic model, the curves of figures 5, 6, and 7 would be shifted more to the right.

In figure 7 the scales have been expanded even farther. The nearly vertical lines represent atmospheric vertical resonance. The nearly horizontal lines represent jet-stream modes. This figure has been shown merely to illustrate an academic matter. Phase velocity curves can't cross.

II-A-1.4 Vertical Group Velocity

Strictly speaking there is no way to define vertical group velocity in the medium we are considering because it can produce such strong reflections. Nevertheless energy does migrate upward from low altitude sources to high altitudes where it is dissipated. Without solving the time transient problem we can calculate reasonable measures of vertical energy transport. Consider a source at a perfectly reflecting ground overlain by a simple layer and halfspace with a 99% reflection coefficient at the halfspace. If the group travel time from the ground to the halfspace is t_0 , an observer just above the layer in the halfspace might regard $50t_0$ or $100t_0$ as a better estimate of the time for vertical energy transport than just t_0 . The time t_0 might perhaps be more accurately called a signal velocity and might very well be the appropriate velocity to consider for some experiments, but it would not be the vertical energy transport time.

PHASE VELOCITY (METERS/SEC) VERSUS PERIOD

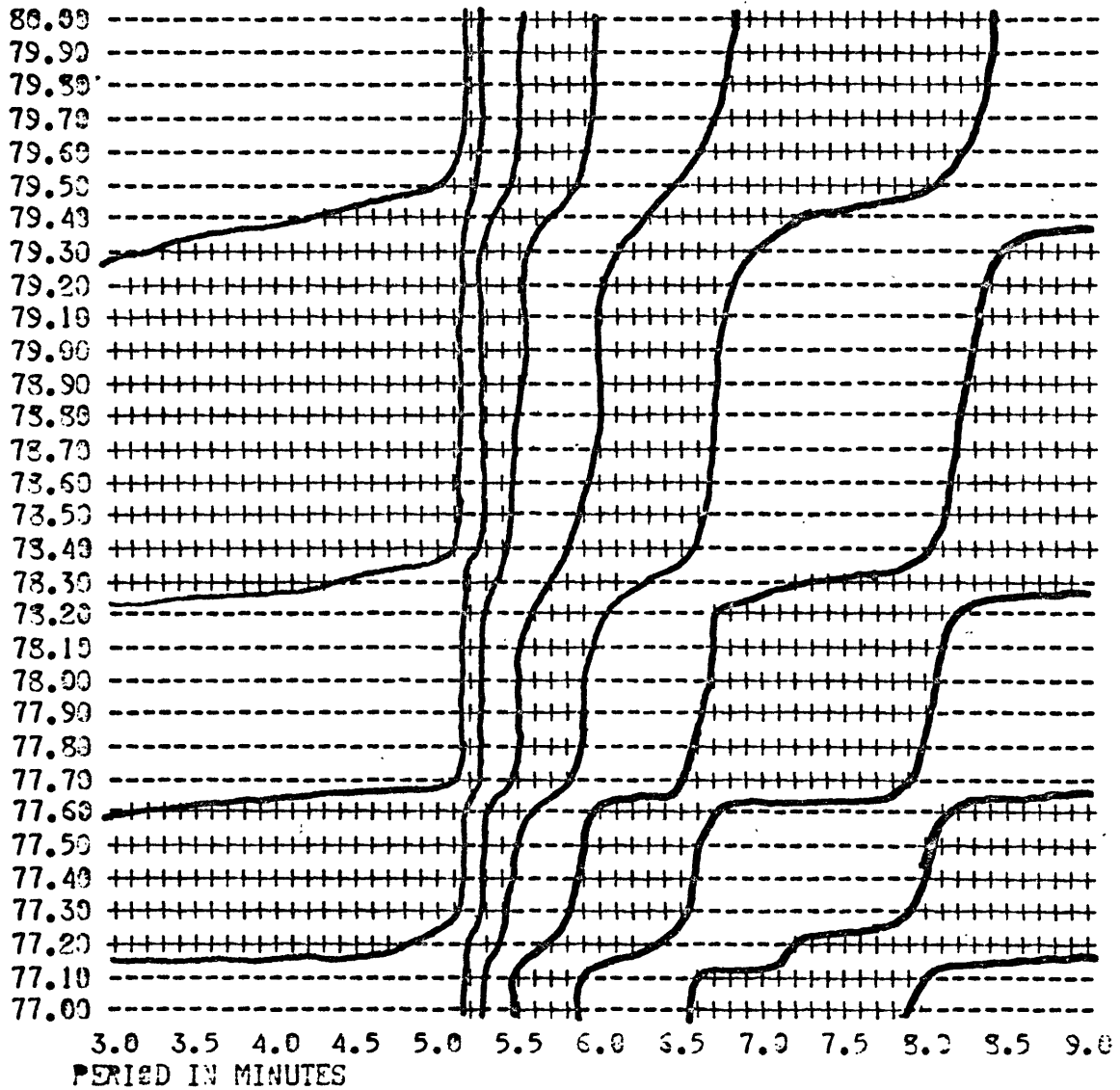


Figure II-A-1.7 This is figure 5 with an even further expansion of the phase velocity scale.

We have here defined the vertical energy travel time from the jet to an altitude h by putting a source just above the jet and a perfect, non-reflecting absorber at h . The travel time is then said to be the integral of the energy density between the two points divided by the vertical energy flux.

$$\text{energy travel time} = \frac{\int_{\text{source}}^{\text{absorber}} \text{energy density } dh}{\text{Energy flux}}$$

When this formula was calculated for the real atmosphere it was found as expected that vertical acoustic waves have just the delays ordinary ray theory would predict because the reflections are small; however for jet stream waves reflections can be very strong. This is graphed in section II-B-2 figure 1 for a range of horizontal phase speeds. The most notable thing about the graph is the very large vertical travel time taken by slow disturbances and the extreme sensitivity of vertical travel time to the horizontal velocity. In going from 60 meter/sec waves to 30 meter/sec waves the transport time to 100 kilometers altitude goes from 20 hours to 2000 hours. It is also clear that temperature gradients around eighty kilometers play a strong role in retarding the energy. Since these temperature gradients are not really well known and are thought to disappear in winter it is clear that situations could arise in which energy could propagate to the ionosphere much more rapidly

than computed in figure II-B-2. Another situation which could result in very rapid vertical transport is if the wind overlying the jet stream were in the opposite direction. This would effectively increase the horizontal phase velocity of the waves and reduce the reflecting effect of temperature gradients.

II-A-2 Particle Motions

The presentation of complicated 3-dimensional vector fields presents a challenge which is well worth taking up for the insight into the physical process which it affords. The figures in this section are computer output and the code for figuring out field direction is as follows:

- "l" indicates a vector within 30° of pointing up because a l looks a bit like a vertical arrow.
- "I" indicates a vector with 30° of point down
- "-" indicates a vector pointing to the right
- "=" indicates a vector pointing to the left
- "/" indicates a vector between 30° and 60° or between $180^\circ + 30^\circ$ and $180^\circ + 60^\circ$ with unspecified direction.
- "N" indicates a vector perpendicular to "/" because it is the best keyboard character with an upward line to the left.
- "." indicates a vector with a more than 60° component coming out of the paper because it is like the tip of an arrow as seen by the target.
- "*" indicates a vector with a more than 60° component going into the paper because it looks a bit like the feathers of an arrow as seen by the archer.

Figure 1 shows the particle motions of the Lamb wave. The wave is propagating to the right along the x-axis in a T-J model atmosphere. Below 100km one sees the horizontal particle velocities one expects, purely longitudinal. Because the thermosphere is hotter, hence lighter than the air beneath, the particles tend to burst out into the thermosphere from the point of maximum compression below. On

the figure this is at 50 kilometers on the x-axis and 100 kilometers on the z-axis.

Figure 2 shows the particle motions in the T-J model for a disturbance of a fast jet stream velocity (85 m/s) and 20 minute period. The most obvious difference with the Lamb waves is the standing wave pattern due to reflections at the thermosphere boundary. The wave is propagating to the right, and as it does the phase fronts in the ionosphere appear to move downward. The air currents are circulating and there are no obvious regions of compression and rarefaction as with the Lamb waves. For the realistic atmosphere particle motions are a great deal more complicated due to their vertical wavelength being comparable in scale to vertical changes in temperature.

Figure 3 shows particle velocities of a wave going just slightly faster than the jet at its peak. The wave propagates to the right and must be sustained by a source at the ground. Phase fronts move downward as the energy is radiated outward. The wind increases linearly (actually in 20 constant layers) to 50 meters/second at 10 km. altitude and then decreases linearly at the same rate. It is notable that the wind gradient does not seem to set up partial reflections as temperature gradients do. As the wave propagates up to the point of maximum wind velocity its frequency is doppler lowered and the phase fronts become parallel horizontal.

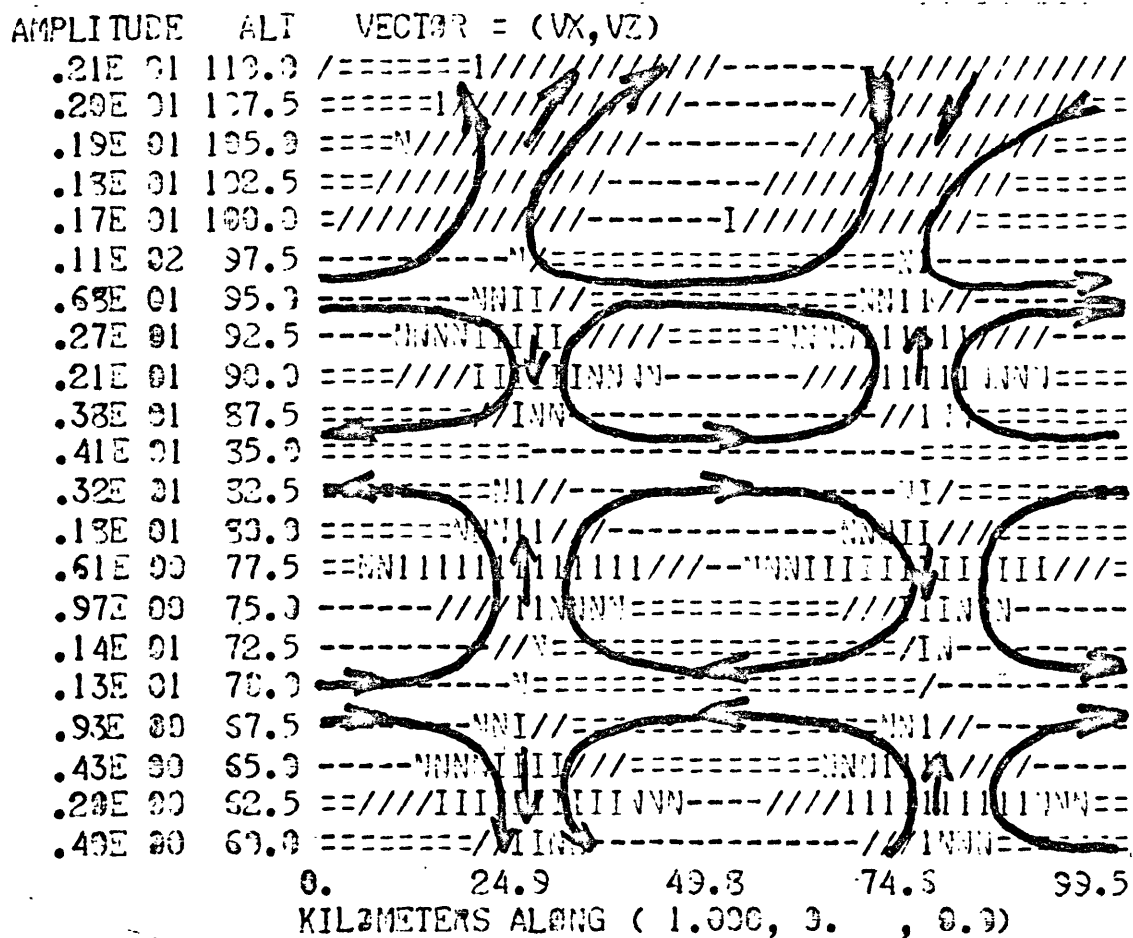


Figure II-A-2.2 Particle motions in the T-J model for a disturbance of a fast jet stream velocity (85 meters/second) and 20 minute period.

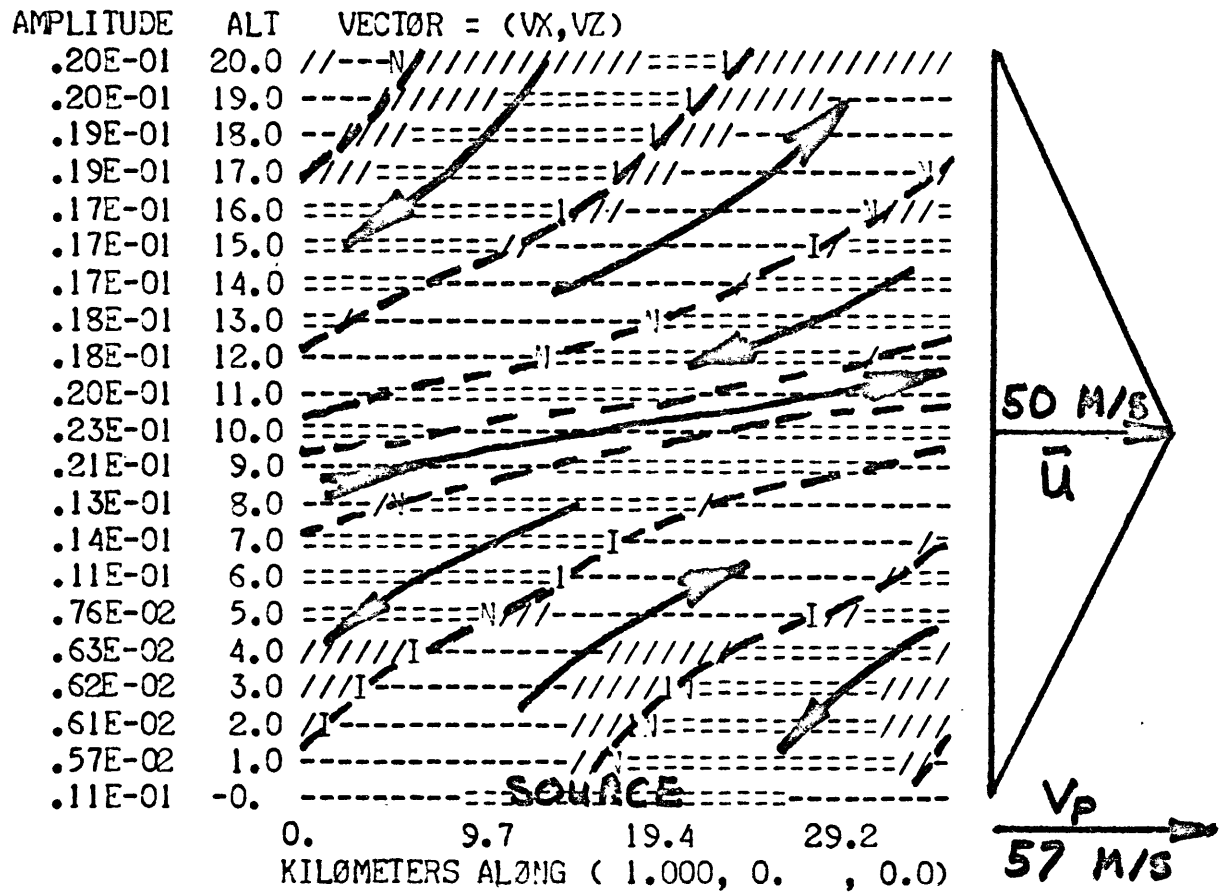


Figure II-A-2.3 Particle velocities of a wave going slightly faster than the peak speed in the jet. The wave propagates to the right and must be sustained by a source at the ground.

In figure 4 the source has been moved up to 5.5 km altitude. This has the effect of producing a standing wave pattern below it due to reflections off the ground.

In figure 5 the phase velocity has been reduced below the maximum jet speed. Thus there are 2 critical heights near 5 and 10 kilometers where the integration must pass through a singularity. (see section I-A-3) The program sidesteps this problem by putting the singularity at a layer interface. This problem was discussed theoretically in chapter I-A-3. Briefly the conclusion was that the group velocity becomes horizontal at the critical height. The source then feeds finite power into the region of the critical height and the energy density becomes so large linearity breaks down. Even before linearity breaks down, the wave has very large horizontal shears and itself violates the Richardson stability criterion at the critical height. For lack of a better approach at the present time we might then regard the critical height as a secondary source, due to the onset of some turbulent motions driven by the waves. The actual effect of this situation on the waves and the waves ability to cross these critical zones remains an important unsolved problem. We will refer to this problem again when we examine the observational data.

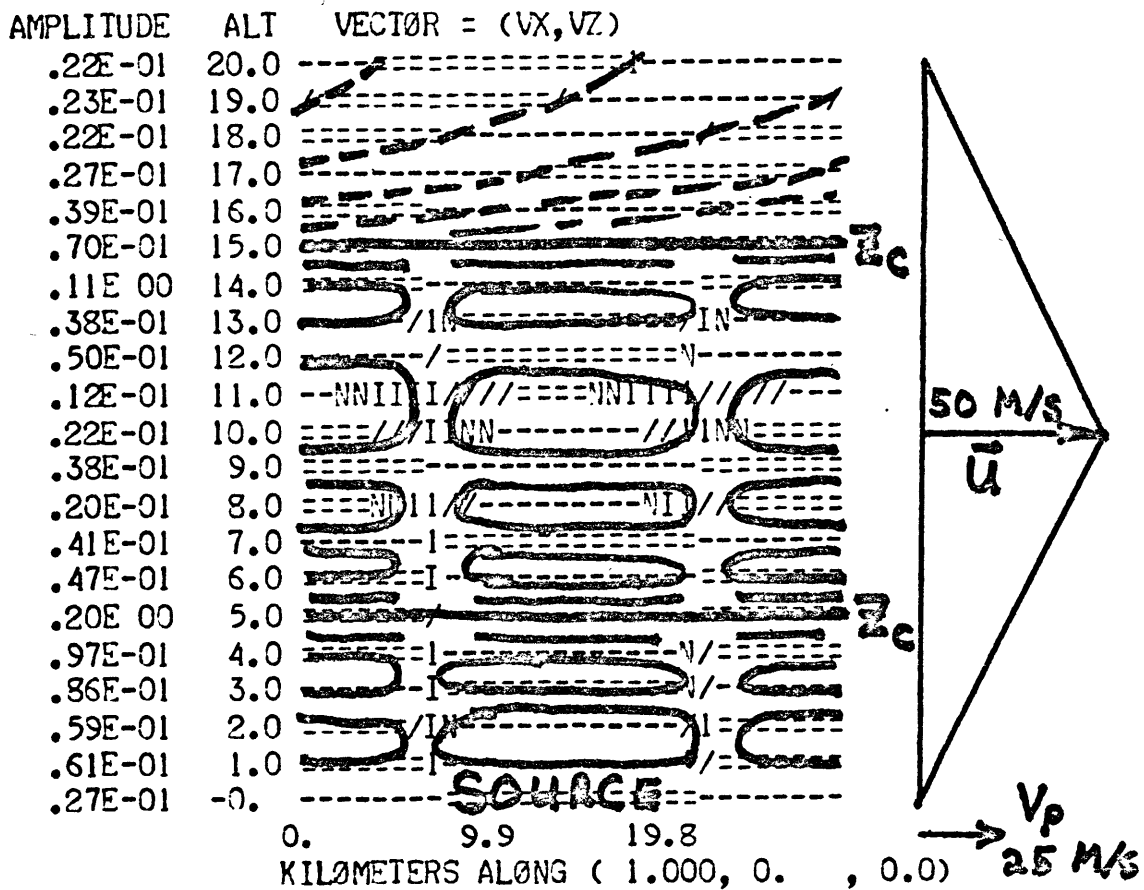


Figure II-A-2.5 Particle velocities of a wave traveling slower than the jet stream.

II-B-2 Ionospheric Winds; Two Dimensional Conductivities

A simplified way to begin the study of ionospheric winds is over a flat earth of infinite extent. Include a uniform horizontal wind and magnetic field with arbitrary inclination. Charged particles try to avoid crossing magnetic field lines, but collisions with molecules of the neutral wind will drag them along. This results in some pattern of current, voltage, ionization drift, and in a loss of the kinetic energy of the neutral wind.

There can be no vertical electric current since even a very small one would set up rapidly growing vertical electric fields. There could, however, be vertical motion of the ionization with both electrons and ions moving at the same velocity. Of course, if one envisions a steady state, this implies that ionization is taking place at one level and recombination at another.

In this section we consider B , E_x , E_y , V_x , and V_y to be prescribed. Along with the assumption that J_z and V_z vanish, we can calculate the complete state of the atmosphere E_z , J_x , J_y , D_x , D_y , D_z , ∇P . The dragging causes a pressure gradient ∇P and the rate of energy dissipation is $-V_3 \cdot \nabla P$. The kinetic energy of the neutral gas is $\frac{1}{2} \rho (V_3 \cdot V_3)$ so the energy decay time is $-\frac{\rho (V_3 \cdot V_3)}{2(V_3 \cdot \nabla P)}$.

We begin with the conductivity from I-B-3.19 and

abbreviate σ^{JE} by σ and σ^{JV} by τ

$$(1) \quad \begin{bmatrix} J_x \\ J_y \\ J_z \end{bmatrix} = \begin{bmatrix} \sigma_{xx} & \sigma_{xy} & \sigma_{xz} \\ \sigma_{yx} & \sigma_{yy} & \sigma_{yz} \\ \sigma_{zx} & \sigma_{zy} & \sigma_{zz} \end{bmatrix} \begin{bmatrix} E_x \\ E_y \\ E_z \end{bmatrix} + \begin{bmatrix} \tau_{xx} & \tau_{xy} & \tau_{xz} \\ \tau_{yx} & \tau_{yy} & \tau_{yz} \\ \tau_{zx} & \tau_{zy} & \tau_{zz} \end{bmatrix} \begin{bmatrix} V_x \\ V_y \\ V_z \end{bmatrix}$$

with $V_z = 0$ the equation $J_z = 0$ gives

$$(2) \quad 0 = \begin{bmatrix} \sigma_{zx} & \sigma_{zy} \end{bmatrix} \begin{bmatrix} E_x \\ E_y \end{bmatrix} + \sigma_{zz} E_z + \begin{bmatrix} \tau_{zx} & \tau_{zy} \end{bmatrix} \begin{bmatrix} V_x \\ V_y \end{bmatrix}$$

Solve for E_z

$$(3) \quad E_z = \frac{-1}{\sigma_{zz}} \left\{ \begin{bmatrix} \sigma_{zx} & \sigma_{zy} \end{bmatrix} \begin{bmatrix} E_x \\ E_y \end{bmatrix} + \begin{bmatrix} \tau_{zx} & \tau_{zy} \end{bmatrix} \begin{bmatrix} V_x \\ V_y \end{bmatrix} \right\}$$

Now (3) may be reintroduced into (1)

$$(4) \quad \begin{bmatrix} J_x \\ J_y \end{bmatrix} = \left\{ \begin{bmatrix} \sigma_{xx} & \sigma_{xy} \\ \sigma_{yx} & \sigma_{yy} \end{bmatrix} - \frac{1}{\sigma_{zz}} \begin{bmatrix} \sigma_{xz} \\ \sigma_{yz} \end{bmatrix} \begin{bmatrix} \sigma_{zx} & \sigma_{zy} \end{bmatrix} \right\} \begin{bmatrix} E_x \\ E_y \end{bmatrix} + \left\{ \begin{bmatrix} \tau_{xx} & \tau_{xy} \\ \tau_{yx} & \tau_{yy} \end{bmatrix} - \frac{1}{\sigma_{zz}} \begin{bmatrix} \tau_{xz} \\ \tau_{yz} \end{bmatrix} \begin{bmatrix} \sigma_{zx} & \sigma_{zy} \end{bmatrix} \right\} \begin{bmatrix} V_x \\ V_y \end{bmatrix}$$

which is the desired 2-dimensional conductivity expression.

It is straightforward to derive a similar expression for ionization drift, say $\vec{D} = \sigma^{DE} \vec{E} + \sigma^{DV} \vec{V}$. Some vertical drifts can be quite large; for example, when \vec{B} is at 45° in the X-Z plane and the neutral wind is in the X direction. Then at high altitudes the vertical component of drift is half the horizontal wind speed. At altitudes where collisions are sufficiently rare a charged particle just follows a field line after a collision. It can go upward about a scale height before it is returned by gravity which we have neglected. When the particle slides back down the field line and recollides with the neutral gas, it will be moving in a direction opposite to the neutral wind and therefore create a greater dissipation than we have calculated. It would seem that this enhanced dissipation could not exceed the dissipation of a vertical B field.

Next we calculate the extent to which charged particles are dragged along by the neutral wind.

We have the basic definitions

$$(5) \quad \begin{aligned} J &= ne (V_1 - V_2) \\ D &= \frac{1}{2} (V_1 - V_3) \end{aligned}$$

which we invert to give

$$(6) \quad \begin{aligned} V_1 &= D + J/(2ne) \\ V_2 &= D - J/(2ne) \end{aligned}$$

A measure of the relative motion is given by dotting V_3

into (6) and dividing by $(V_3 \cdot V_3)$.

$$(7) \quad \frac{V_3 \cdot V_1}{V_3 \cdot V_3} = \frac{1}{V_3 \cdot V_3} \left[V_3 \cdot D + V_3 \cdot J / (2ne) \right]$$

$$\frac{V_3 \cdot V_2}{V_3 \cdot V_3} = \frac{1}{V_3 \cdot V_3} \left[V_3 \cdot D - V_3 \cdot J / (2ne) \right]$$

Terms on the right are computed from (4) and its analog for drifts. Quantities of interest have been profiled and are presented in tables (2) and (3) for various orientations of the vectors during the mean-solar daylight conditions (table (1)).

Table II-B-1.1 Table of ionospheric properties used in ionospheric wind calculations.

THE MEAN SOLAR DAYTIME ATMOSPHERE

ALT KM	NEUTRAL TEMP	ELECTRON TEMP	MOLEC WEIGHT	CP/CV GAMMA	SOUND SPEED
200	1235	1700	26.0	1.46	768
190	1181	1600	26.2	1.45	747
180	1123	1500	26.4	1.45	726
170	1074	1400	26.5	1.44	705
160	1020	1300	26.8	1.44	684
150	866	1200	27.0	1.44	627
140	712	970	27.2	1.43	566
130	531	740	27.4	1.43	486
120	350	510	27.6	1.43	393
110	280	280	27.8	1.42	350
100	210	220	28.0	1.42	301
90	185	160	28.1	1.42	282
80	160	160	28.2	1.41	262
70	203	203	28.3	1.41	294
60	247	247	28.4	1.41	323
50	290	290	28.5	1.41	350
40	264	288	28.6	1.41	333
30	238	286	28.7	1.41	315
20	225	284	28.8	1.40	306
10	225	282	28.9	1.40	305
-00	280	280	29.0	1.40	340

ALT	PRESSURE	DENSITY	ELECTRONS
200	.103E-03	.285E-09	.316E 12
190	.139E-03	.402E-09	.282E 12
180	.187E-03	.567E-09	.251E 12
170	.252E-03	.800E-09	.224E 12
160	.339E-03	.113E-08	.200E 12
150	.500E-03	.199E-08	.178E 12
140	.737E-03	.352E-08	.165E 12
130	.142E-02	.965E-08	.153E 12
120	.272E-02	.265E-07	.142E 12
110	.919E-02	.115E-06	.132E 12
100	.310E-01	.502E-06	1.000E 11
90	.190E 00	.352E-05	1.000E 10
80	.115E 01	.247E-04	.316E 10
70	.534E 01	.930E-04	1.000E 09
60	.245E 02	.350E-03	1.000E 08
50	.113E 03	.132E-02	.316E 08
40	.413E 03	.536E-02	1.000E 07
30	.152E 04	.218E-01	.316E 07
20	.610E 04	.922E-01	1.000E 06
10	.268E 05	.405E 00	.316E 06
-00	.101E 06	.122E 01	1.000E 05

Table II-B-1.2

ATMOSPHERIC EFFECTS OF HORIZONTAL WIND VX=1 METER/SEC

B=30*(0. 1.0000 0.)									
H	EZ	DZ	JX	JY	V3.V1	V3.V2	DISP,	HOURS	
200	-.600E-04	.175E-09	.103E-18	-.000E 00	1.000E 00	1.000E 00	.192E	08	
150	-.600E-04	-.466E-09	.347E-17	-.000E 00	1.000E 00	1.000E 00	.349E	09	
125	-.600E-04	-.000E 00	.111E-15	-.000E 00	1.000E 00	1.000E 00	.510E	08	
105	-.600E-04	-.466E-09	-.000E 00	-.000E 00	1.000E 00	1.000E 00	.149E	09	
90	-.600E-04	-.186E-08	.139E-16	-.000E 00	1.000E 00	1.000E 00	.950E	09	
75	-.600E-04	-.745E-08	.173E-17	-.000E 00	1.000E 00	1.000E 00	.107E	11	
60	-.600E-04	-.466E-08	.673E-20	-.000E 00	.100E 01	1.000E 00	.117E	16	
40	-.600E-04	-.291E-09	.165E-23	-.000E 00	.100E 01	1.000E 00	.103E	17	
B=30*(0. 0. 1.0000)									
H	EZ	DZ	JX	JY	V3.V1	V3.V2	DISP,	HOURS	
200	.000E 00	-.000E 00	.116E-10	-.766E-09	.229E-03	.482E-06	.361E	00	
150	.000E 00	-.000E 00	.303E-09	-.293E-08	.107E-01	.302E-05	.153E	01	
125	.000E 00	-.000E 00	.955E-08	-.116E-07	.405E 00	.287E-04	.319E	01	
105	.000E 00	-.000E 00	.202E-07	-.172E-08	.993E 00	.307E-04	.323E	03	
90	.000E 00	-.000E 00	.160E-08	-.841E-10	1.000E 00	.221E-02	.909E	05	
75	.000E 00	-.000E 00	.194E-09	-.133E-09	1.000E 00	.317E 00	.336E	06	
60	.000E 00	-.000E 00	.461E-12	-.268E-11	.100E 01	.971E 00	.303E	09	
40	.000E 00	-.000E 00	.174E-15	-.167E-13	.100E 01	1.000E 00	.744E	12	
B=30*(.7070 .7070 0.)									
H	EZ	DZ	JX	JY	V3.V1	V3.V2	DISP,	HOURS	
200	-.424E-04	.116E-09	.349E-14	-.103E-18	.100E 01	.100E 01	.300E	00	
150	-.424E-04	-.466E-09	.917E-13	-.347E-17	1.000E 00	1.000E 00	.610E	04	
125	-.424E-04	.186E-08	.289E-11	-.555E-16	1.000E 00	1.000E 00	.111E	05	
105	-.424E-04	-.000E 00	.610E-11	.000E 00	1.000E 00	1.000E 00	.112E	07	
90	-.424E-04	-.140E-08	.483E-12	-.208E-16	1.000E 00	1.000E 00	.244E	09	
75	-.424E-04	-.559E-08	.537E-13	-.173E-17	1.000E 00	1.000E 00	.200E	10	
60	-.424E-04	-.326E-08	.139E-15	-.339E-20	1.000E 00	1.000E 00	.277E	12	
40	-.424E-04	-.175E-09	.524E-19	-.827E-24	1.000E 00	1.000E 00	.383E	13	
B=30*(.7070 0. .7070)									
H	EZ	DZ	JX	JY	V3.V1	V3.V2	DISP,	HOURS	
200	.603E-10	.502E 00	.116E-10	-.542E-09	.503E 00	.502E 00	.173E	01	
150	.653E-10	.495E 00	.303E-09	-.297E-08	.505E 00	.435E 00	.315E	01	
125	.116E-07	.293E 00	.955E-08	-.820E-08	.702E 00	.298E 00	.630E	01	
105	.249E-06	.361E-02	.202E-07	-.128E-08	.997E 00	.366E-02	.616E	03	
90	.281E-05	.275E-03	.159E-08	-.112E-09	1.000E 00	.468E-02	.103E	06	
75	.212E-04	.145E-03	.148E-09	-.142E-09	1.000E 00	.432E 00	.110E	07	
60	.509E-05	.477E-05	.234E-12	-.192E-11	.100E 01	.935E 00	.596E	09	
40	.312E-06	.192E-07	.368E-16	-.118E-13	1.000E 00	1.000E 00	.107E	13	
B=30*(0. .7070 .7070)									
H	EZ	DZ	JX	JY	V3.V1	V3.V2	DISP,	HOURS	
200	-.565E-10	.107E-01	.116E-10	-.198E-08	.229E-03	.115E-05	.861E	00	
150	-.891E-09	.725E-01	.303E-09	-.414E-08	.107E-01	.135E-04	.158E	01	
125	-.200E-07	.347E 00	.955E-08	-.164E-07	.405E 00	.264E-03	.319E	01	
105	-.391E-07	.579E-01	.202E-07	-.244E-03	.993E 00	.385E-03	.323E	03	
90	-.209E-06	.392E-02	.159E-08	-.119E-09	1.000E 00	.466E-02	.971E	05	
75	-.205E-04	.159E-03	.148E-09	-.142E-09	1.000E 00	.482E 00	.110E	07	
60	-.418E-04	.577E-06	.234E-12	-.192E-11	.100E 01	.985E 00	.596E	09	
40	-.424E-04	-.291E-10	.868E-16	-.118E-13	.100E 01	1.000E 00	.149E	13	
B=30*(.5770 .5770 .5770)									
H	EZ	DZ	JX	JY	V3.V1	V3.V2	DISP,	HOURS	
200	-.686E-10	.343E 00	-.430E-09	-.884E-09	.335E 00	.343E 00	.129E	01	
150	-.133E-08	.389E 00	-.139E-08	-.338E-08	.340E 00	.399E 00	.236E	01	
125	-.128E-07	.481E 00	.236E-08	-.134E-07	.603E 00	.432E 00	.478E	01	
105	.212E-06	.490E-01	.192E-07	-.204E-08	.996E 00	.494E-01	.473E	03	
90	.255E-05	.348E-02	.159E-08	-.140E-09	1.000E 00	.103E-01	.101E	06	
75	-.312E-05	.215E-03	.119E-09	-.140E-09	1.000E 00	.582E 00	.137E	07	
60	-.309E-04	.351E-05	.157E-12	-.158E-11	.100E 01	.990E 00	.388E	09	
40	-.344E-04	.126E-07	.580E-16	-.963E-14	.100E 01	1.000E 00	.223E	13	

IONOSPHERIC EFFECTS OF HORIZONTAL E-FIELD, EX=1 VOLT/METER
 B=30*(0. 1.0000 0.)

H	EZ	JX	JY	DX	DY	DZ	GRADP/P
200	.151E-01	.128E-04	.000E 00	-.126E 03	-.000E 00	.167E 05	-.127E-10
150	.104E 00	.489E-04	.000E 00	-.864E 03	-.000E 00	.167E 05	-.327E-08
125	.824E 00	.193E-03	.000E 00	-.686E 04	-.000E 00	.167E 05	-.155E-05
105	.117E 02	.287E-04	.000E 00	-.976E 05	-.000E 00	.159E 05	-.852E-04
90	.190E 02	.140E-05	.000E 00	-.158E 06	-.000E 00	.176E 04	-.144E-04
75	.147E 01	.221E-05	.000E 00	-.122E 05	-.000E 00	.100E 02	-.140E-06
60	.172E 00	.447E-07	.000E 00	-.143E 04	-.000E 00	.161E 00	-.283E-10
40	.104E-01	.273E-09	.000E 00	-.867E 02	-.000E 00	.640E-03	-.593E-15

B=30*(0. 0. 1.0000)

H	EZ	JX	JY	DX	DY	DZ	GRADP/P
200	-.000E 00	.123E-04	.193E-06	.126E 03	-.167E 05	-.000E 00	.112E-06
150	-.000E 00	.483E-04	.500E-05	.855E 03	-.166E 05	-.000E 00	.697E-06
125	-.000E 00	.193E-03	.159E-03	.409E 04	-.133E 05	-.000E 00	.436E-05
105	-.000E 00	.287E-04	.336E-03	.637E 03	-.839E 04	-.000E 00	.120E-05
90	-.000E 00	.140E-05	.266E-04	-.345E 03	-.832E 04	-.000E 00	.842E-03
75	-.000E 00	.221E-05	.324E-05	-.388E 04	-.569E 04	-.000E 00	.781E-10
60	-.000E 00	.447E-07	.769E-08	-.139E 04	-.240E 03	-.000E 00	.188E-13
40	-.000E 00	.278E-09	.289E-11	-.367E 02	-.903E 00	-.000E 00	.553E-18

B=30*(.7070 .7070 0.)

H	EZ	JX	JY	DX	DY	DZ	GRADP/P
200	.107E-01	.969E 01	.959E 01	-.945E 03	-.945E 03	.118E 05	.446E-13
150	.733E-01	.249E 01	.232E 01	-.407E 03	-.407E 03	.118E 05	.166E-02
125	.592E 00	.649E 00	.410E 00	-.858E 07	-.857E 07	.118E 05	.300E-02
105	.828E 01	.376E 00	.386E-01	-.105E 07	-.948E 06	.112E 05	.730E-02
90	.134E 02	.409E-02	.300E-04	-.163E 06	-.937E 04	.125E 04	.131E-03
75	.104E 01	.795E-05	.209E-08	-.122E 05	-.367E 01	.703E 01	.257E-03
60	.122E 00	.454E-07	.223E-12	-.143E 04	-.694E-02	.114E 00	-.126E-10
40	.736E-02	.278E-09	.533E-17	-.867E 02	-.166E-05	.452E-03	-.294E-15

B=30*(.7070 0. .7070)

H	EZ	JX	JY	DX	DY	DZ	GRADP/P
200	-1.000E 00	.959E 01	.273E-06	-.100E 01	-.236E 05	-.253E 03	.420E-01
150	-1.000E 00	.232E 01	.715E-05	-.000E 00	-.234E 05	-.171E 04	.145E-01
125	-1.000E 00	.410E 00	.225E-03	-.325E 01	-.153E 05	-.817E 04	.516E-02
105	-.999E 00	.403E-01	.476E-03	-.691E 02	-.119E 05	-.134E 04	.335E-03
90	-.995E 00	.303E-03	.376E-04	-.780E 03	-.117E 05	-.923E 02	.354E-05
75	-.518E 00	.577E-05	.348E-05	-.539E 04	-.610E 04	-.354E 01	.711E-07
60	-.146E-01	.454E-07	.552E-03	-.141E 04	-.172E 03	-.137E-01	.195E-11
40	-.541E-04	.278E-09	.205E-11	-.867E 02	-.638E 00	-.333E-05	.249E-17

B=30*(0. .7070 .7070)

H	EZ	JX	JY	DX	DY	DZ	GRADP/P
200	.142E-07	.123E-04	.273E-06	.126E 03	-.118E 05	.118E 05	.112E-06
150	.154E-05	.483E-04	.715E-05	.855E 03	-.118E 05	.117E 05	.637E-06
125	.274E-03	.193E-03	.225E-03	.408E 04	-.118E 05	.792E 04	.475E-05
105	.537E-02	.273E-04	.476E-03	.603E 03	-.118E 05	.851E 02	.113E-05
90	.662E-01	.155E-06	.376E-04	-.734E 03	-.117E 05	.651E 01	-.024E-07
75	.499E 00	.137E-05	.348E-05	-.538E 04	-.610E 04	.341E 01	-.672E-07
60	.120E 00	.440E-07	.552E-03	-.141E 04	-.172E 03	.112E 00	-.234E-10
40	.736E-02	.278E-09	.205E-11	-.867E 02	-.638E 00	.452E-03	-.592E-15

B=30*(.5770 .5770 .5770)

H	EZ	JX	JY	DX	DY	DZ	GRADP/P
200	-1.000E 00	.253E-04	.131E-04	.961E 04	-.194E 05	.936E 04	.439E-05
150	-1.000E 00	.103E-03	.575E-04	.951E 04	-.200E 05	.786E 04	.402E-05
125	-.999E 00	.570E-03	.469E-03	.572E 04	-.214E 05	-.244E 04	.106E-04
105	-.992E 00	.444E-03	.699E-03	-.407E 02	-.151E 05	-.107E 04	.963E-05
90	-.912E 00	.321E-04	.460E-04	-.117E 04	-.144E 05	-.943E 00	.334E-06
75	.753E-01	.377E-05	.348E-05	-.711E 04	-.692E 04	.519E 00	-.327E-03
60	.836E-01	.443E-07	.452E-03	-.142E 04	-.141E 03	.931E-01	-.171E-13
40	.597E-02	.278E-09	.167E-11	-.367E 02	-.521E 00	.367E-03	-.392E-15

II-B-2 Gravity Wave Dissipation and Heating

Quantitatively, the energy lost by the neutrals due to their interaction with charged particles is $-\nabla p \cdot V$, which is determined by dotting V_3 into formula (I-B-2.8c)

$$\begin{aligned}
 (1) \quad \frac{\nabla p}{\rho} &= \nu_{31} V_1 + \nu_{32} V_2 + \nu_{33} V_3 \\
 &= (\nu_{31} + \nu_{32}) \left(\frac{V_1 + V_2}{2} \right) + (\nu_{31} - \nu_{32}) \left(\frac{V_1 - V_2}{2} \right) + \nu_{33} V_3 \\
 &= (\nu_{31} + \nu_{32}) D + (\nu_{31} - \nu_{32}) J / (2ne) + (-\nu_{31} - \nu_{32}) V_3
 \end{aligned}$$

$$\frac{\nabla p \cdot V_3^*}{\rho (V_3 \cdot V_3^*)} = (\nu_{31} + \nu_{32}) \left(\frac{D \cdot V_3^*}{V_3 \cdot V_3^*} - 1 \right) + \frac{(\nu_{31} - \nu_{32})}{2ne} \frac{J \cdot V_3^*}{V_3 \cdot V_3^*}$$

$$(2) \quad \text{decay time } T = - \frac{\rho (V_3 \cdot V_3^*)}{(\nabla p \cdot V_3^*)}$$

In the case that p and V_3 are coefficients of exponentially varying functions in space or time the asterisk refers to complex conjugate and one takes the real part of the expression. Profiles of dissipation rate (1) have been computed for a variety of acoustic gravity wave modes. Generally the profile is within a factor of 2 or so of the profile of dissipation rate of ionospheric winds. However, for the modes the dissipation is not so smooth a function of altitude due to the vertical wavelengths of the modes.

In fact, at some altitudes electromagnetic effects may be acting to strengthen the gravity wave rather than diminish it.

As a mechanism for dissipation of acoustic gravity waves electromagnetic effects are fairly independent of frequency and wave-number quite unlike dissipation due to heat conduction and molecular viscosity.

A comparison of the results of this thesis with Midgley and Liemohn's calculation of viscons damping shows that electromagnetic dissipation is more important for all velocities comparable to the jet stream. At some lower velocity (shorter vertical wavelength) these must become equal but exact comparison is difficult due to differences in techniques and thermal models.

Finally we come to the heating of the ionosphere by energy lost from ionospheric winds and gravity waves. Along with wind profiles and the specific heat C_p everything needed is a profile of formula (1) or (2) because the heating rate is

$$\begin{aligned} \text{heating reat} &= - \frac{\nabla p \cdot V_3}{\rho C_p} \quad \text{degrees C/sec} \\ \text{heating time} &= - \frac{\rho C_p}{\nabla p \cdot V_3} = \frac{C_p T}{V_3 \cdot V_3} = \frac{10^3 T}{V_3 \cdot V_3} \quad \text{sec/degree C} \end{aligned}$$

Since T is actually graphed in units of hours we may also read the same graph as hours to raise the temperature one degree if the time axis is scaled by $10^3/V^2$.

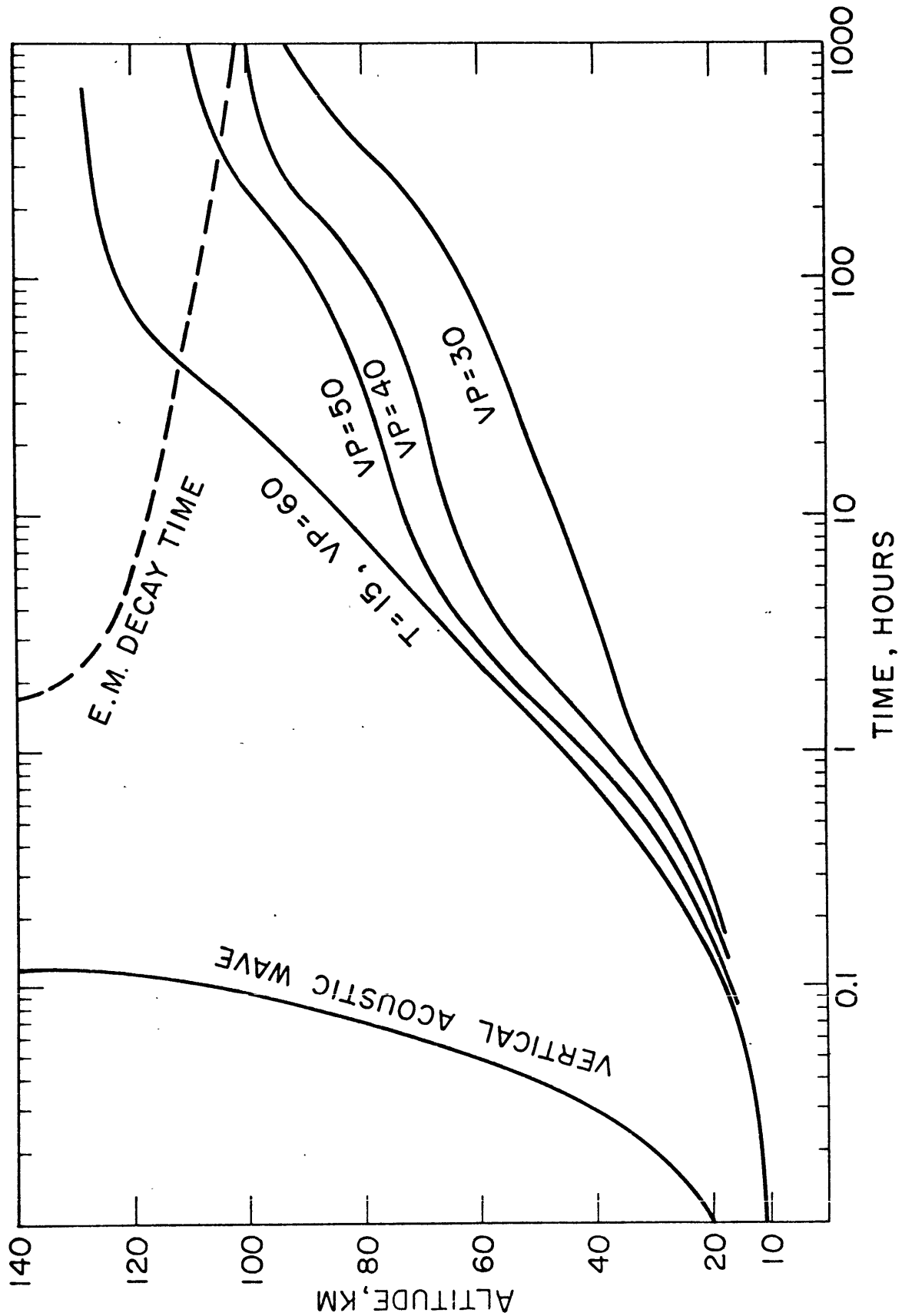


Figure II-B-2.1 Vertical energy transport time for acoustic gravity waves originating in the jet stream.

Since ionospheric winds of 100 meters/sec at 125 km altitude are fairly typical where decay times are typically 20 hours we get

$$\text{heating time} = \frac{10^3 \cdot 20}{100^2} = 2 \text{ hours/degree centigrade}$$

Gravity waves associated with the jet stream are dissipated at about 110 ± 10 km. altitude where the vertical group velocity is 50 hours per kilometer and the decay time is 300 hours. Both observations and modal calculations agree that 100 meters/sec is a reasonable particle velocity at that altitude and this implies a heating rate of 30 hours per degree. Due to uncertainties in the altitude and velocity magnitude involved the reliability of this number is taken to be an order of magnitude.

II-B-3 Electromagnetic Effects of the Lamb Wave

Figure 1 shows the particle motions of the Lamb wave in a realistic temperature model.

The amplitude of the vectors is scaled to correspond to what we consider the quietest atmospheric conditions, an r.m.s. pressure at the ground of 10 microbars. Everything scales linearly. Multiply by a factor of 10 to get typical noise amplitudes observed on the ground (100 microbars) or by a factor of 50 to get unusually large amplitudes (.5 millibar). All vector amplitudes are in rationalized MKS units.

Subsequent figures are calculated from the theory developed in section I-B-4. Superposed on the T-J model we have a uniform magnetic field at 45° in the x - z plane. The wave we are considering is traveling southward at midlatitude in the northern hemisphere. The neutral particles collide with charged particles and tend to drag them along. This is depicted in figure 2. At high altitudes however, the charged particles tend to follow magnetic field lines. In figure 3 we see the electric fields induced by the Lamb wave. At high altitudes the electric fields tend to be perpendicular to the magnetic field due to the high conductivity along field lines. At low altitudes charge concentration produces a divergence of E which is clearly apparent on the figure at

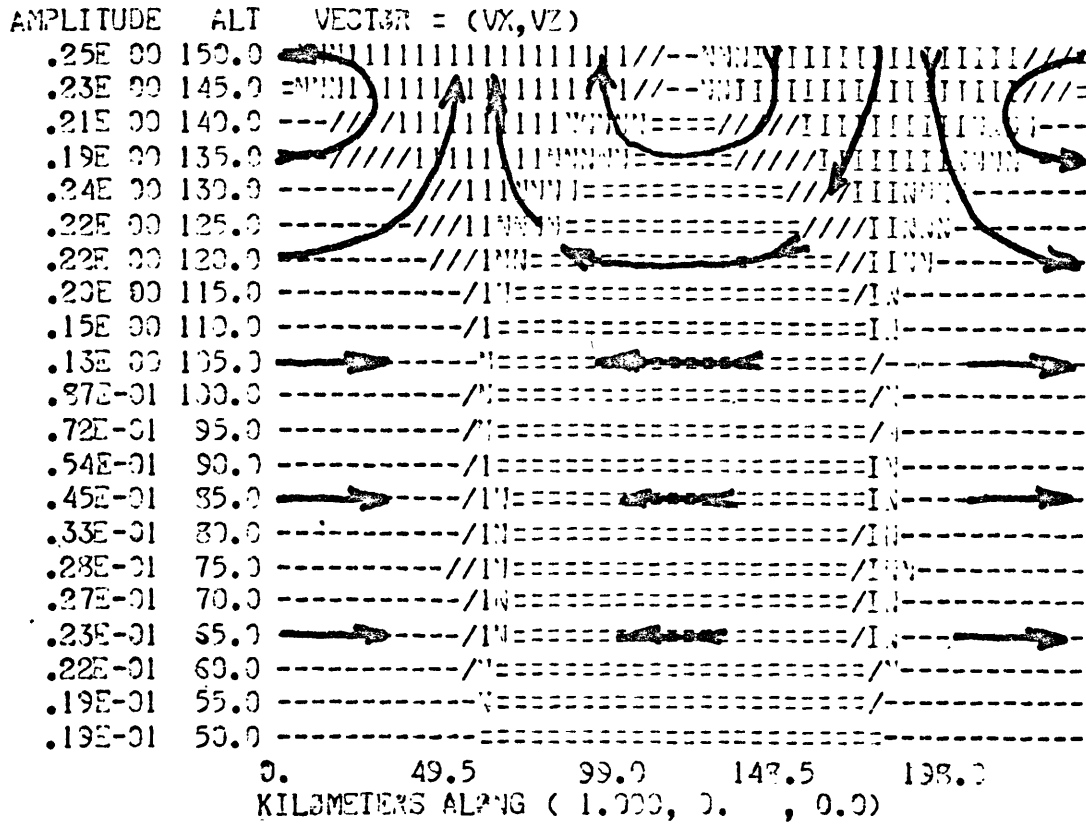


Figure II-B-3.1 Particle velocities (MKS Units) for a Lamb wave propagating along the x-axis in a realistic atmosphere.

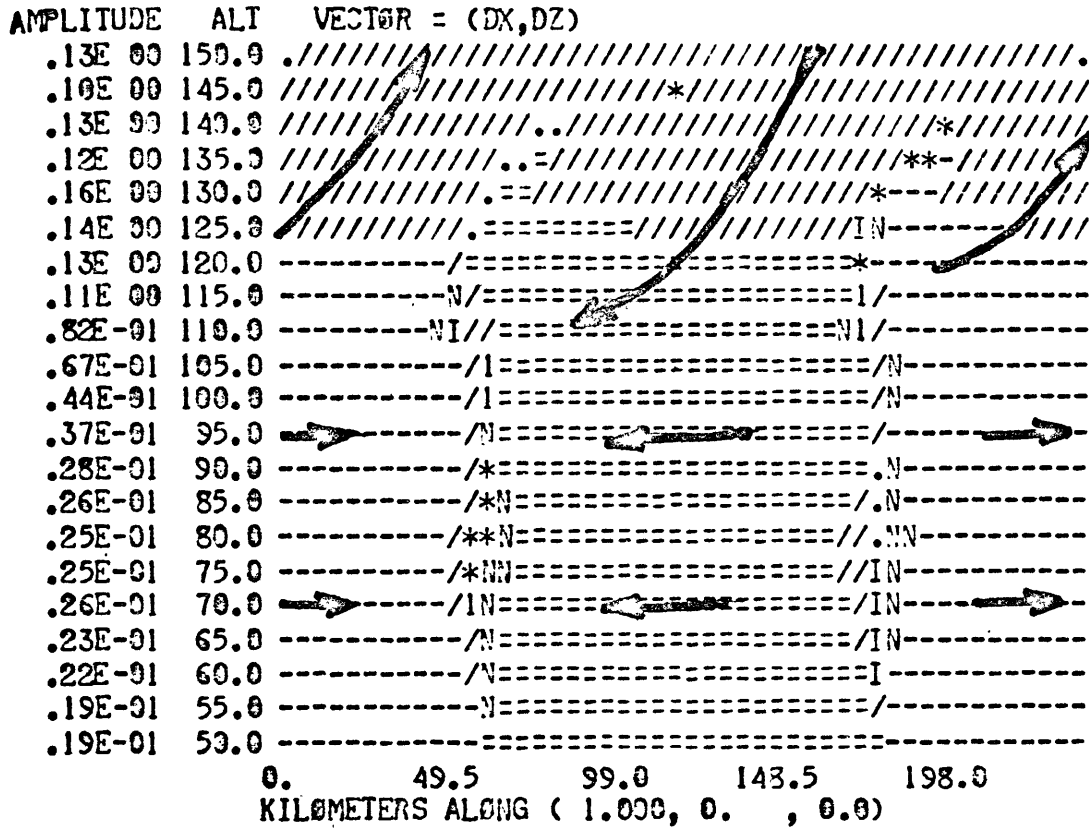


Figure II-B-3.2 Drift = $(V_{ion} + V_{electron}) / 2$ in meters/sec induced by the Lamb wave in figure 1. Drift follows neutrals at low altitude and follows magnetic field lines at high altitudes.

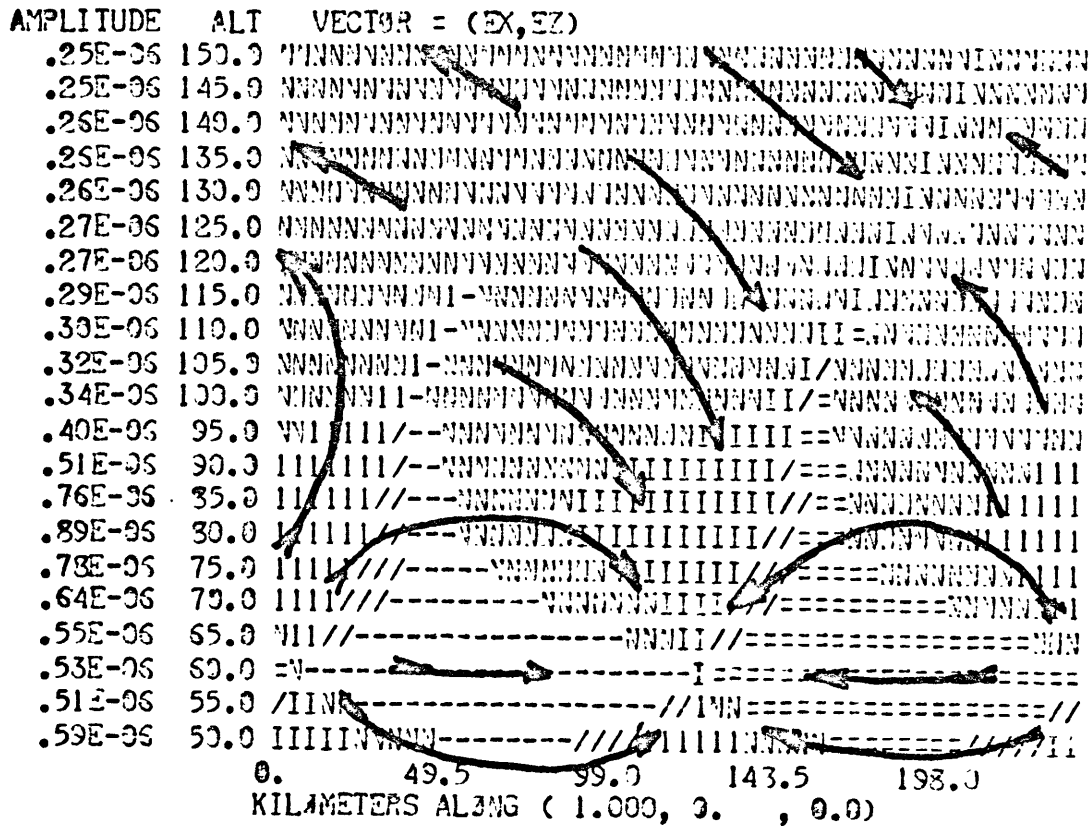


Figure II-B-3.3 Electric fields induced by the Lamb wave. The induced electric fields are perpendicular to the magnetic field at high altitude. At low altitude charge concentration gives a divergence of E .

10 and 135 kilometers on the x-axis.

Figure 4 shows the induced electrical currents. They behave somewhat like the charged particle drift but differ at low altitudes because they are influenced in addition by the electric fields. Figure 5 shows the induced magnetic fields. One may crudely verify $\text{curl } H=J$ by comparison of figures 4 and 5. Near the bottom one sees the magnetic field satisfying $\text{curl } H=0$.

Figure 6 shows the electrical effects of the Lamb wave fo figure 1 propagating toward the east.

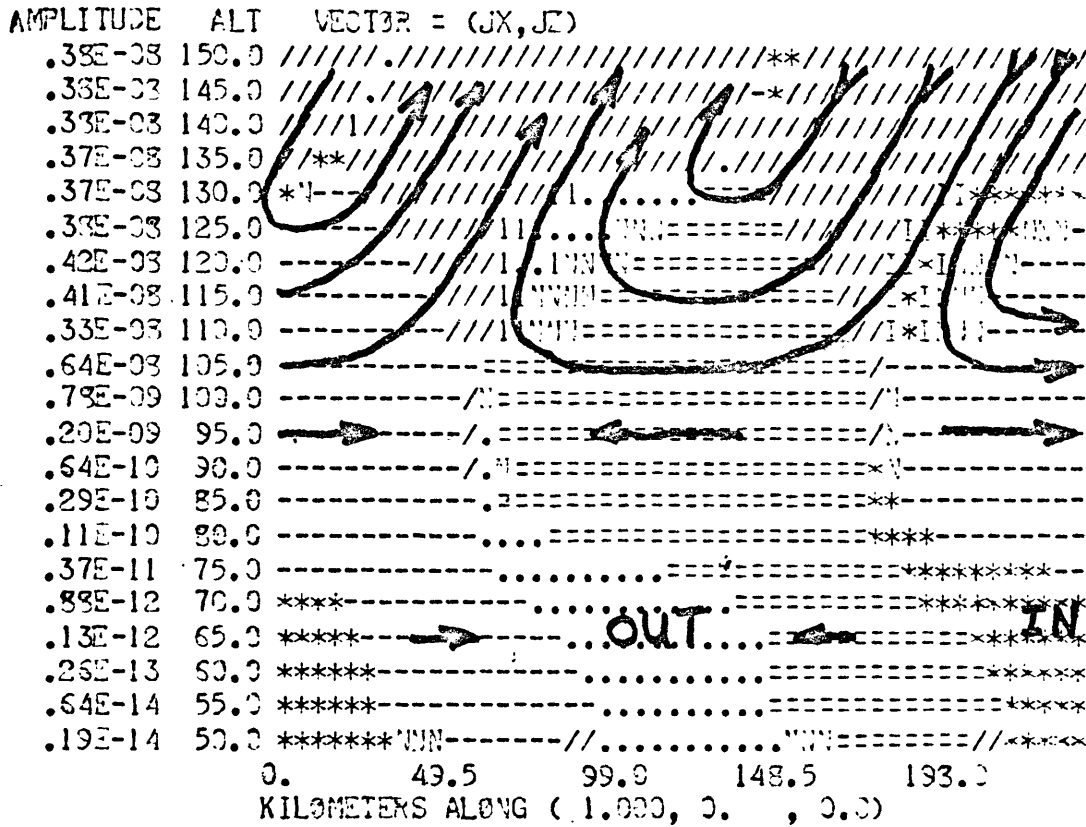


Figure II-B-3.4 Electric currents induced by the Lamb wave. The electrical currents behave like the drifts except at low altitude where electric fields influence the currents.

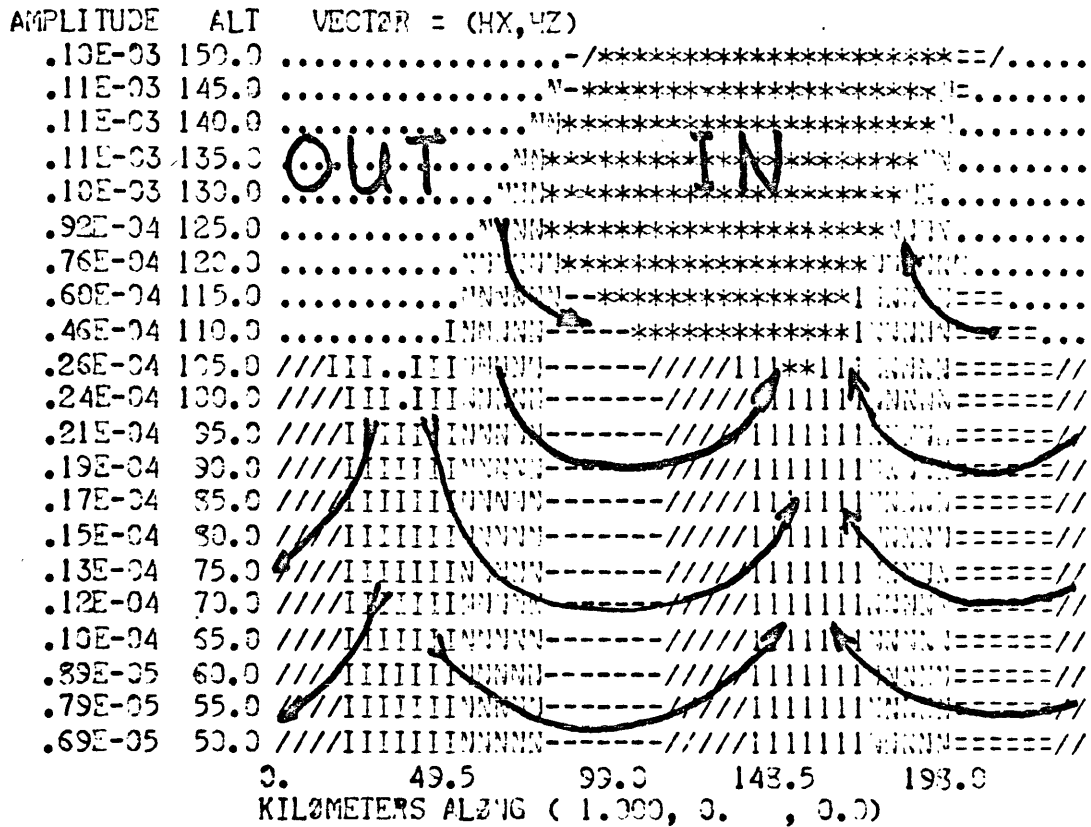
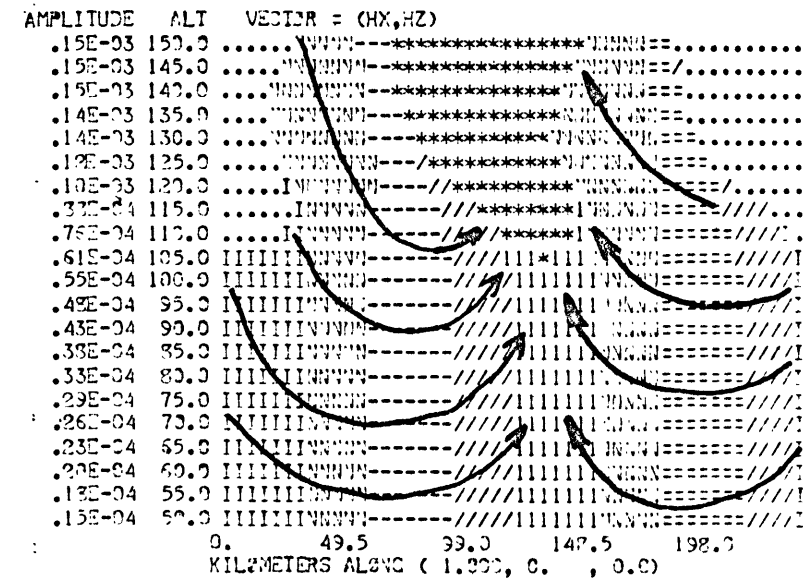
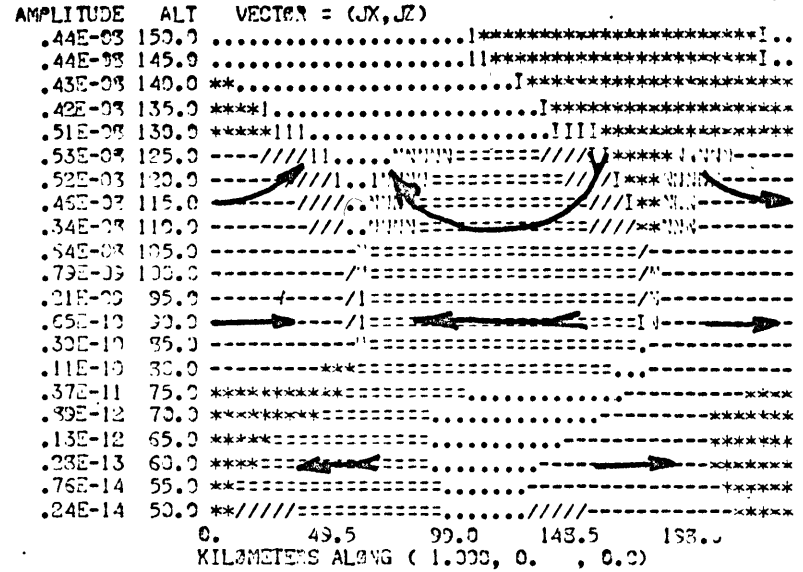
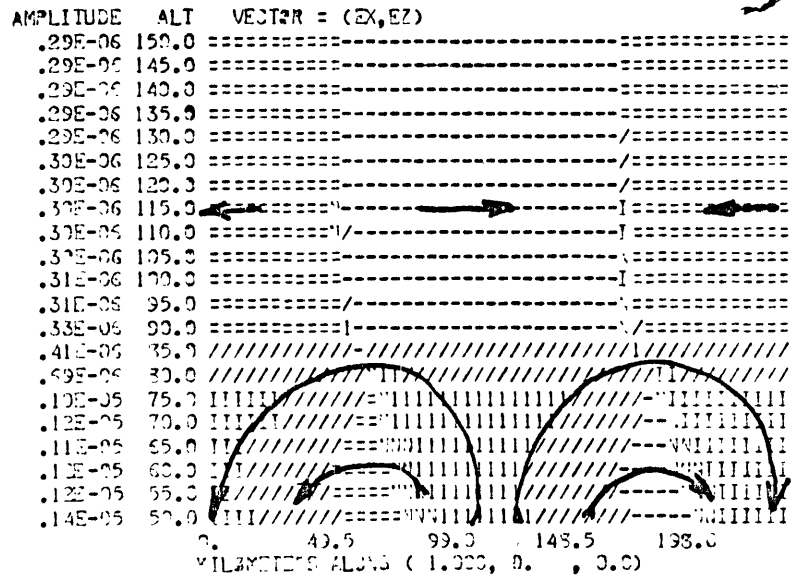
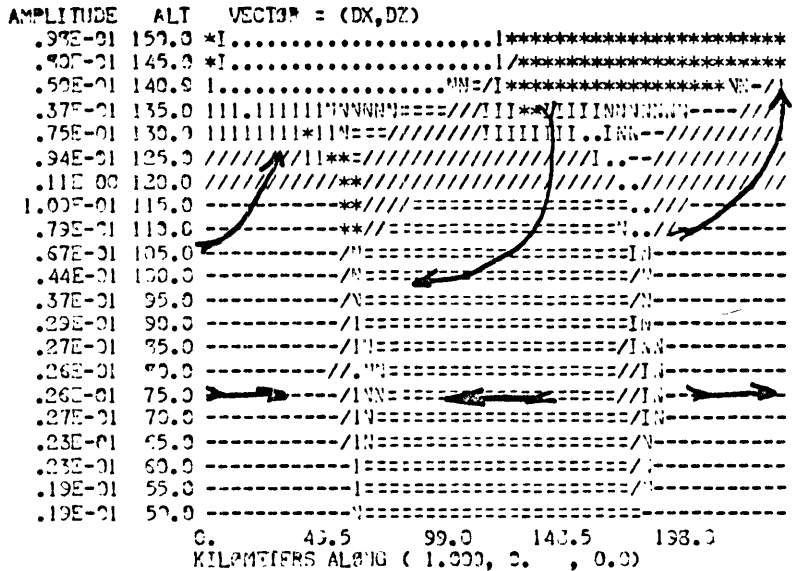


Figure II-B-3.5 The magnetic field induced by the Lamb wave. The magnetic fields are obtained by solving curl H=J. This may be qualitatively verified by comparison with figure 3.4 .

Figure II-B-3.6 The electrical effects of the Lamb wave of Figure 1 propagating toward the east.



II-B-4 The Westerly Jet Wave

The jet stream in our locality is usually from the west. In this section we show the calculated electromagnetic effects of this wave. Figure 1 shows the T-J model for a wave of 20 minute period wave propagating at 85 meters/second. (A more typical velocity would be 50 meters/second but 85 makes a clearer presentation.) Figure 2 shows the same wave with a realistic temperature profile. In these calculations some quite crude approximations have been made which invalidate the results at high altitude. Since the gravity waves are damped out around 110 kilometers altitude but the modal solutions have neglected the damping, the current sources have been neglected above 120 kilometers. A more correct procedure would follow the outline of section I-B-5. In view of the substantial differences which could also result by changing the period, phase velocity, and thermal or ionization structure it does not appear that the extra effort of the method of I-B-5 would be adequately rewarded.

The fairly large difference between the T-J model and the realistic model arises because the T-J model has an unrealistic temperature jump at 100 kilometers and this is a crucial altitude for the electrical phenomena.

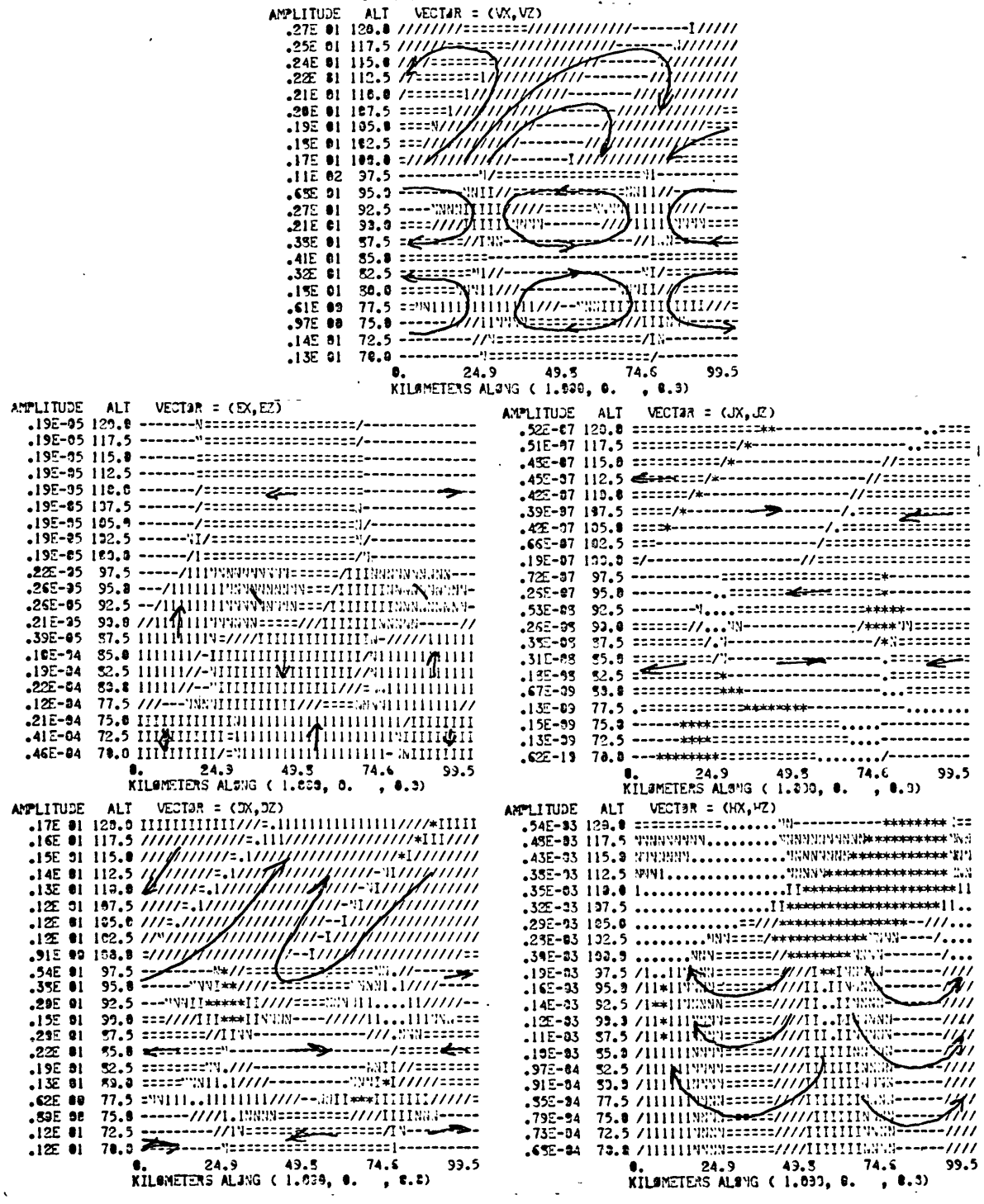


Figure II-B-4.1 Electrical effects of jet wave in T-J model.

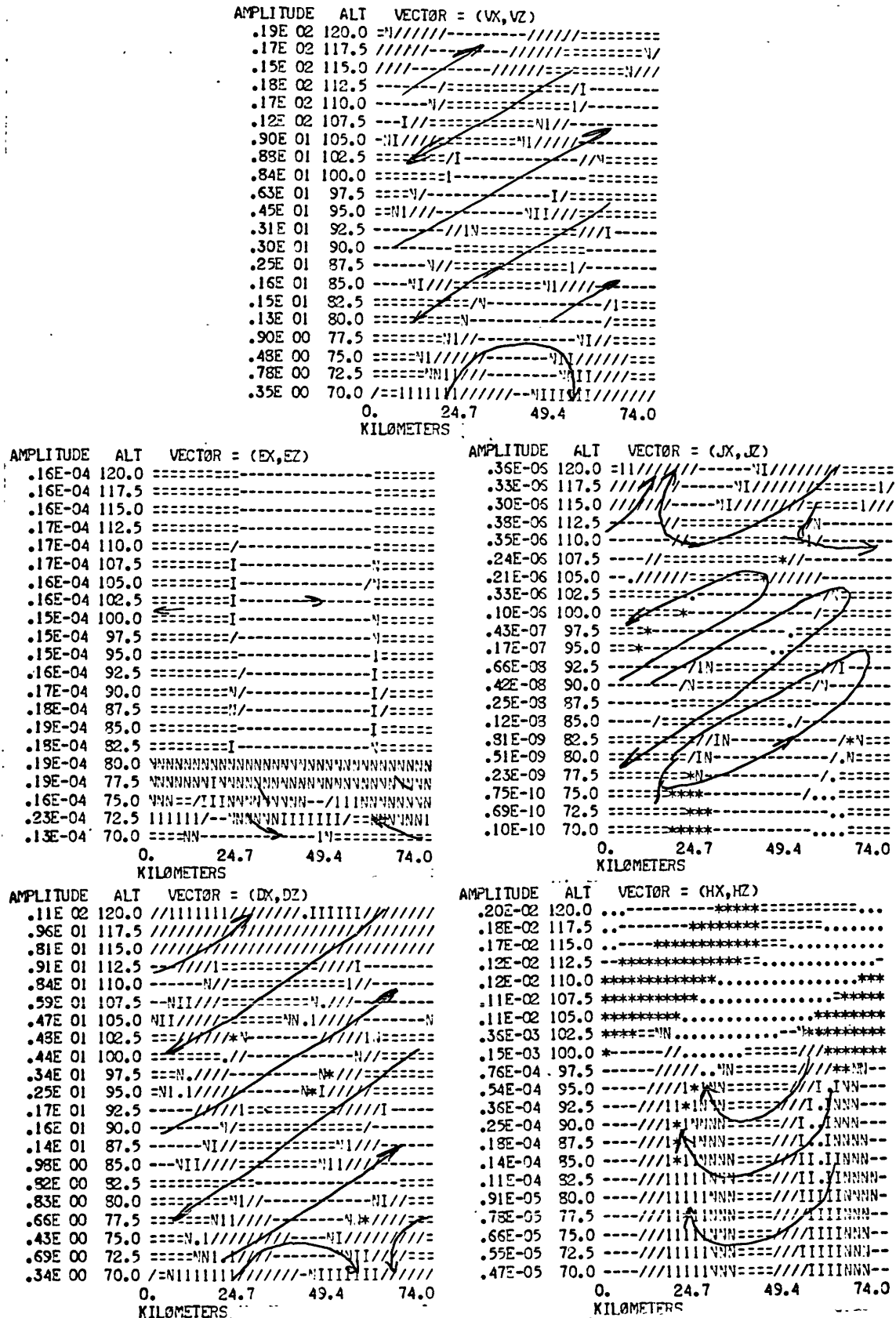


Figure II-B-4.2 Electrical effects of jet wave in realistic model.

II-B-5 Finite Transverse Wavelength

In all of the mathematics so far we have considered plane wave disturbances when in fact the observations we have made of the jet waves indicate that the coherence between microbarograph time series perpendicular to the wave velocity (transverse coherence) was far from unity as one would expect for plane waves. In fact the transverse coherence was usually less than the coherence in the direction of propagation (longitudinal coherence.) Thus one might interpret our observations as standing wave patterns in the y direction which are moving in the x direction. For a jet in the x direction at a speed V_x one might say we observe waves with a given $v_x = \omega/\lambda_x$ and a range of $\pm k_y$. The k_y dependence in the acoustic equations appears in the terms $(k_x^2 + k_y^2)$ and $(\Omega = \omega - \lambda \cdot \bar{u})$, so a solution to a problem with $k_y = 0$ would be almost like one for k_y small. One feels that although introducing k_y may produce quantitative differences it will not produce anything unexpected. The situation in the electromagnetic case is not nearly so obvious. Electrical currents obviously cannot go off to infinity in the transverse direction. How will the potential, drift, and the magnetic field change when the currents are forced to circulate by a cosine or sine y -dependence? What we have done in this section is to

solve two problems, one for $+k_y$ and one for $-k_y$. Due to the arbitrary orientation of the earth's magnetic field with respect to the propagation direction these two problems may have very different solutions. Adding the two solutions

φ_+ and φ_- we get

$$\begin{aligned} \varphi_+ e^{+ik_y y + i(k_x x - \omega t)} + \varphi_- e^{-ik_y y + i(k_x x - \omega t)} &= \\ = \left[(\varphi_+ + \varphi_-) \left(\frac{e^{ik_y y} + e^{-ik_y y}}{2} \right) + i (\varphi_+ - \varphi_-) \left(\frac{e^{ik_y y} - e^{-ik_y y}}{2i} \right) \right] e^{i(k_x x - \omega t)} \\ = \left[(\varphi_+ + \varphi_-) \cos k_y y + i (\varphi_+ - \varphi_-) \sin k_y y \right] e^{i(k_x x - \omega t)} \end{aligned}$$

For the acoustic variables $\tilde{p}, \tilde{p}, \tilde{u}$, and \tilde{w} where the propagation is parallel to the wind ($\tilde{u}_y = 0$) the coefficient of the sine vanishes by the equivalence of $+k_y$ and $-k_y$ in the equations. Thus a single "snapshot" of the x-z plane at $y = 0$ is sufficient to show what is going on. The acoustic variable \tilde{v} is antisymmetric in $\pm k_y$ so it has sine k_y y-dependence where \tilde{u} has cosine k_y y-dependence. Thus air parcels circulate in the x-y plane. For the electromagnetic variables the situation is more complex, both the sine and the cosine dependence being important. Thus for e.m. variables two "snapshots" are presented, one at

$y = 0$ and one at $y = \pi/2$.

Now that we recognize that the solutions are sums and differences of solutions we have already seen we do not expect orders of magnitude differences to result from forcing current loops to close. For the sake of completeness we present figure 1. The cosine dependence is on the left and the sine dependence is on the right.

```

AMPLITUDE ALT VECTOR = (W,VZ)
.23E-00 120.0 ////////////////
.21E-00 117.5 ////////////////
.19E-00 115.0 ////////////////
.27E-00 112.5 ////////////////
.21E-00 110.0 ////////////////
.28E-00 107.5 ////////////////
.22E-00 105.0 ////////////////
.27E-00 102.5 ////////////////
.19E-00 100.0 ////////////////
.31E-00 97.5 ////////////////
.19E-00 95.0 ////////////////
.31E-00 92.5 ////////////////
.16E-00 90.0 ////////////////
.17E-00 87.5 ////////////////
.16E-00 85.0 ////////////////
.56E-01 82.5 ////////////////
.49E-01 80.0 ////////////////
.23E-01 77.5 ////////////////
.31E-01 75.0 ////////////////
.20E-01 72.5 ////////////////
.13E-01 70.0 ////////////////
0. 24.7 49.4 74.0
KILOMETERS ALONG ( 1.000, 0. , 0.0)

```

```

AMPLITUDE ALT VECTOR = (X,Z)
.17E-00 120.0 ////////////////
.15E-00 117.5 ////////////////
.11E-00 115.0 ////////////////
.13E-00 112.5 ////////////////
.16E-00 110.0 ////////////////
.15E-00 107.5 ////////////////
.99E-01 105.0 ////////////////
.14E-00 102.5 ////////////////
.12E-00 100.0 ////////////////
.16E-00 97.5 ////////////////
.13E-00 95.0 ////////////////
.16E-00 92.5 ////////////////
.11E-00 90.0 ////////////////
.93E-01 87.5 ////////////////
.95E-01 85.0 ////////////////
.36E-01 82.5 ////////////////
.35E-01 80.0 ////////////////
.20E-01 77.5 ////////////////
.27E-01 75.0 ////////////////
.20E-01 72.5 ////////////////
.14E-01 70.0 ////////////////
0. 24.7 49.4 74.0
KILOMETERS ALONG ( 1.000, 0. , 0.0)

```

```

AMPLITUDE ALT VECTOR = (E,Z)
.25E-06 120.0 ////////////////
.30E-06 117.5 ////////////////
.37E-06 115.0 ////////////////
.41E-06 112.5 ////////////////
.43E-06 110.0 ////////////////
.49E-06 107.5 ////////////////
.52E-06 105.0 ////////////////
.43E-06 102.5 ////////////////
.43E-06 100.0 ////////////////
.37E-06 97.5 ////////////////
.33E-06 95.0 ////////////////
.73E-06 92.5 ////////////////
.11E-05 90.0 ////////////////
.74E-06 87.5 ////////////////
.97E-06 85.0 ////////////////
.89E-06 82.5 ////////////////
.94E-06 80.0 ////////////////
.38E-06 77.5 ////////////////
.93E-06 75.0 ////////////////
.79E-06 72.5 ////////////////
.69E-06 70.0 ////////////////
0. 24.7 49.4 74.0
KILOMETERS ALONG ( 1.000, 0. , 0.0)

```

```

AMPLITUDE ALT VECTOR = (U,VZ)
.44E-08 120.0 ////////////////
.40E-08 117.5 ////////////////
.38E-08 115.0 ////////////////
.56E-08 112.5 ////////////////
.37E-08 110.0 ////////////////
.68E-08 107.5 ////////////////
.74E-08 105.0 ////////////////
.11E-07 102.5 ////////////////
.19E-07 100.0 ////////////////
.20E-07 97.5 ////////////////
.49E-07 95.0 ////////////////
.65E-07 92.5 ////////////////
.19E-07 90.0 ////////////////
.19E-07 87.5 ////////////////
.12E-07 85.0 ////////////////
.26E-07 82.5 ////////////////
.14E-07 80.0 ////////////////
.43E-07 77.5 ////////////////
.61E-07 75.0 ////////////////
.24E-07 72.5 ////////////////
.77E-07 70.0 ////////////////
0. 24.7 49.4 74.0
KILOMETERS ALONG ( 1.000, 0. , 0.0)

```

```

AMPLITUDE ALT VECTOR = (X,HZ)
.33E-04 120.0 ////////////////
.23E-04 117.5 ////////////////
.23E-04 115.0 ////////////////
.40E-04 112.5 ////////////////
.29E-04 110.0 ////////////////
.43E-04 107.5 ////////////////
.45E-04 105.0 ////////////////
.63E-04 102.5 ////////////////
.14E-04 100.0 ////////////////
.12E-04 97.5 ////////////////
.29E-05 95.0 ////////////////
.50E-05 92.5 ////////////////
.18E-05 90.0 ////////////////
.95E-06 87.5 ////////////////
.84E-06 85.0 ////////////////
.93E-06 82.5 ////////////////
.41E-06 80.0 ////////////////
.27E-06 77.5 ////////////////
.19E-06 75.0 ////////////////
.14E-06 72.5 ////////////////
1.00E-07 70.0 ////////////////
0. 24.7 49.4 74.0
KILOMETERS ALONG ( 1.000, 0. , 0.0)

```

```

AMPLITUDE ALT VECTOR = (W,VZ)
.26E-00 120.0 ////////////////
.24E-00 117.5 ////////////////
.21E-00 115.0 ////////////////
.39E-00 112.5 ////////////////
.19E-00 110.0 ////////////////
.43E-00 107.5 ////////////////
.24E-00 105.0 ////////////////
.41E-00 102.5 ////////////////
.17E-00 100.0 ////////////////
.43E-00 97.5 ////////////////
.10E-00 95.0 ////////////////
.46E-00 92.5 ////////////////
.24E-00 90.0 ////////////////
.23E-00 87.5 ////////////////
.51E-01 85.0 ////////////////
.69E-01 80.0 ////////////////
.93E-02 77.5 ////////////////
.47E-01 75.0 ////////////////
.24E-01 72.5 ////////////////
1.00E-02 70.0 ////////////////
0. 24.7 49.4 74.0
KILOMETERS ALONG ( 1.000, 0. , 0.0)

```

```

AMPLITUDE ALT VECTOR = (X,Z)
.13E-00 120.0 ////////////////
.15E-00 117.5 ////////////////
.19E-00 115.0 ////////////////
.26E-00 112.5 ////////////////
.13E-00 110.0 ////////////////
.17E-00 107.5 ////////////////
.87E-01 105.0 ////////////////
.21E-00 102.5 ////////////////
.70E-01 100.0 ////////////////
.23E-00 97.5 ////////////////
.37E-01 95.0 ////////////////
.23E-00 92.5 ////////////////
.34E-01 90.0 ////////////////
.13E-00 87.5 ////////////////
.13E-00 85.0 ////////////////
.44E-01 82.5 ////////////////
.42E-01 80.0 ////////////////
.98E-02 77.5 ////////////////
.42E-01 75.0 ////////////////
.24E-01 72.5 ////////////////
.76E-02 70.0 ////////////////
0. 24.7 49.4 74.0
KILOMETERS ALONG ( 1.000, 0. , 0.0)

```

```

AMPLITUDE ALT VECTOR = (E,Z)
.35E-06 120.0 ////////////////
.35E-06 117.5 ////////////////
.33E-06 115.0 ////////////////
.29E-06 112.5 ////////////////
.29E-06 110.0 ////////////////
.29E-06 107.5 ////////////////
.35E-06 105.0 ////////////////
.67E-06 102.5 ////////////////
.74E-06 100.0 ////////////////
.56E-06 97.5 ////////////////
.54E-06 95.0 ////////////////
.19E-05 92.5 ////////////////
.94E-06 90.0 ////////////////
.18E-05 87.5 ////////////////
.33E-05 85.0 ////////////////
.89E-07 82.5 ////////////////
.13E-05 80.0 ////////////////
.39E-06 77.5 ////////////////
.10E-05 75.0 ////////////////
.77E-06 72.5 ////////////////
.59E-06 70.0 ////////////////
0. 24.7 49.4 74.0
KILOMETERS ALONG ( 1.000, 0. , 0.0)

```

```

AMPLITUDE ALT VECTOR = (U,VZ)
.66E-08 120.0 ////////////////
.64E-08 117.5 ////////////////
.51E-08 115.0 ////////////////
.63E-08 112.5 ////////////////
.34E-08 110.0 ////////////////
.11E-07 107.5 ////////////////
.53E-08 105.0 ////////////////
.15E-07 102.5 ////////////////
.26E-08 100.0 ////////////////
.31E-08 97.5 ////////////////
.54E-09 95.0 ////////////////
.99E-09 92.5 ////////////////
.16E-09 90.0 ////////////////
.23E-09 87.5 ////////////////
.13E-09 85.0 ////////////////
.45E-10 82.5 ////////////////
.29E-10 80.0 ////////////////
.19E-11 77.5 ////////////////
.69E-11 75.0 ////////////////
.23E-11 72.5 ////////////////
.82E-12 70.0 ////////////////
0. 24.7 49.4 74.0
KILOMETERS ALONG ( 1.000, 0. , 0.0)

```

```

AMPLITUDE ALT VECTOR = (X,HZ)
.55E-04 120.0 ////////////////
.43E-04 117.5 ////////////////
.35E-04 115.0 ////////////////
.25E-04 112.5 ////////////////
.12E-04 110.0 ////////////////
.15E-04 107.5 ////////////////
.28E-04 105.0 ////////////////
.40E-04 102.5 ////////////////
.51E-05 100.0 ////////////////
.75E-05 97.5 ////////////////
.42E-05 95.0 ////////////////
.27E-05 92.5 ////////////////
.73E-05 90.0 ////////////////
.90E-05 87.5 ////////////////
.71E-06 85.0 ////////////////
.53E-06 82.5 ////////////////
.32E-06 80.0 ////////////////
.22E-06 77.5 ////////////////
.16E-06 75.0 ////////////////
.12E-06 72.5 ////////////////
.89E-07 70.0 ////////////////
0. 24.7 49.4 74.0
KILOMETERS ALONG ( 1.000, 0. , 0.0)

```

Figure II-B-5.1 Electrical effects of westerly jet wave with a 50 kilometer traverse wavelenth. Because of the short vertical wavelenth the vector fields are nearly aliased on this presentation.

III. Data Acquisition and Interpretation

The purpose of this chapter is to describe the data, typical and atypical, and to show how the most coherent data is associated with the jet stream. To begin with we describe the instrumentation, both the microbarographs and the overall system. Then a two weeks stretch of data is presented and interpreted to give an idea of the frequency of jet stream observations, other observations, and instrumentation problems. Finally we will consider the jet phenomena more closely, its spectrum, its coherency in space and its time variations and show how these tie in with the theory derived in preceding chapters.

III-A Instrumentation

We have been recording 3-30 minute period atmospheric pressure variation in eastern Massachusetts for about a year. The map on figure 1 shows the four recording sites at Bedford, Weston, Cambridge, and Groton (the same as Millstone Hill). We have since discovered that a quite similar array was set up by Flauraud, Mears, Crowley, and Crary in 1954.

Figure 2 gives an overall view of our data collection and analysis hardware. Signals are sent directly over DC telephone lines to our laboratory from the pressure observation stations. The pressure transducer at MIT is not in our building because of the interference caused by elevators and central air conditioning. The pressure transducers in Bedford and Weston are in the basements of private homes and the transducer at Groton is in a warehouse. No spatial filtering at the transducers was attempted because of the long wavelengths (more than 10 kilometers) of interest in this thesis.

The digitizer and tape recorder are shared with other experiments so digital data was collected at irregular intervals amounting in total to about 1/3 of the year. This data is sorted on cards. Analog multiplexed recordings were made continuously and some examples are shown in the next section.

The microbarograph is depicted in figure 3. A dif-

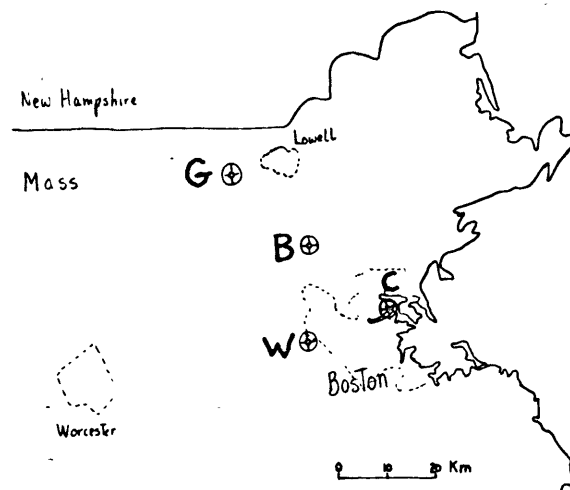
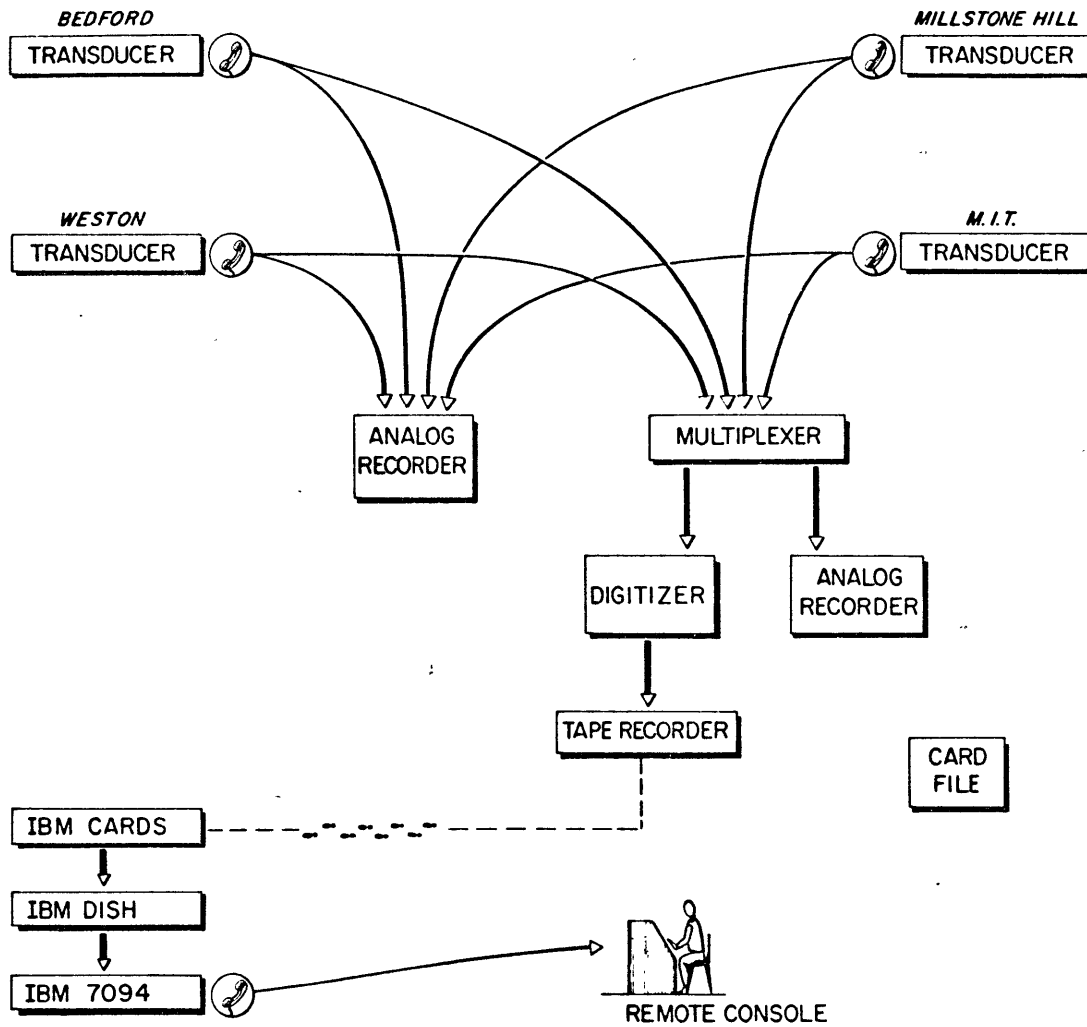


Figure 1 Map showing pressure recording sites

Figure III-A-1



COLLECTION AND ANALYSIS OF MICROBAROGRAPH
ARRAY DATA

Figure III-A-2

ferential pressure measurement is made between two air reservoirs which leak at different rates. The differential pressure is measured by a Sanborn model 270-300 gas pressure transducer. The manufacturer's functional diagram is shown in figure 4. The air reservoirs are two 16 oz. glass bottles which leak to the atmosphere through stainless steel capillary tubing. One bottle leaks with a time constant of 36 seconds and the other with a constant of 15 minutes. Consequently the device is most sensitive to atmospheric pressure variations in the $2 \cdot \pi \cdot 36/60$ to $2 \cdot \pi \cdot 15$ minute period range. Some additional filtering is done in the electronic amplifiers to further reduce the long period cut-off. The final bandpass is depicted on figure 5.

After two of the instruments were constructed they were run in separate buildings about 200 meters apart. A comparison of the records obtained, shown in figure 6, shows nearly identical recordings. The principal differences apparent on figure 6 are due to slight differences in the leak rates of the capillaries. We have found the manufacturer's calibration to be accurate and normally run unmultiplexed strip chart data with ± 3 centimeter full scale at $\pm .7$ millibar full scale.

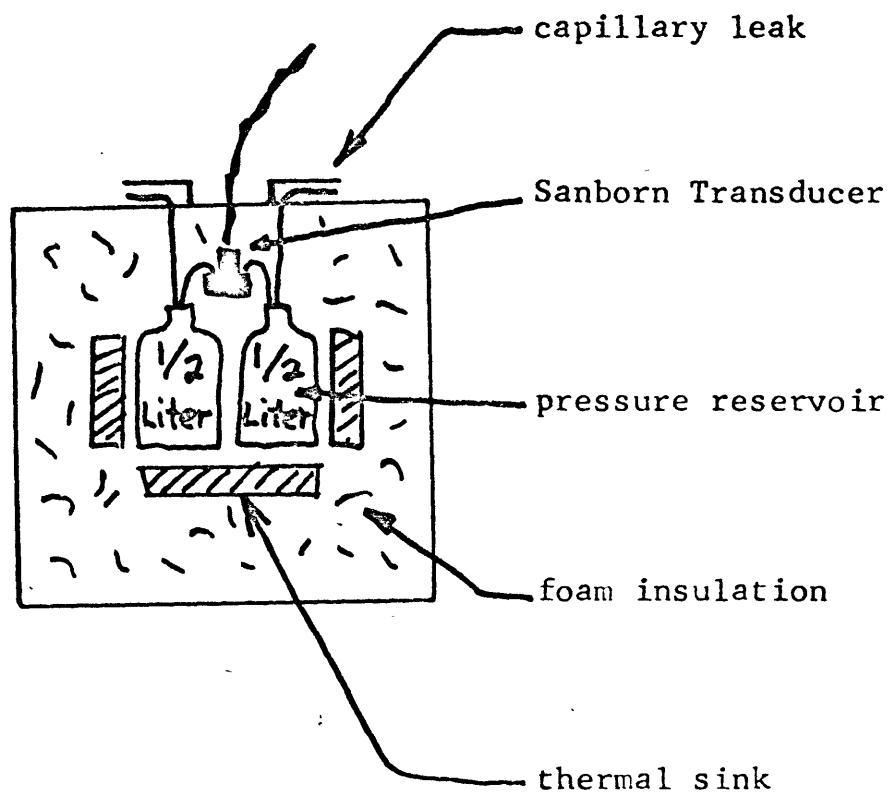


Figure 3 Microbarograph System 0.5 - 30.0 minute periods

Figure III-A-3

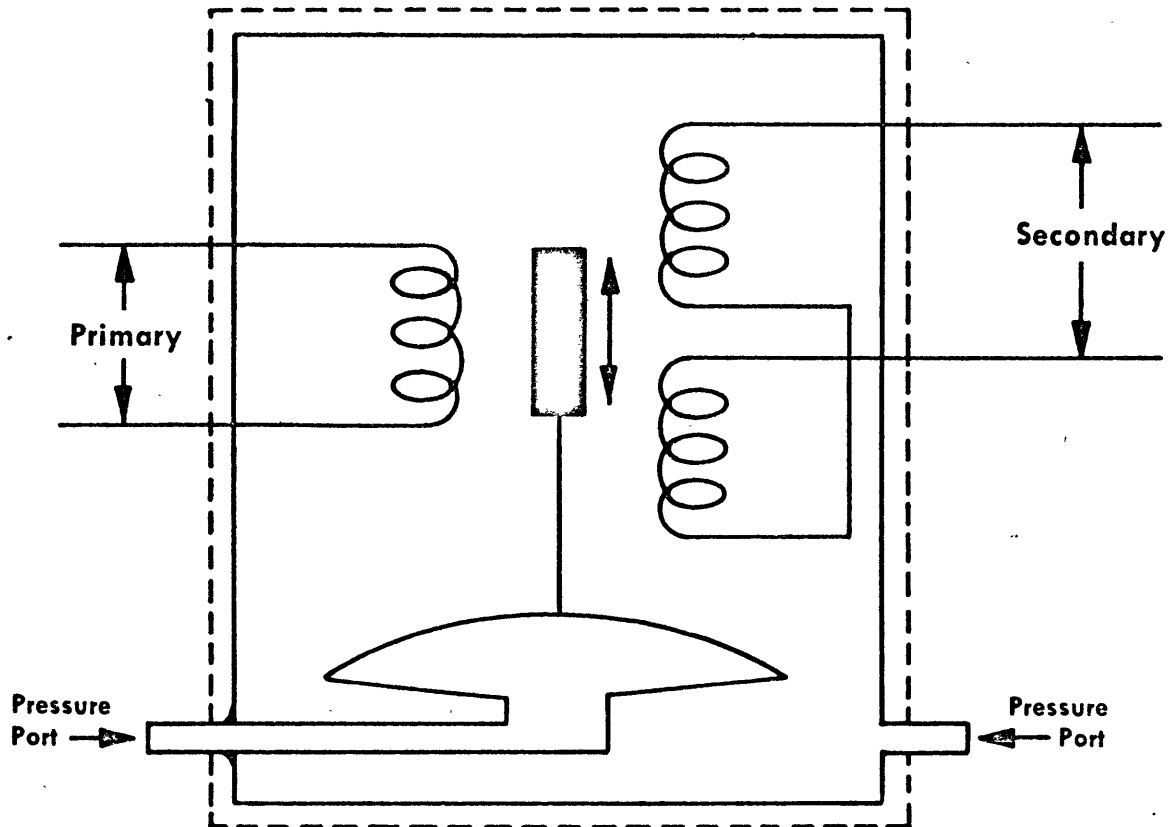
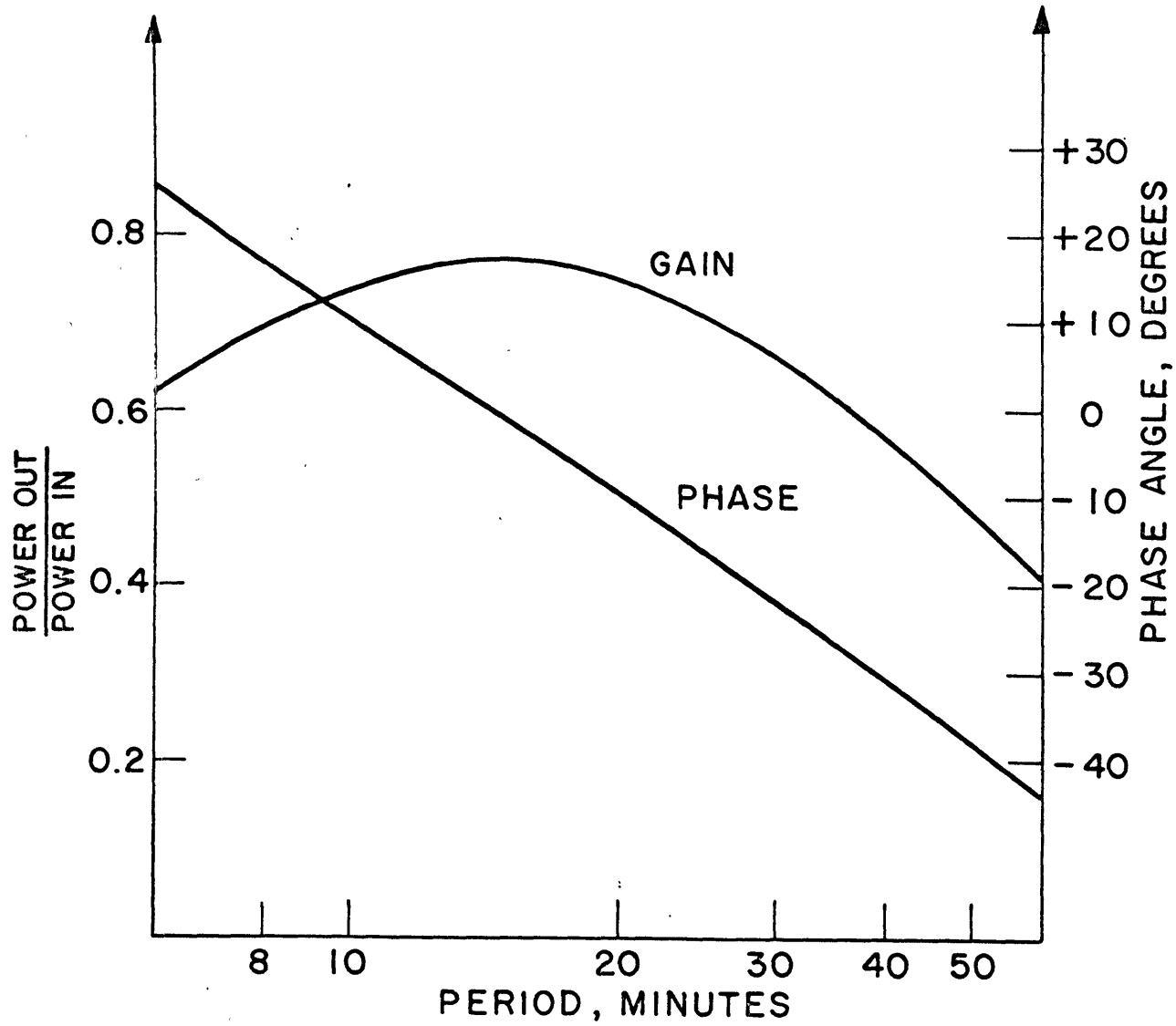


Figure III-A-4 Functional diagram of differential gas pressure transducer.

Figure III-A-5 Overall power gain and phase lag of microbarographs.



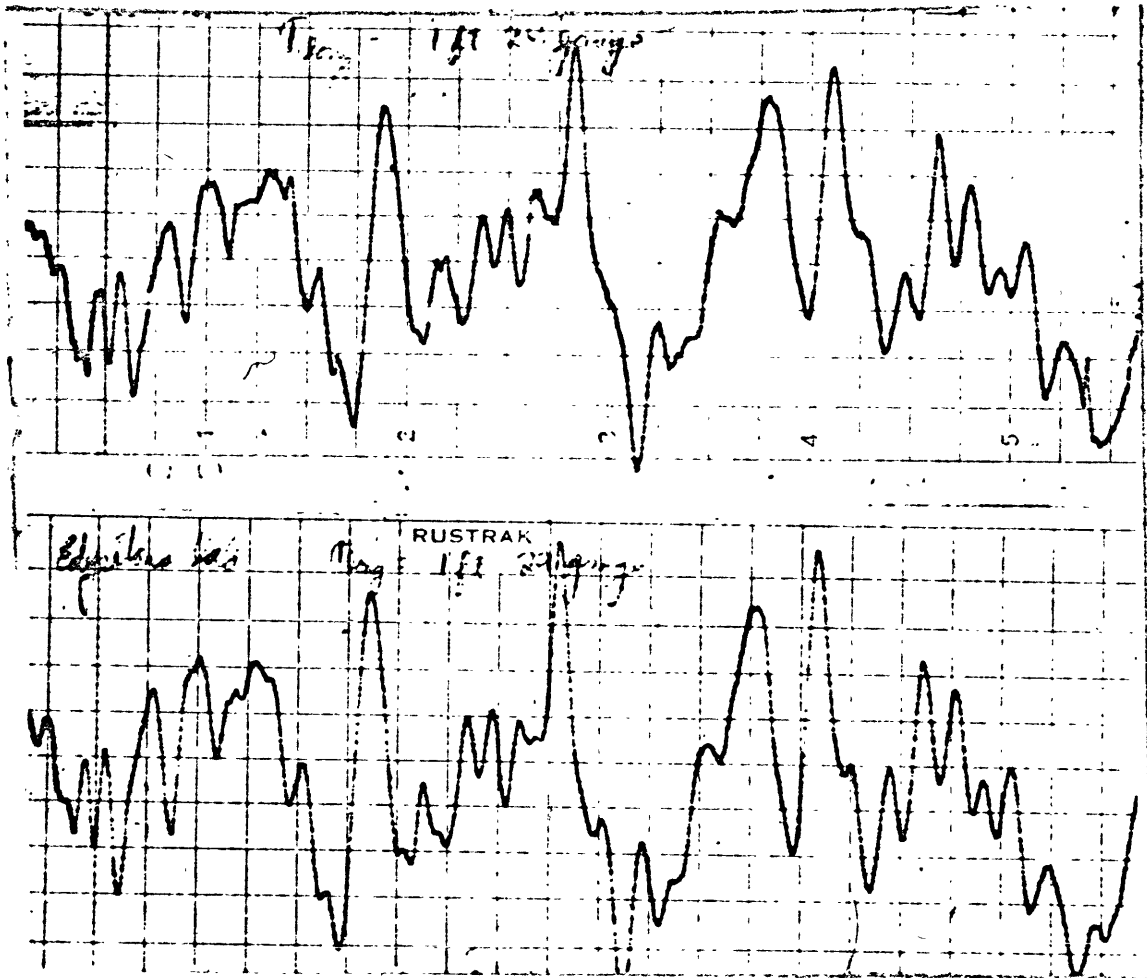


Figure III-A-6 Pressure recorded by two instruments
200 meters apart.

Typical data illustrates four physical processes, moving weather fronts, ground level winds, storms, and jet stream associated disturbances. Unsuccessful attempts were made to identify waves from 5 French atomic explosions in the South Pacific and 2 Chinese explosions in western China. This is attributed to low source strength, great distance, and possibly the frequency band of recording.

Moving weather fronts like the one shown in figure 1 can sometimes be identified by large transients with large relative time delays. Jet stream disturbances may appear impulsively as in figure 2 or they may appear as a high correlation among channels for 24 hours or more.

Data from the first two weeks of 1967 is presented in figures 3 and 4 . Each figure shows 7 strip charts, one for each day of the week. Each strip chart shows 5 channels which from the top are telluric currents, Groton, Bedford, Weston, and Cambridge. We next describe features of this data on a day to day basis.

2 Jan. The wind is frequently stronger during the day than at night. This appears as a higher frequency content in the pressure records at midday than at midnight. Another good example of this is on 6 Jan.

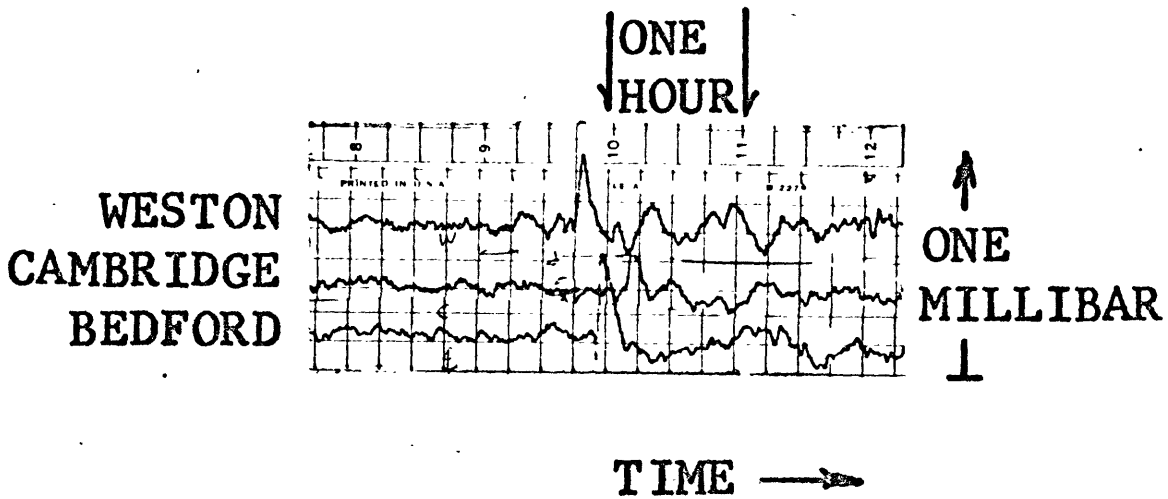


Figure III-B-1 Pressure transient associated with weather front moving about 13 meters/second (25 miles/hour).

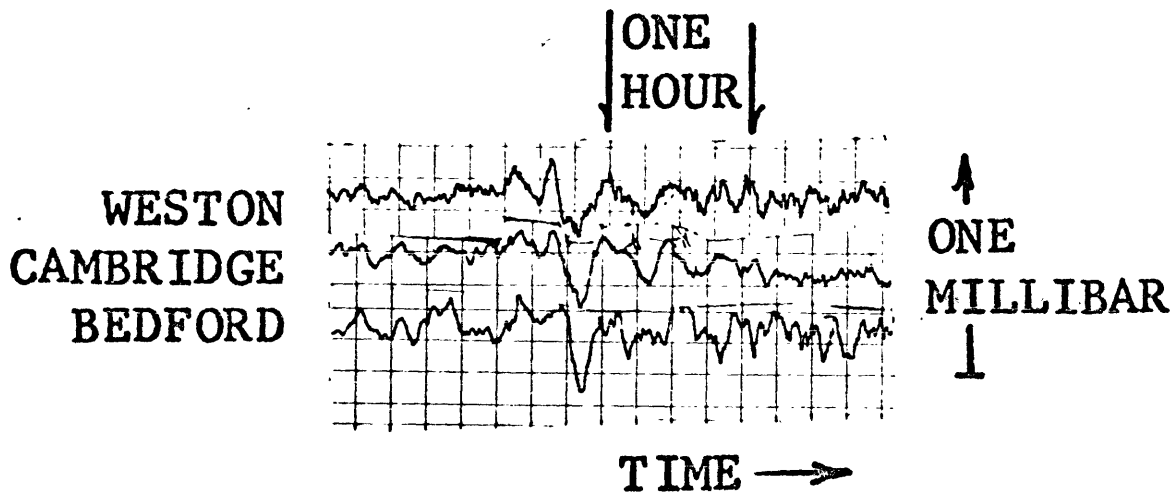
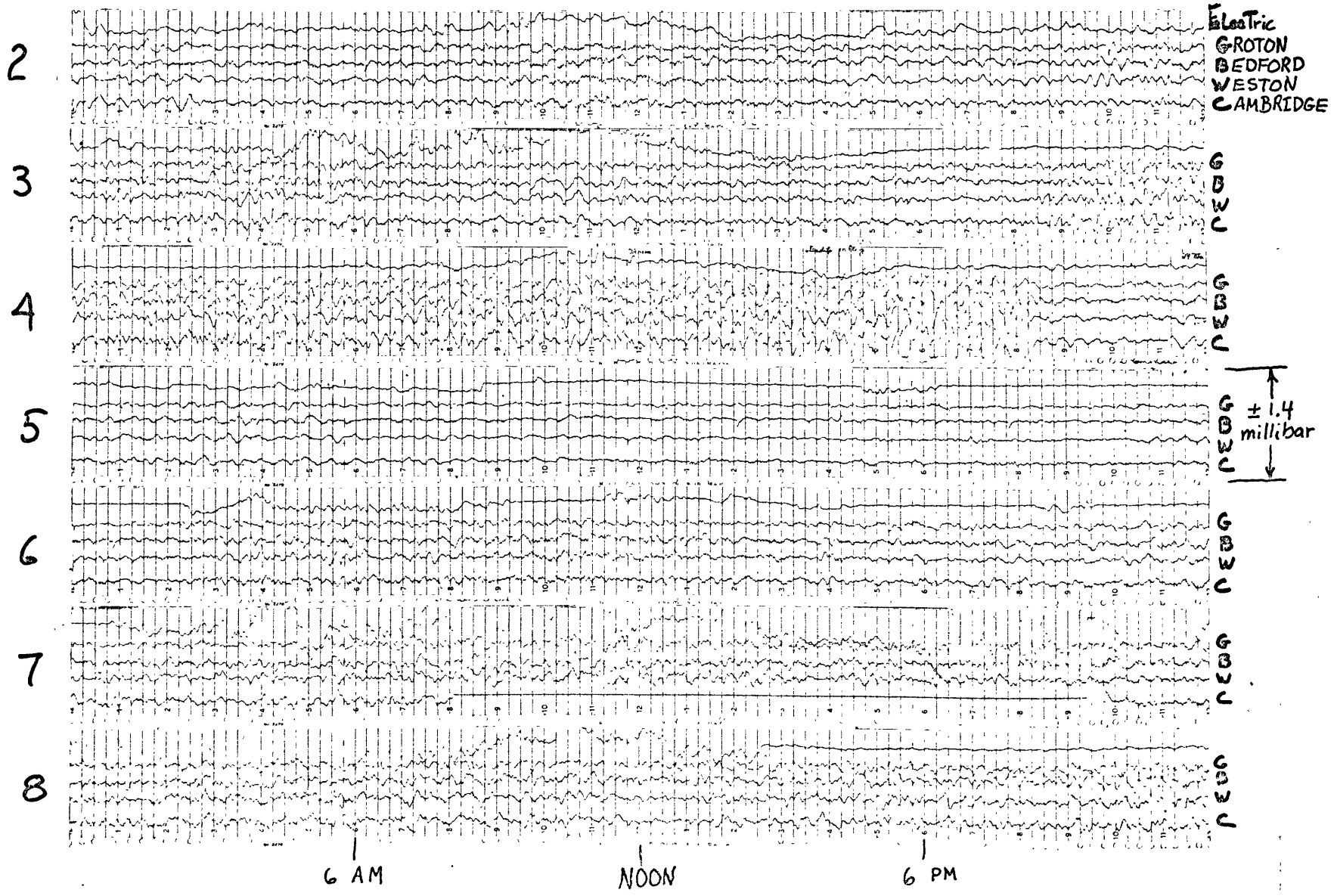


Figure III-B-2 Pressure transient associated with jet stream moving about 60 meters/second (120 miles/hour).

- 4 Jan. A fairly continuous coherency is apparent until about 11 A.M. Weston and Cambridge are especially coherent with Weston leading Cambridge by about 5 minutes which corresponds to a jet stream speed.
- 4 Jan. A storm moves off to the northeast at 8 P.M. It is interesting that the pressure disturbances cease so abruptly compared to the onset of the disturbance a day before.
- 5 Jan. The Groton pressure channel occasionally suffers electrical interference with an ionosonde housed nearby. This appears as pulses at half hourly intervals.
- 7 Jan. Large telluric currents are observed without an associated pressure disturbance.
- 7 Jan. The Cambridge channel phone line went dead for awhile. We have found polarity reversals associated with such cutoffs, but it is apparent from the signal received at 2 A.M. the next day that the polarity was not reversed this time.
- 9 Jan. A transient arrives at 1:40 P.M. on the Bedford channel which is thought to be associated with a transient in the power supply at Bedford.
- 10 Jan. Good jet stream coherency at 2 A.M.
- 14 Jan. Multiplexer difficulty causes double imaging.
- 15 Jan. Good jet stream coherency up to 8A.M.

Pressure

2 Jan 1967 to 8 Jan 1967



Pressure
Jan 1967

Figure III-B-4 Pressure data the second week of January 1967



15 Jan. Some very quiet telluric currents with average to noisy barographic conditions.

An unusual pressure disturbance took place on 13 November 1966. All stations recorded a very sinusoidal disturbance for about 18 hours. The period was about 13 minutes around noon and decreased to about 8 minutes after midnight. A similar observation was made by Flauraud et. al. on 18 January 1952 but their example persisted only a few hours and the changing period was not observable. Visual inspection of the records yielded no unambiguous velocity determination. The digitizer was not operating at the time so a more precise analysis is not possible.

III-C Spectrum and Plane Wave Interpretation

The high frequency end of the spectrum of pressure fluctuations is caused by local wind gusts and the low frequency end is meteorology. The principle feature of interest in between is the "jet waves". At times the coherency of data channels is 90% or more with delays related to the jet stream velocity. Even when the coherence is considerably less, the pressure variations may be almost completely a result of the presence of the jet stream. Coherence with the jet time delays shows that the phenomena is strongly influenced by, or a result of, the jet stream, but, as we will see, a purely jet stream phenomena need not result in perfect coherence.

Flauraud et. al. reported that these jet waves show no dispersion. Pulses have a different shape from one station to the next suggesting dispersion, noise, or that the waves are composed of a mixture of velocities. Fourier transforms of one day data sections showed no statistically reliable dispersion. Figure 1 shows an example of an attempt to resolve velocity and direction as a function of frequency. The changing pulse shape is presumably due to the non-unity coherence among observing points. This non-perfect coherence may be interpreted as the interference of random waves from various directions. The fact that the downstream and cross-stream coherencies differ suggest that the problem cannot be solely a result of random noise.

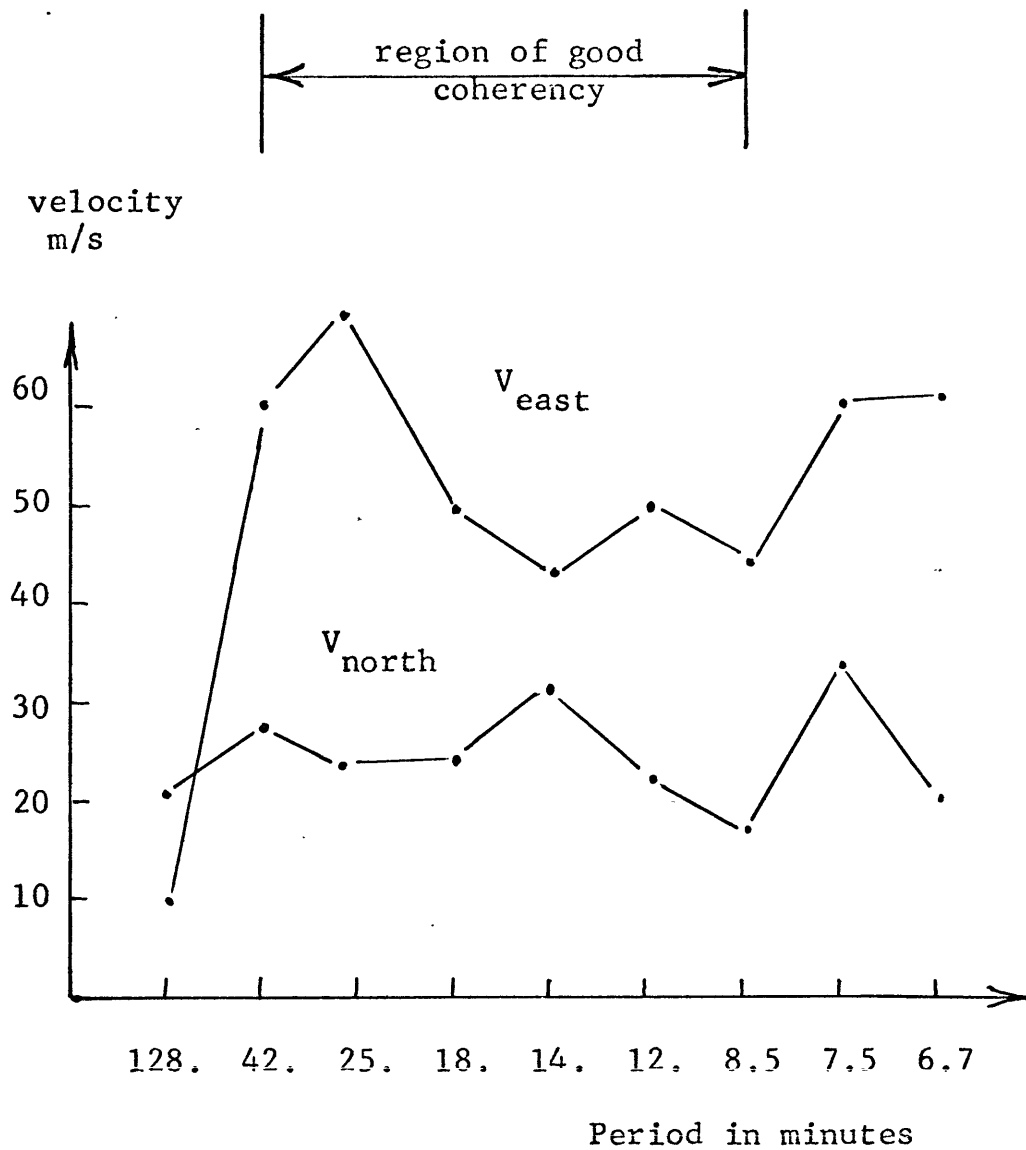


Figure III-C-1 Microbarograph disturbance velocities as a function of frequency do not show significant dispersion.

The observed velocity and period of the jet disturbance gives us the horizontal wavelength. If the jet is in the x direction we may say k_x is known. The coherency of the waves gives us crude information about k_y . An example of the coherency of a 12 hour stretch of data is shown in figure 2. It is rather typical in that the Weston-Cambridge coherence is usually the highest because this is along the line of the most typical jet stream direction. The fact that the cross-stream coherence is less than the downstream coherence as it would be under the assumption of plane waves in the x direction forces us to interpret the data in terms of a k_y as well as a k_x . If the disturbance were made up of two waves with wave vectors (k_x, k_y) and $(k_x, -k_y)$ we would have a cosine dependence of pressure in the y direction. A decreasing coherency in the y direction is obtained by integrating over a distribution in k_y . Of course we don't know what weighting to give to different values of k_y but if we take the distribution to be constant over the range $\pm K_y$ one gets a coherency of the form $(\sin K_y y)/K_y y$ which has its first root at $K_y y = \pi$. If one assumed an isotropic distribution in direction with $k_x^2 + k_y^2 = K_y^2$ one would get a cross-stream coherency of Bessel function form $J_0(K_y y)$ with its first root at $K_y y = 2.4$. Roughly, we may expect the coherency in the y direction to drop off to near zero around $K_y y = 3$. This occurs at 8 minute period on figure 2. Since the stations are about a 20 kilometer triangle and the

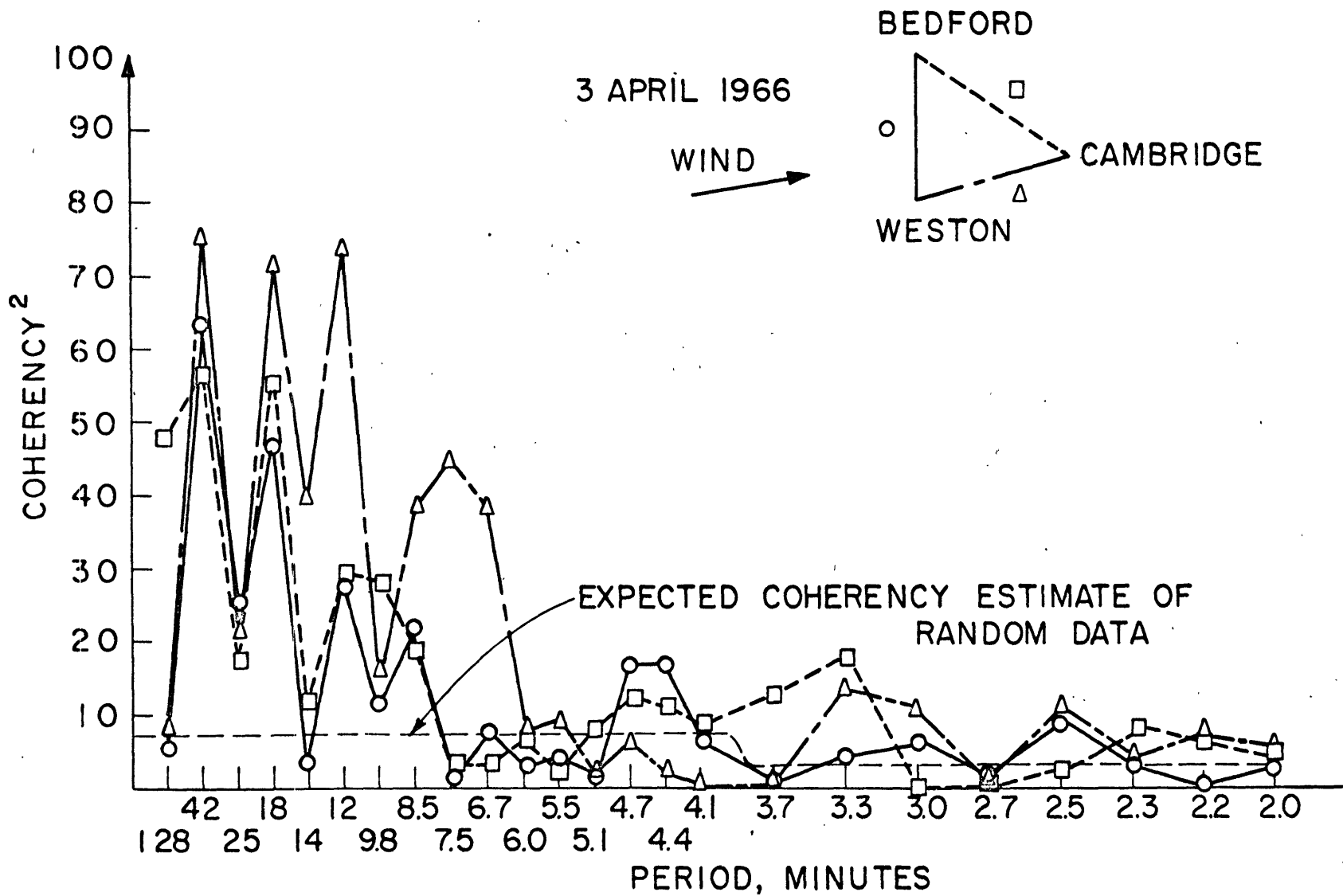


Figure III-C-2 Pressure coherencies among three locations as a function of wave period.

velocity is about 60 meters per second we conclude that

$$k_x = \omega/v_p = 2\pi/(8 \times 60 \times 60) \text{ m}^{-1} = .2 \text{ km}^{-1}$$

$$\pm k_y = 3/20 \text{ km} = .15 \text{ km}^{-1}$$

It is notable that these are about the same. One sometimes hears the term cellular waves (Martyn 1950) in distinction to internal waves. A cellular wave is thought of as a swirl or vortex of air being carried past overhead by the jet stream. An analysis like that of section II-B-5 shows that a cellular wave is really nothing more than the sum of two internal waves with wave vectors (k_x, k_y) and $(k_x, -k_y)$. The fact that $k_x \approx k_y$ simply means the cells are approximately circular. Interpreting the data as approximately circular cellular waves is reasonable and the idea of small vortices peeling off the jet stream is appealing. The crucial question is whether wave packets in (ω, k) space are really organized into vortices or whether we are looking at something like turbulence. (disorganization in (ω, k) space).

A minor difficulty in the above interpretation is that it hinges on a coherency cutoff at 8 minute period where another aspect of the problem becomes important. Figure 3 shows a cross-spectrum between the Cambridge and Weston pressure records. The predominant feature is the

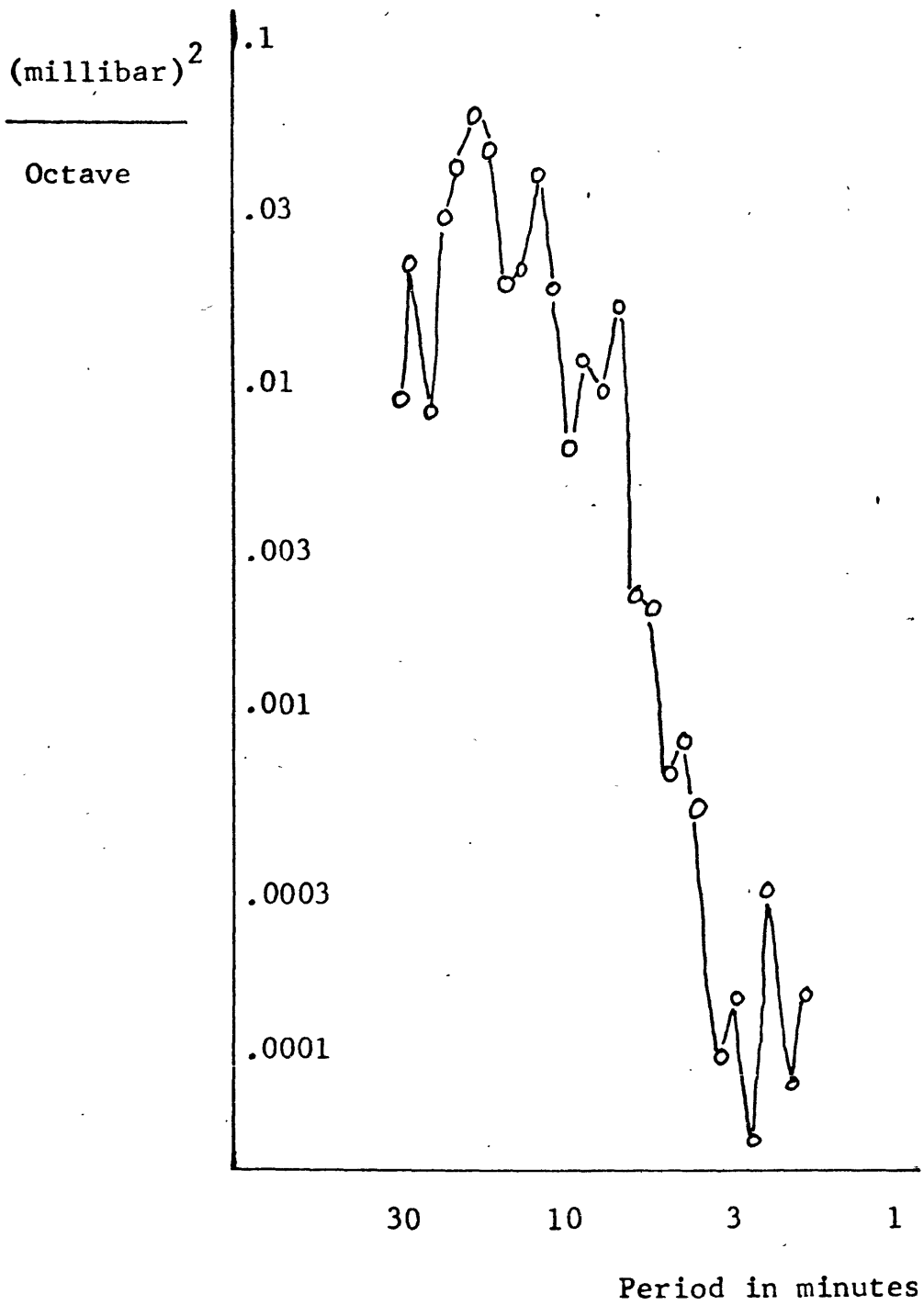


Figure III-C-3

CROSS POWER CAMBRIDGE-WESTON PRESSURE
01:00 E.S.T. APRIL 4, 1966

sharp cutoff about 8 minute period. The cutoff would appear even more sharply if power per unit bandwidth were plotted instead of power per octave. The coherency cutoff is far less abrupt than the crosspower cutoff. In fact the trend toward zero is well established before the cutoff. Therefore the coherency cutoff is not simply a result of the crosspower dropping to near zero. The sharp crosspower cutoff may be predicted from the theoretical considerations of section II-A-13. Briefly, disturbances above the cutoff frequency may exist in the jet where their doppler shifted frequency makes them gravity waves, but once outside the jet they are acoustic in nature and cannot propagate at velocities less than the speed of sound. Therefore they attenuate strongly before reaching ground observers. Quantitatively the decay scale is approximately given by

$$-k_z^2 = \left(\frac{1}{c^2} - \frac{1}{V_p^2} \right) (\omega^2 - \omega_b^2)$$

which for a frequency twice the Brunt frequency in a typical jet stream is about

$$k_z \approx \frac{\sqrt{3} \omega_b}{V_p} \approx 1.5 \text{ km}^{-1}$$

III-D Correlation With Jet Stream Behavior

Wind and temperature profiles are measured up to an altitude of about 15 kilometers every 12 hours by meteorologists at several hundred places around the world. These are obtained with balloons and expendable radio transmitters. The nearest observation point to our array is 150 kilometers at Nantucket Island. Better correlation with our pressure data has been found with Albany, New York which is 220 kilometers distant but more in line with the jet stream. Figure 1 shows altitude profiles of temperature, wind, and shear instability number at Albany for the period 2 April to 5 April 1966. Profiles are numbered 1-4 consecutively. Since the instability number is determined by taking derivatives of the wind and temperature, it tends to be jagged and no attempt has been made to draw a continuous profile.

Figure 2 shows successive maps of the height of the 500 millibar surface. This map is nearly the same as a map of pressure at 5.5 kilometers altitude. The flow is controlled by the coriolis force and the geostrophic wind equations. The wind tends to be along lines of constant pressure and the velocity inversely proportional to contour separation. These maps show a gradual changing of wind direction from west by northwest to west by southwest. The separation of contours over Albany reaches a minimum on 4 April, which corresponds to high winds and the lost balloon (profile

ATMOSPHERIC PROFILES
2-5 APRIL AT ALBANY, NEW YORK

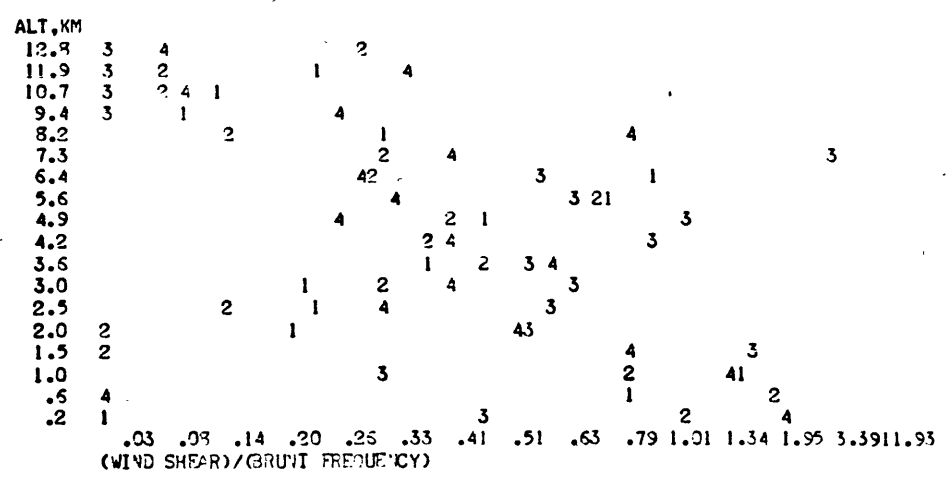
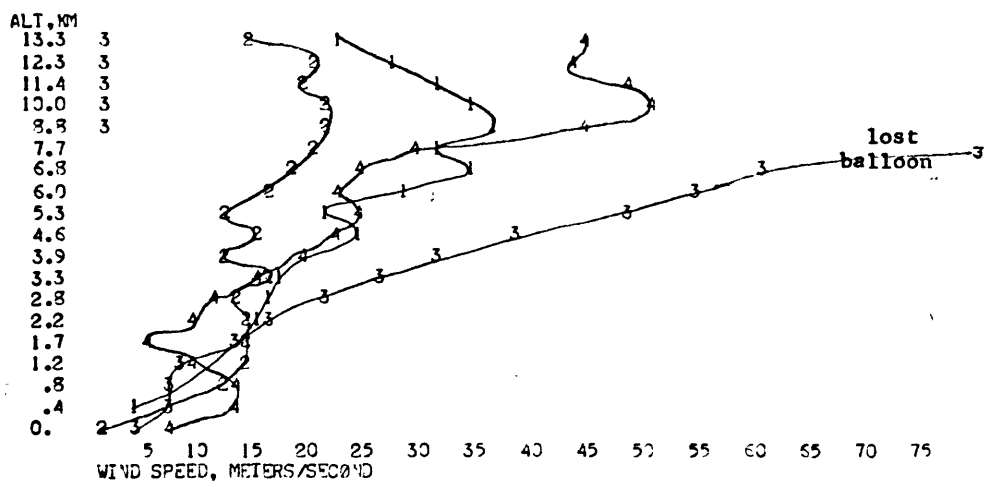
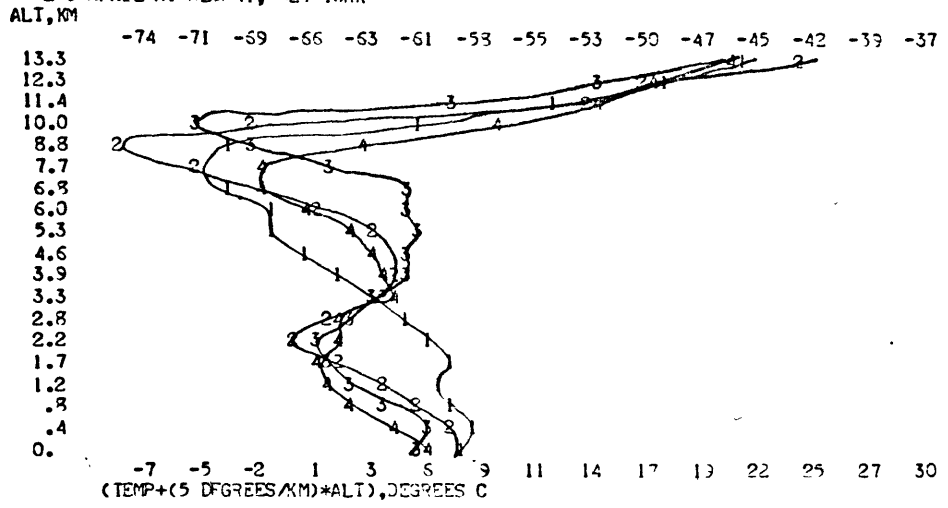


Figure III-D-1 Atmospheric profiles of temperature, wind, and instability.

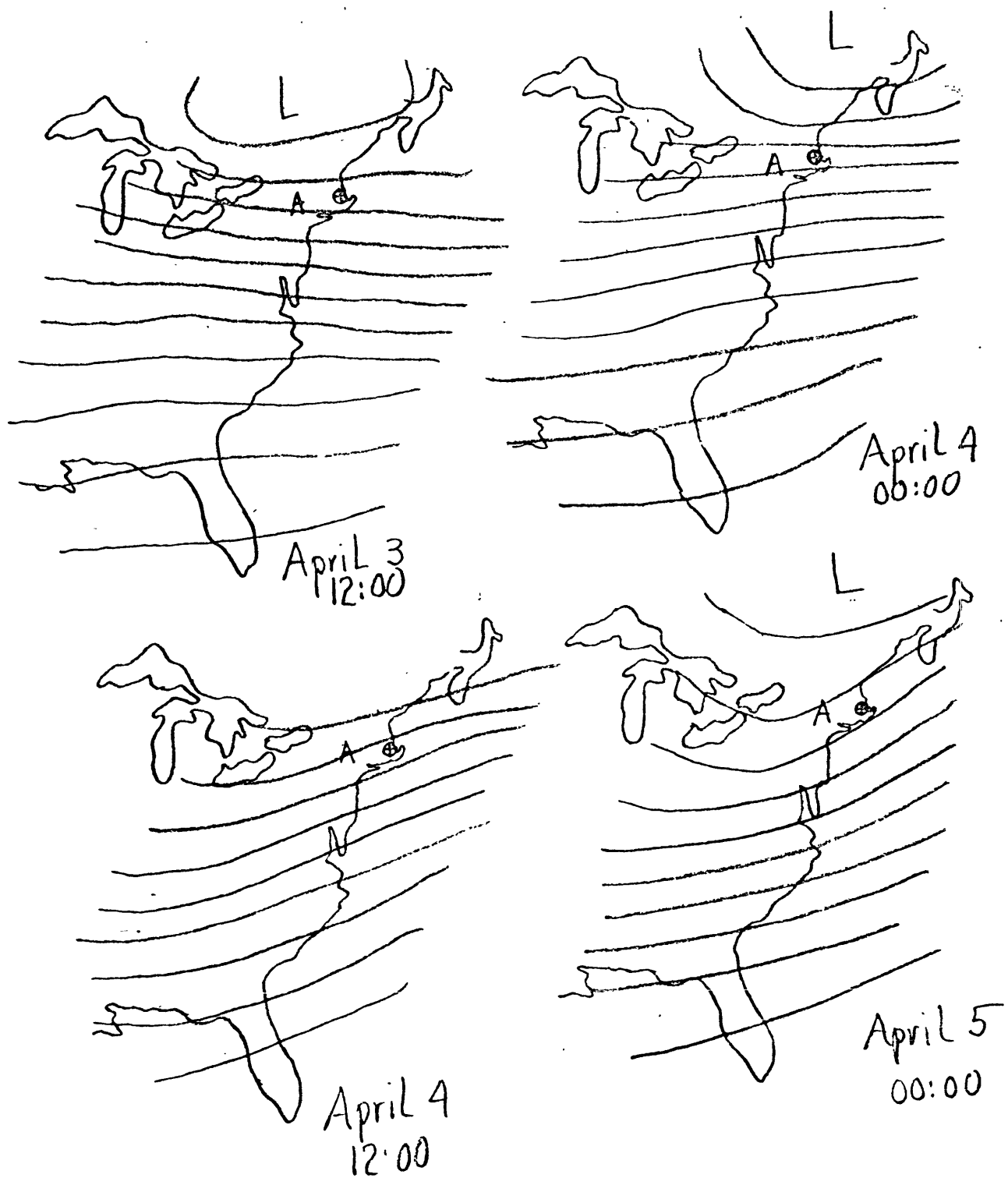


Figure III-D-2 500 millibar map April 3-5, 1966

number 3) on figure 1.

Figure 3 shows three velocity versus time functions for six days in April 1966. They are: (1) the maximum velocity of winds aloft, (2) the apparent velocity of disturbances over the microbarograph array, and (3) the velocity of the wind at the height of minimum Richardson number. The latter is not always a unique function of time because of the possibility of multiple altitudes having practically the same Richardson number. The unstable points near the ground have been neglected because they produce very slow waves which are incoherent by the time they traverse the array. The apparent phase velocities were determined from the time delays at the peaks of a running correlation calculation with a 4 hour averaging time sampled every two hours. The correlation between (2) and (3) is remarkable especially when the velocity is large.

The final correlation between theory and data is to take the observations and integrate them up toward the critical height. We will calculate that the linear theory breaks down first because of the wave introduced wind shear. The later non-linearity is unimportant. At the height of shear breakdown the vertical wavelength is 2 kilometers and wave parcel horizontal velocity is +5 meters per second. These are quite comparable to the variations on the basic trend observed in figure 1 and may be used to explain the small scale variations in these winds. The remainder of

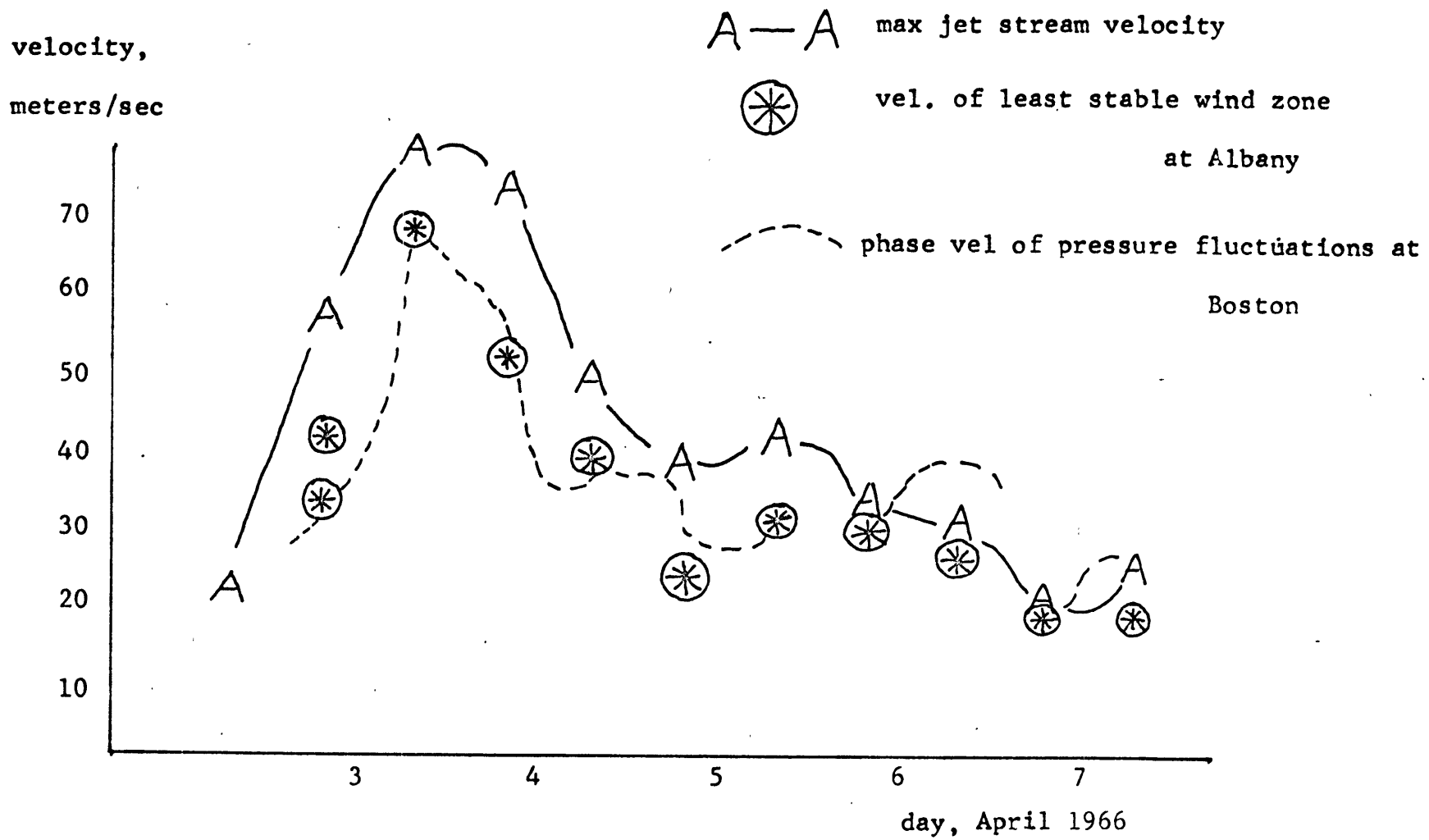


Figure III-D-3

ASSOCIATION OF PRESSURE FLUCTUATIONS WITH STABILITY CRITERIA

this section contains the calculation justifying the assertions of this paragraph.

The following we take to be typical parameters based on observations.

$$\mu^2 \approx R = 2$$

$$2\pi/k = 72 \text{ kilometers}$$

$$2\pi/\omega = 20 \text{ minutes}$$

$$2\pi/\omega_b = 10 \text{ minutes}$$

$$z_c = 10 \text{ kilometers}$$

$$u_c = 60 \text{ meters/sec}$$

$$u_o = 1 \text{ meter/sec} = \text{wave particle velocity at ground}$$

In the theory of section I-A-3 we have used the approximation that terms multiplying the inverse doppler frequency $1/\Omega$ dominate all others. Closer inspection shows that this approximation amounts to assuming that the local wave frequency is much less than the Brunt frequency. This approximation is reasonable for our pressure observations in a realistic jet stream geometry so we can use the formulas of that section. Those we need are

$$\bar{u} = u_c z/z_c$$

$$u_z = \frac{du}{dz} = u_c/z_c$$

$$\Omega = (ku_z) (z_c - z)$$

$$\mu \approx \sqrt{R} = \omega_b/|u_z|$$

$$\tilde{p} = i (k/u_z) (a_c - z)^{1/2} + i$$

$$\tilde{w} = i (k/u_2) (a_c - a)^{1/2} + i$$

$$\tilde{u} = u_0 (1 - z/z_c)^{-1/2}$$

$$\text{time } (z) = \int_0^z \text{momentum density } dz / \text{momentum flux}$$

$$= \frac{\int_0^z \frac{1}{\Omega} \left\{ \frac{1}{\bar{\rho}} \frac{k^2}{\Omega^2} \tilde{p} \tilde{p}^* + \bar{\rho} \tilde{w} \tilde{w}^* \right\} dz}{\text{Re } \tilde{p} \tilde{w}^* / \Omega}$$

from which by substitution we obtain time as a function of height.

$$\begin{aligned} &= \frac{\int_0^z \frac{1}{k \bar{u}_2 (z_c - z)} \left\{ \frac{(z_c - z)}{\bar{\rho} u_2^2 (z_c - z)^2} |-\frac{1}{2} + i\mu|^2 + \frac{1}{\bar{\rho}} \left(\frac{k}{u_2}\right)^2 (z_c - z) \right\} dz}{\left\{ \frac{1}{\bar{\rho}} \frac{\mu k}{u_2} (z_c - z) \frac{1}{k u_2 (z_c - z)} \right\}} \\ &= \frac{\bar{\rho} \int_0^z \frac{1}{\bar{\rho}} \left\{ \frac{R}{k u_2^2 (z_c - z)^2} + \frac{k}{u_2^2} \right\} dz}{\mu / u_2^2} \\ &= \frac{\bar{\rho}}{\mu k \bar{u}_2} \int_0^z \frac{R dz}{\bar{\rho} (z_c - z)^2} \quad k \ll \frac{1}{z_c - z} \end{aligned}$$

Since we are interested in z such that $\bar{\rho}_c$ is less than about 300 millibars we introduce a modest error by taking $\bar{\rho}$ out of the integral. Also take $R = \mu^2 = \text{const.}$

$$\text{time } (z) = \frac{\mu}{k u_2} \int_0^z \frac{dz}{(z_c - z)^2} = \frac{\omega_b}{k u_2^2} \left(\frac{-1}{z - z_c} \right)^2$$

$$= \frac{\omega_b z_c^2}{k u_2^2} \left(\frac{-1}{z - z_c} - \frac{-1}{-z_c} \right)$$

$$= \frac{\omega_b z_c^2}{\omega u_c} \left(\frac{z/z_c}{z_c - z} \right) \quad (\omega/k = u_c)$$

$$t(z) = \frac{\omega_b}{\omega} \frac{1}{u_c} \frac{z}{1 - z/z_c}$$

The time $t(z)$ is readily inverted to give the height $z(t)$

$$z(t) = \frac{t}{\left(\frac{\omega_b}{\omega} \frac{1}{u_c} + t/z_c\right)}$$

We can use these expressions to integrate the heights at which the waves observed on the ground would, when projected back towards the sources, attain certain critical magnitudes and the travel times involved. Consider first the onset of non-linear behavior. For this we calculate the height at which the wave particle velocity equals the wind velocity

$$\tilde{u} = \bar{u}$$

$$\tilde{u}_0 (1 - z/z_c)^{-1/2} = U_c z/z_c$$

$$(1 - z/z_c) = \frac{u_0^2}{u_c^2} \frac{z_c^2}{z^2} \approx \frac{u_0^2}{u_c^2}$$

Inserting the typical values we get

$$(1 - z/z_c) = \left(\frac{1}{60}\right)^2 = \frac{1}{3600}$$

so z is within about 3 meters of z_c and the time required to propagate from the ground to z is

$$t = \frac{\omega_b}{\omega} \frac{1}{u_c} \frac{z_c}{1 - z/z_c} = \frac{2}{60} 10000 \cdot 3600 = 1,200,000 \text{ seconds}$$

$$= 12 \text{ days}$$

This time is unrealistic in view of the close simultaneous correlations between the observed pressure wave velocities and the wind velocities. We can also show that this time is

meaningless because the wave when projected back will develop unstable shears well before reaching this height. It is at this height where the wind shear violates the Richardson criteria that we should expect the sources. To find this height we set

$$\frac{\omega_b}{\tilde{u}_z} = \frac{1}{2}$$

$$2\omega_b = \tilde{u}_z$$

$$= \frac{d}{dz} U_0 \left(1 - z/z_c\right)^{-1/2 + i\mu}$$

$$= U_0 (-1/2 + i\mu) \left(1 - z/z_c\right)^{-3/2 + i\mu} \left(-1/z_c\right)$$

Drop the phase angle. Take $\mu = 1/2 + i\mu \approx \mu$

$$\approx \frac{U_0}{z_c} \frac{\omega_b}{\tilde{u}_z} \left(1 - z/z_c\right)^{-3/2}$$

$$\left(1 - z/z_c\right) = \left(\frac{U_0}{2U_c}\right)^{2/3} = \left(\frac{1}{120}\right)^{2/3} = \frac{1}{25}$$

So z is within 400 meters of z_c and the travel time is

$$t = \frac{2}{60} \times 10000 \times 25 \text{ seconds} = 2 \text{ hours} = .1 \text{ day}$$

These time and altitude scales are within the persistence and reliability of our knowledge of the stratosphere. Let us therefore go back and calculate the particle velocity of the wave at the height where its shear gives dynamic instability.

$$\tilde{u} = \tilde{u}_0 \left(1 - z/z_c\right)^{-1/2} = 1 \cdot (25)^{1/2} = 5 \text{ meters/sec}$$

This is a good result because it is in very good agreement with observed wind profiles, they are not linear as we have presumed, but superposed on the linear profile are short vertical wave lengths with about ±5 meters/second amplitude. Finally we calculate the vertical wavelength superposed on the presumed linear wind profile.

$$\tilde{p} \sim (z_c - z)^{i\mu + 1/2}$$

$$\text{phase} = \text{Im} \ln(z_c - z)^{i\mu + 1/2}$$

$$= \mu \ln(z_c - z)$$

$$k_z = \frac{d}{dz} \text{phase} = \frac{\mu}{z_c(1 - z/z_c)} = \frac{1.4 \times 25}{10 \text{ km}}$$

$$\lambda_z = \frac{2\pi}{k_z} = 2$$

kilometers

This is certainly typical of balloon observations as may be seen by figure 1.

Appendix A. Weight Factors In First Order Matrix Differential Equations

First order linear matrix differential equations can frequently be transformed to a new set of variables which accomplish the following:

- 1) simplifies
- 2) eliminates singular points
- 3) converts irregular singular points to regular ones
- 4) gets a matrix of constant coefficients
- 5) avoids complex numbers
- 6) keeps integral from extreme growth or decay reducing round off problems

Consider a set

$$\frac{d}{dz} \begin{bmatrix} x_1 \\ x_2 \\ x_3 \end{bmatrix} = \begin{bmatrix} A_{11} & A_{12} & A_{13} \\ A_{21} & A_{22} & A_{23} \\ A_{31} & A_{32} & A_{33} \end{bmatrix} \begin{bmatrix} x_1 \\ x_2 \\ x_3 \end{bmatrix}$$

One can derive an "addition" transformation

$$\frac{d}{dz} \begin{bmatrix} X_1 + X_2 \\ X_2 \\ X_3 \end{bmatrix} = \begin{bmatrix} (A_{11} + A_{21}) & (A_{12} + A_{22} - A_{11} - A_{21}) & (A_{13} + A_{23}) \\ A_{21} & A_{22} - A_{21} & A_{23} \\ A_{31} & A_{23} - A_{31} & A_{33} \end{bmatrix} \begin{bmatrix} X_1 + X_2 \\ X_2 \\ X_3 \end{bmatrix}$$

and a "weighting" transformation

$$\frac{d}{dz} \begin{bmatrix} w_1 X_1 \\ X_2 \\ X_3 \end{bmatrix} = \begin{bmatrix} (A_{11} + \frac{1}{w_1} \frac{dw_1}{dz}) & w_1 A_{12} & w_1 A_{13} \\ A_{21} / w_1 & A_{22} & A_{23} \\ A_{31} / w_1 & A_{32} & A_{33} \end{bmatrix} \begin{bmatrix} w_1 X_1 \\ X_2 \\ X_3 \end{bmatrix}$$

In non-dissipative problems it should be possible to avoid complex numbers. If the eigenvalues of a constant matrix are pure real or pure imaginary, the solutions are pure exponential or pure sinusoidal. If by transformations one can get a matrix of constant coefficients to real symmetric form, the roots must be real. More usually one gets it to real and antisymmetric form where the roots are pure real or pure imaginary, but not complex. (This follows since the square of an antisymmetric matrix is symmetric so the square of the roots of an antisymmetric matrix must be real.) A 2x2 matrix with real constant coefficients and zero trace has pure real or pure imaginary roots since the characteristic equation is $\lambda^2 = -\text{determinant}$.

Appendix B. Matrix Sturm-Liouville Formulation

A basic technique in geophysical wave propagation problems is to reduce partial differential equations to ordinary differential equations by means of trial solutions. Since all classical physical laws are first order equations, trial solutions reduce them to a set of first order ordinary differential equations. Traditionally one further reduced the set to a single equation of higher order and sought analytic solutions to it. Many special features of these ordinary differential equations such as self adjointness, completeness and orthogonality of solutions, real eigenvalues, conservation principles, etc. were well known especially for second order equations. With the advent of electronic computers the reduction from a first order set of equations to a single equation of higher order became an unnecessary and often undesirable step, especially for equations of higher than second order. The special features were unclear to people beginning to work with the first order matrix equations because there are very few books written from the newer point of view. One is Discrete and Continuous Boundary Problems by F.V. Atkinson. An inclusive framework for a wide variety of problems is provided by the system

$$(1) \quad J \frac{dy}{dz} = [\lambda A(z) + B(z)] y \quad a \leq z \leq b$$

where J, A, B are square matrices of fixed order k , $y(z)$ is a $k \times 1$ column vector of functions of z , and λ is a scalar parameter. Matrices A and B are hermitian and J is skew-symmetric, that is

$$(2) \quad J^* = -J, \quad A^* = A, \quad B^* = B$$

We will later see that the acoustic-gravity wave problem can be put into this form. Suppose the continuous functions of z were approximated by their sampled values at equal intervals within the interval. The the $\frac{d}{dz}$ operator in (1) would be approximated by a matrix like

$$(3) \quad \frac{d}{dz} \sim \frac{1}{\Delta z} \begin{bmatrix} +1 & -1 & & & & \text{zeros} \\ & +1 & -1 & & & \\ & & +1 & -1 & & \\ & & & +1 & -1 & \\ & & & & +1 & \cdot \\ & & & & & \cdot \\ & & & & & \cdot \\ & & & & & \cdot \\ & & & & & \cdot \\ & & & & & \cdot \\ \text{zeros} & & & & & \cdot \end{bmatrix}$$

The matrix analog of $J \frac{d}{dz}$ would be a (Kronecker) product of two skew matrices which is a symmetric matrix so (1) takes the form

$$(4) \quad [\text{symmetric matrix}] y = \lambda Ay$$

This is simply the generalized eigenvector problem of matrix algebra. The real eigenvalues and orthogonal eigenvectors have their analogs in the differential equation (1). There seems to be no systematic method to put various physical problems into the form (1). It turns out to be easy for acoustic-gravity waves. Either equation I-A-1.14 or I-A-2.3 is of the form

$$(5) \quad \frac{d}{dz} \begin{bmatrix} x_1 \\ x_2 \end{bmatrix} = \begin{bmatrix} A_{11} & A_{12} \\ A_{21} & -A_{11} \end{bmatrix} \begin{bmatrix} x_1 \\ x_2 \end{bmatrix}$$

Multiplying through by a unit 2x2 skew matrix gives the desired form

$$(6) \quad \begin{bmatrix} 0 & -1 \\ +1 & 0 \end{bmatrix} \frac{d}{dz} \begin{bmatrix} x_1 \\ x_2 \end{bmatrix} = \begin{bmatrix} A_{21} & A_{11} \\ A_{11} & A_{12} \end{bmatrix} \begin{bmatrix} x_1 \\ x_2 \end{bmatrix}$$

With formula I-A-2.3 we may identify the parameter λ with k^2 , so (6) may be written in the form (1).

$$(7) \quad \begin{bmatrix} 0 & -1 \\ 1 & 0 \end{bmatrix} \frac{d}{dz} \begin{bmatrix} \tilde{p} \\ \tilde{w}/\Omega \end{bmatrix} = \left\{ k^2 \begin{bmatrix} \frac{1}{\rho \Omega^2} & 0 \\ 0 & 0 \end{bmatrix} + \begin{bmatrix} -\frac{1}{\rho c^2} & -g/c^2 \\ -g/c^2 & \rho(\Omega^2 - \omega^2) \end{bmatrix} \right\} \begin{bmatrix} \tilde{p} \\ \tilde{w}/\Omega \end{bmatrix}$$

In some other problems one has the choice of ω^2 or k^2 as the eigenvalue. Formula (7) is in the desired form only if

there is no wind because otherwise $\Omega = \omega - ku$ is dependent on k so (7) would not really be an eigenvalue problem for k^2 . Given only that equation (7) is in the form (1), conservation of wave momentum follows from a formula in Atkinson's book (pages 252-8). Also, one has the orthogonality relation among modes

$$0 = \int_a^b P(k_n, z) \frac{1}{\rho \omega^2} P^*(k_m, z) dz \quad m \neq n$$

which has many uses.

A primary advantage of Atkinson's approach is that one can understand the basic underlying principles, the orthogonality of eigenvectors for example, and the principles are applicable to any size matrices. The traditional Sturm-Liouville approach is only for a second order differential equation and generalization is far from obvious.

Appendix C. Atmospheric Constants and Basic Physical
Formulas

The purpose of this appendix is to bring together a miscellany of simple formulas about the atmosphere which are frequently used in this thesis.

- 1) sea level pressure

$$P = 10^5 \text{ Newton/meter}^2 = 1 \text{ bar}$$

- 2) sea level density

$$\rho = 1.2 \text{ kg/meter}^3$$

- 3) specific heat at constant pressure

$$C_p = 1003 \text{ joules/kg/degree C}$$

- 4) typical sound speed at sea level

$$c = 340 \text{ meters/sec}$$

- 5) gravity

$$g = 9.8 \text{ meters/sec}^2$$

- 6) ratio of specific heats

$$\gamma = 1.4$$

- 7) scale height

$$H = \frac{c^2}{\gamma g} = \frac{kT}{mg} \quad (\approx 8 \text{ km at sea level})$$

- 8) hydrostatic equation

$$\frac{dP}{dz} = -\rho g$$

- 9) perfect gas law

$$P = \rho \frac{k}{m} T = \frac{c^2}{\gamma} \rho \quad \left(\frac{m}{k} \approx .0034 \text{ MKS units} \right)$$

- 10) isothermal atmosphere

$$P = P_0 \exp(-(z-z_0)/H)$$

- 11) atmosphere with constant temperature gradient

$$T = T_0 + \alpha z$$

$$\rho = \rho_0 \left(\frac{T}{T_0} \right)^{-\left(1 + \frac{mg}{k\alpha}\right)} \quad \alpha \neq 0$$

- 12) adiabatic atmosphere

$$\frac{dT}{dz} = -\frac{mg}{k} \frac{(\gamma-1)}{\gamma}$$

- 13) Brunt frequency

$$\omega_b^2 = \frac{g}{\rho} \left(\frac{1}{c^2} \frac{d\rho}{dz} - \frac{d\rho}{dz} \right)$$

$$= \frac{g}{T} \left(\frac{\gamma-1}{\gamma} \frac{mg}{k} + \frac{dT}{dz} \right)$$

$$\approx \frac{g}{T} (0.0095 + \frac{dT}{dz}) \quad (\text{radians/sec})^2$$

- 14) typical Brunt period

isothermal $2\pi/\omega_b = 5$ minutes

troposphere $2\pi/\omega_b = 10$ minutes

REFERENCES

- Atkinson, F.V., Discrete and continuous boundary problems, Academic Press, New York, 1964
- Axford, W.I., The formation and vertical movement of dense ionized layers in the ionosphere due to neutral wind shears, JGR, 68 No. 3 pp. 769-779, 1963
- Biot, M.A., General fluid-displacement equations for acoustic gravity waves, J. of the Phys. of Fluids, 6, No. 5, 621-626, 1963
- Booker, J.R., Bretherton, F.P., Critical layer for internal gravity waves in a shear flow, J. of Fluid Mech., 27 513-539, 1967
- Bretherton, F.P., The propagation of groups of internal gravity waves in a shear flow, Transaction of Royal Society, 551.511.3:532.59,466-480, Mar. 25, 1966
- Bourdeau, R.E., Research within the ionosphere, Science 148, No. 3670, 585-594, April 30, 1965
- Campbell and Young, Auroral zone observations of infrasonic disturbances and geomagnetic activity, J.G.R. Nov. 1963
- Charney, J.G., and Drazin, P.G. Propagation of planetary scale disturbances from the lower into the upper atmosphere, J.G.R., 66, 83-109, 1961
- Chrzanawski, Green, Lemmon, and Young, Traveling pressure waves associated with geomagnetic activity, J.G.R., Nov. 1961
- Cox, E.F., Microbarometric pressures from large high explosive blasts, J.A.S.A., 19, 832-846, 1947
- Cox, E.F., For transmission of air blast waves, Phys. Fluids I, 95-101, 1958
- Daniels, F.B., Bauer, S.J., Harris, A.K., Vertical traveling shock waves in the ionosphere, J. Geophys. Res. 65, No.6 1848-1850, 1960
- Dickenson, R.E., Propagators of atmospheric Motions, Mass, Inst. of Tech., Dept. of Meteorology, Planetary Circulations Report No. 18, July 1, 1966
- Donn, W.L. and Ewing, M., Atmospheric waves from nuclear explosions, Part II - The Soviet test of Oct. 30, 1961, J. Atmos. Sci., 19, 246, 1962

- Eckart, C., Hydrodynamics of oceans and atmospheres, London, Pergamon Press, 1960
- Eckart, C., and Ferris, H.G., Equations of motion of the ocean and atmosphere, *Reviews of Modern Phys.*, 28, No. 1 48-52, Jan. 1956
- Eliassen, A., and Palm, E., On the transfer of energy in stationary mountain waves, *Geophysica Norvegica*, XXII, No. 3 1-23, Dec. 9, 1960
- Fejer, J.A., The electrical conductivity of the ionosphere: a review, *J. Atmos. and Terr. Physics*, 18, No. 23, 135-146, 1960
- Flauraud, Mears, Crowley, and Crary, Investigation of Microbarometric oscillations in eastern Massachusetts. Geophysical Research paper, No. 27, Air Force Cambridge Research Center, 1954
- Gantmacher, F.R., The theory of matrices, I and II, Chelsea, N.Y., 1960
- Gilbert, F., Backus, G.E., Propagator Matrices in Elastic Wave and Vibration Problems, *Geophysics*, XXXI, No. 2, 326-332, 1966
- Gintsburg, M.A., Low-frequency waves in a multi-component plasma, *Geomagnetism Aeronomy*, 3, 610-614, 1963
- Gossard, E., Vertical flux of energy into the lower ionosphere, *J.G.R.*, 67, 745-757, 1962
- Gossard, E., and Munk, W., Gravity waves in the atmosphere, *Quart. J. of Royal Meteorological Soc.*, 81, No. 349, July, 1955
- Hines, C.O., Internal atmospheric gravity waves at ionospheric heights, *Can. J. Physics*, 38, 1440-1481, 1960
- Hines, C.O., and Reddy, C.A., On the propagation of atmospheric gravity waves through regions of wind shear, *J.G.R.*, 72, No. 3, 1015-1034, 1967
- Ingard, U., A review of the influence of meteorological conditions on sound propagation, *J. Acoustical Soc. of Amer.*, 25, No. 3, 405-411, 1953
- Johnson, F.S., Satellite Environment Handbook, Stanford University Press, Stanford, Calif., 1961
- Lamb, H., Hydrodynamics, Dover Publications, Inc. New York, 1945

- Lighthill, M.J., Group Velocity, *J. Inst. Maths Applic.* I, No. 28, 1-28, 1964
- MacDonald, G.J.F., Spectrum of Hydromagnetic Waves in the Exosphere, *J.G.R.*, 66, No. 11, p. 3639-3670, Nov. 1961
- Martyn, D.F., Cellular atmospheric waves in the ionosphere and troposphere, *Proc. Royal Soc., London, Ser. A*, 201, 216-234, 1950
- Midgley, J.E., and Liemohn, H.B., Gravity waves in a realistic atmosphere, *J.G.R.*, 71, No. 15, p. 3729-3748, Aug. 1966
- Mitra, S.K., The upper atmosphere, *The Asiatic Soc.*, I Park Street, Calcutta 16, 1952
- Mook, C.P., The apparent ionospheric response to the passage of hurricane Diane at Washington D.C. (1955), *J.G.R.* 63, 569-570, 1958
- Murphy, C.H., Bull, G.V. Edwards, H.D., Ionospheric winds measured by hun launched projectiles, *J.G.R.*, 66, No. 11, p. 4535-4544, Nov. 1961
- Pfeffer, R.L., and Zarichny, J., Acoustic gravity wave propagation in an atmosphere with two sound channels, *Geofisica Pura e Applicata, Milano*, 55, 175-199, 1963/II
- Pierce, A.D., Geometrical acoustics' theory of waves from a point source in a temperature and wind stratified atmosphere, *Scientific Document-Avco Corp.* Ap 636 159, Aug. 2, 1966
- Pierce, A.D. and Friedland, A., The reflection and transmission of acoustic waves by a fluid layer with an ambient velocity gradient, *AVCO Report, AUSSO-0064-PP*, Feb. 8, 1961
- Pierce, A.D., Propagation of acoustic-gravity waves from a small source above the ground in an isothermal atmosphere, *J. of Acous. Soc. of Amer.*, 35, No. 11, 1798-1807, Nov. 1963
- Pierce, A.D., A suggested mechanism for the generation of Acoustic-gravity waves during thunderstorm formation, submitted to *Nature*, Nov. 1965
- Pitteway, M.L.V., and Hines, C.O., The viscous damping of atmospheric gravity waves, *Can. J. of Phys.*, 41, No. 12, 1935-1948, Dec. 1963
- Press, F., and Harkrider, D., Propagation of acoustic-gravity waves in the atmosphere, *J. Geophys. Res.*, 67, 3889-3908, 1962

- Radio Science, Feb. 1966, The entire issue is devoted to the wind shear theory of sporadic E.
- Rosenberg, Edwards and Wright, Chemilluminous rocket trails observed between 100 and 150 km., Space Research V
- Rosenberg, and Justus, Space and time correlations of ionospheric winds, Radio Science, 149, Feb. 1966
- Smith, R.L., and Brice, N., Propagation in multicomponent plasmas, J.G.R. 5029, Dec. 1964
- Thrane, E.V., and Piggott, W.R., The collision frequency in the E and D regions of the ionosphere, J. Atmos. and Terr. Phys., 28, 721-737, 1966
- Tolstoy, J., The theory of waves in stratified fluids including the effects of gravity and rotation, Reviews of Mod. Phys., 35, No. 1, 207-230, Jan. 1963

ACKNOWLEDGEMENT

I would like to acknowledge the extensive contribution of my thesis advisor Professor T. R. Madden who besides giving the principal direction did much of the actual work on data collection, organization and analysis and who designed all of the electronic circuits.

Dr. Allen Pierce critically reviewed Chapter I-A at various stages of development. Helpful discussions were held with J. Chapman, R. Dickenson, W. Donn, A. F. Gangi, F. Gilbert, P. Green, C.O. Hines, E. Illiff, P. H. Nelson, W. R. Sill, C. M. Swift and C. Wunsch.

The author held a NASA traineeship during the last two years of his graduate studies. General support was received from the U.S. Army Research Office Project 2M014501B52B. The M.I.T. Center for Space Research financed the microbarographs. The M.I.T. computation center donated computer time for two years at the beginning of the study.

BIOGRAPHICAL NOTE

The author was born on 14 February 1938 in Sheboygan, Wisconsin and attended Sheyboygan Falls elementary and secondary schools. He received his Bachelor's Degree in Physics from M.I.T. in 1960 and his Master's Degree from M.I.T. in Geophysics in January 1963. He spent 1963 working for United Electrodynamics, Inc. (now Tele-dyne) in Alexandria, Virginia and 1964 at the University of Uppsala, Sweden. In 1965 he returned to the M.I.T. Department of Geophysics.